Study of Natural Radioactivity Levels in Environmental Samples (Building Materials) in Dejen district, East Gojjam, Ethiopia

By

Gizachew Zihon Cherie

A DISSERTATION

SUBMITTED TO THE GRADUATE PROGRAMS OF
COLLEGE OF NATURAL AND COMPUTATIONAL SCIENCES
ADDIS ABABA UNIVERSITY
IN FULFILLMENT OF THE REQUIREMENTS FOR THE DEGREE OF

DOCTOR OF PHILOSOPHY

(NUCLEAR PHYSICS)

ADDIS ABABA, ETHIOPIA
DECEMBER 2023

Addis Ababa University
Graduate Programs

Study of Natural Radioactivity Levels in Environmental Samples (Building Materials) in Dejen district, East Gojjam, Ethiopia

By
Gizachew Zihon Cherie
Department of Physics
Addis Ababa University

Approved by the Examining Board:

Dr. Tilahun Tesfaye Signature _____
Advisor

TBA Signature _____
Examiner

TBA Signature _____
Examiner

Dated: December 2023

ADDIS ABABA UNIVERSITY

Date: **December 2023**

Author: **Gizachew Zihon Cherie**
Title: **Study of Natural Radioactivity Levels in Environmental Samples (Building Materials) in Dejen district, East Gojjam, Ethiopia**
Department: **Department of Physics**
Degree: **PhD** Submission: **September. 2023** Convocation Year: **2023**

Permission is herewith granted to Addis Ababa University to circulate and to have copied for non-commercial purposes, at its discretion, the above title upon the request of individuals or institutions.

Signature of Author

This Work is Dedicated
to my family for their encouragement and loving support throughout my PhD studies. I will never forget my wife, Zewdie Araya, and my three special children, Dawit, Kidist, and Henok, who have provided continuous and unending support in all aspects of my life throughout my studies. My studies would not have been possible without their motivation and assistance.

Table of Contents

List of Tables

List of Figures

Acknowledgements

All praise is due to Almighty God, the most beneficent and merciful, to bestow courage, strength, patience, and health on me to start and complete this research project.

I'd like to express my heartfelt appreciation and gratitude to my supervisor, Dr. Tilahun Tesfaye, for his invaluable advice, unwavering support, and insightful comments.

Debre Markos University deserves my gratitude for sponsoring my PhD study. I would like to express my gratitude and indebtedness to the Physics Department of the AAU for providing the financial support and facilities needed; to the Ethiopian Radiation Protection Authority (ERPA) for availing, free of cost, their laboratory to conduct all experiments of the research; the physics department and its staff members for the opportunities given to me and encouragement and constructive comments for the successful completion of this study.

Above all, I'd like to express my gratitude to my beloved wife, Zewdie Araya, for her encouragement and financial support throughout the study period. My children, Dawit, Kidist, and Henok, deserve special gratitude for their well-wishes and moral support throughout this study. I will never forget Kidist's assistance in proofreading and checking manuscripts for submission to journals, despite her busy schedule in her MSC study.

Addis Ababa University — Gizachew Zihon Cherie

September. 2023

Acronyms

AEDE	Annual Effective Dose Equivalent
$Bq\,kg^{-1}$	Becquerel per kilogram
DNA	Deoxyribonucleic acid
ELCR	Excess Life time Cancer Risk
IAEA	International Atomic Energy Agency
ICRP	International commission of radiation protection
ICRP 66	International commission of radiation protection publication 90
$mSv\,y^{-1}$	mill Sievert per year
$nGyh^{-1}$	nano Gray per hour
NORM	Natural Occurring Radioactivity Materials
NRPB	National Radiological Protection Board (NRPB)
Ra_{eq}	Radium equivalent activity
TENORM	Technological Enhanced Natural Occurring Radioactivity Materials
UNSCEAR	United Nation Scientific Commission Effects of Atomic Radiation

Abstract

All materials derived from rock and soil contain varying levels of natural radioactive isotopes such as ^{238}U and ^{232}Th and their decay products as well as ^{40}K. Therefore, whether willingly or unwittingly, humans are constantly exposed to radiation emitted by radionuclides.

The purpose of this study is to determine the levels of naturally occurring radioactivity and their risk indices in raw gypsum, soil samples, and building-related raw materials (sand, limestone, clay, gypsum, pumice, and coal used in cement production) in East Gojjam, Dejen district, Ethiopia.

Raw gypsum samples were collected from the production site of five gypsum factories, while soil samples were collected from agricultural and virgin lands. Raw building materials that are used for cement production were also collected from cement factories. All the samples were prepared and packed for measurement using standard methods [1].

The specific activities of ^{238}U, ^{232}Th, and ^{40}K were computed using a p-type, coaxial, Canberra High Purity Germanium (HPGe) detector. The detector is used in conjunction with a multichannel analyzer that features an analog-to-digital converter for data acquisition and Genie 2000 multichannel analyzer software with 8192 channels to analyze spectra.

In raw gypsum samples it was determined that ^{238}U, ^{232}Th, and ^{40}K are found, with mean specific activities of 1.90 $\pm$ 0.33, 1.99 $\pm$ 0.39, and 28.16 $\pm$ 2.57 Bqkg^{-1}, respectively, which are significantly lower than the intercontinental approved values. All the radioactive risk indices calculated were significantly lower than the global recommended values. The results of various radioactive indices show that using gypsum powder obtained from studied samples in the construction of residences is safe.

The calculated mean activity concentrations of ^{226}Ra, ^{232}Th, and ^{40}K in agricultural soils were 33.44 $\pm$ 2.01, 66.02 $\pm$ 4.54, and 214.16 $\pm$ 8.90 Bqkg^{-1}, respectively, while in virgin soils they were 38.05 $\pm$ 2.48, 61.78 $\pm$ 4.76, and 240.32 $\pm$ 10.79 Bqkg^{-1}, respectively. The findings were discussed and compared to those of other studies. The mean values of absorbed dose rate, annual effective dose rate, radium equivalent activity, external hazard index, internal hazard index, radioactivity level index and excess lifetime cancer risk in agricultural land soils are 67.24 nGyh^{-1}, 0.083 mSvy^{-1}, 144.57 Bqkg^{-1}, 0.39, 0.48, 1.03 and 0.29$\times$10^{-3}, and in virgin land soils are 67.53 nGyh^{-1}, 0.082 mSvy^{-1}, 144.90 Bqkg^{-1}, 0.39, 0.49, 1.03 and 0.29$\times$10^{-3}, respectively. These results were compared and contrasted to the internationally recommended value.

The activity concentrations of ^{226}Ra, ^{232}Th, and ^{40}K, as well as their radiation risk indices, were measured in raw material samples (sand, limestone, clay, gypsum, pumice, and coal) used in cement production. ^{226}Ra, ^{232}Th, and ^{40}K activity concentrations in the tested samples ranged 4.90 $\pm$ 0.49 to 37.43 $\pm$ 2.57, 2.97 $\pm$ 0.42 to 72.08 $\pm$ 5.53, and 2.58 $\pm$ 1.28 to 208.78 $\pm$ 9.70 Bqkg^{-1}, respectively. For ^{226}Ra, ^{232}Th, and ^{40}K, the clay sample had the highest activity concentration (37.33 $\pm$ 2.36, 71.06 $\pm$ 5.45, 208.66 $\pm$ 9.69 Bqkg^{-1}) and the gypsum sample had the lowest activity concentration (5.18 $\pm$ 0.55, 4.95 $\pm$ 0.61, 54.36 $\pm$ 3.40 Bqkg^{-1}). With the exception of clay samples for radium and thorium, these values are significantly lower than the corresponding worldwide mean values. The average results were compared to those of comparable studies conducted in other countries, as well as global average values. The received doses and radiological hazard characteristics were calculated and compared to global average values to determine the exposure risk associated with the use of these raw materials. Except for the increased lifetime cancer risk, the mean total estimated radiation hazard indices are below the recommended limits.

This study demonstrated that the evaluated samples for raw gypsum; raw materials used in cement production and soil samples used in building construction are safe for residents and those involved in agricultural activities, and no additional radiological health risks are present in any of the studied samples.

Chapter 1
Introduction

Natural ionizing radiation arises in outer space, where cosmic rays are found, and in and on the earth, where radionuclides normally present and undergo radioactive decay. Penetrating radiations and radioactive materials pervade the natural environment. Human exposure occurs by irradiation from sources outside the body (external exposure) and upon the decay of radionuclides taken into the body through ingestion and inhalation. The assessment of radiation doses in humans from natural sources is important because natural ionizing radiation is the largest contributor to the collective effective dose received by the world's population. Measuring radionuclide levels is crucial for limiting radiation levels to which humans are exposed both externally and internally [2]. Thus, in this study, gamma-ray emitting nuclide activity concentrations in the investigated samples was measured using a P-type high purity germanium detector. The findings were utilized to assess the doses received and potential radioactive risks associated with the use of these materials in buildings by calculating various indices.

1.1 Background of the Study

Henri Becquerel discovered radioactivity in 1896, and the science of radioactivity has been extensively studied since then. Radioactivity is present everywhere and has been part of the natural environment since the earth's formation. Radioactivity is a phenomena that comes from the heart of atoms that are specifically known as radionuclides. Radionuclides that manifest radioactivity most of the time emit radiations that are identified as α, β or γ radiations [3]. Emission from a given radionuclide can be one or any combination of these radiation types. Radionuclides are radioactive elements that emit nuclear radiation, which has become a part

of our everyday lives. Alpha particles, beta particles, and gamma rays are the most common types of ionizing radiation [3].

Radionuclides and resulting nuclear radiation is an integral part of our lives because it is present in our food we take in, in the air we inhale, in the shelter we are housed and in medications we practice. Radionuclides are not only limited to be constituent particles of the natural environment but also are exploited for the betterment of human life in numerous areas of human life including medicine, agriculture, industry, biotechnology and energy generation [4].

Radionuclides are categorized as primordial, anthropogenic and cosmic on the basis of their origin. The primary primordial (half-lives comparable to the age of the earth) radionuclides in terms of dose are ^{40}K, ^{232}Th, and ^{238}U. Both ^{232}Th and ^{238}U belong to the radionuclide head series that cause significant human exposure. Anthropogenic radionuclides are produced artificially by explosions resulting from thermonuclear reactions, discharges from nuclear installations, or production for different isotopes . Both natural and man-made radionuclides emit background radiation, which is present everywhere in the environment. Human-made radionuclides have entered the environment through activities such as medical imaging with radionuclides and electricity generation with radioactive uranium as fuel. Humans are constantly exposed to radiation from both outsides and inside their bodies. Space radiation and terrestrial radiation are examples of external sources. Inside sources include radionuclides that enter our bodies through the food and water we consume, as well as the air we breathe [5].

As a result of natural radioactivity in building components, the inhabitants are exposed both internally and externally. All raw materials used in construction made from rock and soil (also used in agricultural activities) contain varying levels of the radioactive isotope ^{40}K, as well as the naturally occurring radionuclides ^{238}U and ^{232}Th and their decay products. Radionuclides originate in the Earth's crust, but they also end up in food, air, water, building materials, and the human body. The specific activities of natural radionuclides can vary greatly depending on their geographical locations and geochemical properties in environmental samples [2, 6, 7].

To protect the general public's health from the radiation risk posed by naturally occurring radioactive materials, radioactivity in the environment must be measured in order to assess the biological effect on humans. In recent years, the IAEA has paid increased attention to this issue [8]. Thus, measurements of the specific activities of natural radionuclides in environmental samples are important for evaluating the radiation impacts on the environment, population, and occupational personnel exposed to radiation [9].

1.2 Statement of the problem

The natural background radiation, and the resulting exposure rates, have large variations depending on geography, geology, and housing environments. This variation implies the importance of measurement in different localities and environmental samples of radiological importance. In this regard studies related to measurement of radioactivity concentrations in building materials are hardly available in Ethiopia. There is no national data-base that indicates the natural radioactivity level in different parts of Ethiopia and exposure level.

This study aims to contribute toward accumulation of baseline data related to activity concentration of primordial radionuclides in building materials, thus the activity concentrations of primordial radionuclides in raw gypsum, soil, and raw materials for cement production from Ethiopia's East Gojjam Amhara regional state, are studied. The amounts of naturally occurring radionuclides such as ^{226}Ra, ^{232}Th and ^{40}K in the analyzed samples were measured with a coaxial P-type high-purity germanium (HPGe) detector and their radiation risk was assessed. Knowing the activity levels of naturally occurring radioactive materials in the environment ensures the health of the environment for life, raises awareness of radiation risk in factory workers and allows for restrictions or regulations on their use in the study area.

1.3 Objectives of the Study

1.3.1 General objective

The overall goal of this study is to measure the levels of natural radioactivity in soil and raw building materials used in the Dejen district, East Gojjam, Ethiopia, using a P-type high-purity germanium detector, and then estimate the effective dose based on the measured radioactivity levels.

1.3.2 Specific objectives

- To determine the natural radionuclides and their specific activities in the samples under consideration.
- To compare and contrast the obtained specific activities with other similar studies.
- To calculate the radiation dose based on the activity concentration obtained in the analyzed samples.
- To evaluate the radiation hazard indices in all samples tested and compare them to the global average recommended values.
- To make recommendations to the appropriate body regarding building material restrictions or regulations in the studied area.

1.4 Motivation for the study

There are six gypsum factories and two cement factories in Dejen town, East Gojjam, Ethiopia, which use raw materials such as gypsum to produce gypsum powder and sand, limestone, clay, gypsum, pumice, and coal to produce cement. Even though neither factory had radiological regulatory control, naturally occurring radioactive elements such as ^{226}Ra, ^{232}Th and ^{40}K exist in these raw materials and emit background radiation into the environment. People in the studied area who work in factories and live in buildings made of cement and decorated with gypsum products were not aware of their exposure to radiation. Thus, the purpose of this research is to assess the levels of naturally occurring radioactivity and their risk indices in building-related raw materials.

1.5 Scope of the study

This study includes raw gypsum samples obtained from Abay gorge in the Dejen district by digging out an area of ground where the raw gypsum materials are found and produced in Dejen town, East Gojjam Ethiopia, by five factories. Furthermore, the raw materials used in cement production, such as sand, limestone, clay, gypsum, pumice, and coal, were obtained from Abay gorge in East Gojjam, Ethiopia, with the exception of coal, which was obtained from Sudan as well. At the same time, soil samples from Berchgiyorgis village in Dejen district, Ethiopia, which uses artificial fertilizer for agricultural activities, were included in the study.

1.6 Limitation of the study

This research is constrained by the dissertation design and methodology. The method of collecting samples that represent the study area is the major limitation of this study. The raw materials samples must be collected from the site, but the site area of Abay gorge is far from the factory, and there is no way of transportation to get to the site area, so the materials collected from the factory are stored outside in the field. The factories have more than two site areas in Abay gorge, and some raw materials are taken from the surface while others are taken from depth, which could be a barrier to this study. Another methodology constraint for this study's laboratory work is limited access to gamma-ray spectrometry. The experiment was carried out at the Ethiopian Radiation Protection Authority, the country's only laboratory. As a result, they limit the number of samples we collect, the time allotted to us is insufficient. As a result, the author used few number of samples to complete this thesis.

1.7 Dissertation structure

This thesis is divided into five chapters. Chapter one provides a general overview of background radiation, as well as an explanation of the problems, research objectives, and limitations.

The second chapter deals on literature review and discusses radioactivity

and its decay laws, naturally occurring radioactive materials in the environment, radiation detectors, ionizing radiation health effects, and a review of previous related studies in environmental samples.

The third chapter discusses the sampling methodology and sample preparation used in this research from East Gojjam, Ethiopia, as well as the operational properties and experimental setup of the HPGe detector and the assessment of radiation risk indices.

Chapter four contains the research date (results) and its evaluation, and its discussion, which is its overall analysis. The experimental results from this study are compared to published data from other parts of the world.

This study's conclusion and recommendations are presented in Chapter 5.

Chapter 2
Literature Review

2.1 Radioactivity

Radioactivity is the spontaneous decay of nuclide that results in the emission of radiation. Radiation is made up of particles (alpha and beta radiation) that are usually accompanied by electromagnetic waves (gamma radiation and X-rays). During the decay process, the so-called parent nuclide transforms into a different type of nucleus, known as the daughter nuclide. As a result of the decay type, the chemical element changes, or an isotope is created. The energy of the emitted radiation is enough to ionize atoms by stripping electrons along the radiation's path. This occurs either directly (alpha and beta radiation) or indirectly (gamma radiation and X-rays). Alpha (α) radiation is made up of α-particles with two protons and two neutrons that are identical to ionized $^{4}_{2}$He nuclei. Because of its large mass and twice elementary positive electric charge, α-particle has a low penetrating power. Its path through biological tissues is only a few tens of micrometers long. Alpha radiation is densely ionizing, which means that it produces more ions per unit length of matter it passes through than other types of radiation. This is because the particles lose all of their energy over a short distance. Internal exposure is primarily caused by alpha emitters, which include inhalation, ingestion, and skin contact. Beta (β) radiation is composed of β^- particles, which are electrons with a negative elementary charge or, less frequently, positrons with a positive elementary electric charge. Because the mass of an electron is much lower than that of an α-particle (about 8000 times), β^- radiation has moderate penetrating power. Finally, beta particle exposure causes more external irradiation hazards and fewer internal radiation hazards than alpha particle exposure. The external irradiation caused by beta particles is mostly restricted to the epidermis and outer skin tissue, but it can also harm the eye lens. Gamma (γ)

radiation is made up of high-energy photons (electromagnetic waves) that are emitted by the nucleus. This radiation is only weakly ionizing, but it has high penetrating power and can travel hundreds of meters through the air. To protect against γ-radiation, thick concrete or lead shielding is typically used. It is primarily in charge of external exposure. In terms of internal radiation exposure, the high penetrating power of gamma rays means that the energy released by gamma rays and taken up by a small volume of tissue is comparatively smaller than that released by alpha and beta radiation. As a result, the internal radiation exposure risk posed by gamma rays is less severe than that posed by other types of radiation (alpha and beta) [9].

2.1.1 Radioactive decay law

As we have seen, unstable nuclei can often transmute into other nuclei through the emission of α, β, and γ particles. Radioactive decay refers to any such spontaneous transition from one state to another. Radioactive decay can be described statistically. Specifically, if there are a large number of radioactive nuclei, we cannot predict which nucleus will decay at any given time. Each nucleus, however, has a distinct constant decay probability. Thus, if N denotes the number of radioactive nuclei of any specified type at a given time and λ is the constant probability of decay per unit of time (that is, the decay constant), then the change in nuclei during an infinitesimal time interval dt is defined by [10]:

$$\frac{dN}{N} = -\lambda dt \tag{2.1}$$

The negative sign in the above equation represents, the fact that the number of nuclei decreases as a result of decay. If we assume N_o to be the initial number of nuclei at $t = 0$, then the number of nuclei $N(t)$ at any later time can be obtained from the above equation.

$$N_\circ e^{-\lambda t} \tag{2.2}$$

In other words, the number of nuclei that survive in a radioactively decaying system decreases exponentially and vanishes only infinitely. A radioactive system can be associated with several time scales. The half-life ($t_{\frac{1}{2}}$) is the amount of time it takes for half of the nuclei in the sample to decay. It can be calculated using the following equation:

$$t_{\frac{1}{2}} = \frac{\ln 2}{\lambda} \tag{2.3}$$

Another useful time scale for describing decay is the average or mean life (τ) of a radioactive material. The mean life of the sample is the inverse of the decay constant and is given as:

$$\tau = \frac{1}{\lambda} \tag{2.4}$$

Activity (A) is the number of disintegrations per unit time of radionuclides and is defined as follows [10]:

$$A(t) = \frac{dN(t)}{dt} = \lambda N_0 e^{-\lambda t} \tag{2.5}$$

2.1.2 Radioactive equilibrium

If a radioactive parent nucleus generates a radioactive daughter nucleus, which decays into a granddaughter nucleus, and so on, then each radioactive parent nucleus initiates a series of decays, with each decay product having its own characteristic decay constant and, thus, a different half-life. In general, the parent nucleus has a much longer mean life than any other member of the decay chain [10].

Consider a radioactive parent nucleus that has a very long lifetime and thus the number of parent nuclei barely changes over a short time interval, while the daughter, granddaughter, and so on decay relatively quickly. After a certain lapse in time, a situation may develop where the number of nuclei of any member of the decay chain stops changing, at this time it is said to be radioactive equilibrium. Let us denote the number of nuclei

in the series of species 1, 2, 3, ... by N_1, N_2, N_3, ... at some specific time, and the decay constant by λ_1, λ_2, λ_3, ... respectively, in the decay chain. The change in the number of parent, daughter, granddaughter nuclei, etc., in a time interval Δt, can be written as follows [10]:

$$\Delta N_1 = -\lambda_1 N_1 \Delta t \tag{2.6}$$

$$\Delta N_2 = -\lambda_1 N_1 \Delta t - \lambda_2 N_2 \Delta t \tag{2.7}$$

$$\Delta N_3 = -\lambda_2 N_2 \Delta t - \lambda_3 N_3 \Delta t \qquad etc. \tag{2.8}$$

Dividing the above equations by Δt, and taking the limit of infinitesimal time intervals we can write as follows [10]:

$$\frac{dN_1}{dt} = -\lambda_1 N_1 \tag{2.9}$$

$$\frac{dN_2}{dt} = -\lambda_1 N_1 - \lambda_2 N_2 \tag{2.10}$$

$$\frac{dN_3}{dt} = -\lambda_2 N_2 - \lambda_3 N_3 \qquad etc. \tag{2.11}$$

When the activity of parent, daughter, granddaughter nuclei, etc., is the same, the activity of a radionuclide is said to be secular equilibrium, and we can write for this as follows [10]:

$$\frac{dN_1}{dt} = \frac{dN_2}{dt} = \frac{dN_2}{dt} = ... = 0 \tag{2.12}$$

As a result, under these conditions, the parent, daughter, granddaughter, and so on will all be in equilibrium with one another, which means their numbers will not change over time [10].

The parent and daughter radionuclides are said to be in secular equilibrium if the parent's half-life is significantly greater than the daughter's, i.e. $(t_{\frac{1}{2}})_p \gg (t_{\frac{1}{2}})_d$ or $\lambda_p \ll \lambda_d$ [11].

If the activities of parent and daughter nuclide are not equal but differ by a constant fraction, the activity of a radionuclide is said to be transient equilibrium. This occurs when the parent's half-life is only slightly greater than the daughter's, i.e. $(t_{\frac{1}{2}})_p > (t_{\frac{1}{2}})_d$ or $\lambda_p < \lambda_d$ [11].

If the half-life of the parent is less than the half-life of the daughter radionuclide, i.e. $(t_{\frac{1}{2}})_p < (t_{\frac{1}{2}})_d$ or $\lambda_p > \lambda_d$, and the activity of the parent nuclide will diminish quickly as it decays into the daughter, then the state is said to be non-equilibrium. Consequently, the net activity will be solely determined [11].

2.2 Natural radioactivity in the environment

Natural radioactivity originates from extraterrestrial sources as well as from radioactive elements in the earth's crust. About 340 nuclides have been found in nature, of which about 70 are radioactive and are found mainly among the heavy elements. All elements having an atomic number greater than 80 possess radioactive isotopes, and all isotopes of elements heavier than number 83 are radioactive [12]. Other than naturally occurring radionuclides (NORs), naturally occurring radioactive material (NORM) contains no significant amounts of radionuclides. Natural radionuclides exist because their half-life time is comparable to the age of the Earth and they are constantly created. Uranium, thorium, and potassium are found in abundance, either as primary constituents of some rock materials or as trace elements. This means that NORM can be found almost anywhere and, depending on its concentration and application, can cause radiological problems. Some NORs can concentrate in specific minerals due to their geochemical behavior. As a result, some important raw materials have higher NOR concentrations [9]. The majority of environmental radioactivity comes from natural sources, but radionuclides and ionizing radiation are also produced by humans. Ionizing radiation, which has always existed naturally, is constantly exposed to all living organisms.

The sources of that exposure are cosmic rays from outer space and the Sun's surface, terrestrial radionuclides found in the Earth's crust, building materials, air, water, and foods, and the human body itself [5]. Radionuclides, both terrestrial and cosmogenic, enter the body through the food we eat, the water we drink, and the air we breathe [3]. Some exposures, such as the dose from ingestion of potassium-40 in foods, are fairly constant and uniform for all individuals everywhere. Other exposures differ greatly depending on location. Cosmic rays, for example, are more intense at higher altitudes, and uranium and thorium concentrations in soils are elevated in isolated areas. Human activities and practices can also alter exposure levels. Building materials, as well as the design and ventilation systems of houses, have a strong influence on indoor levels of the radioactive gas radon and its decay products, which contribute significantly to doses through inhalation [5].

2.2.1 Cosmogenic radionuclides

Cosmogenic radionuclides are the result of interactions between cosmic rays (primarily protons with some helium and other heavier ions) and atoms in the atmosphere. Radiation entering the Earth's atmosphere from space can come from as close as the Earth's radiation belts and the sun to as far away as beyond the solar system's boundaries and even beyond the Milky Way galaxy. Beyond-solar-system radiation contains enough energy to generate additional radiation as it passes through Earth's atmosphere, resulting in radionuclides in the air or secondary particles. When energetic particles, primarily protons, enter the atmosphere, they can interact with the nuclei of atmospheric gases (nitrogen, oxygen, and argon) in a variety of nuclear reactions. Tritium (hydrogen-3), beryllium-7, carbon-14, and sodium-22 are the four most important cosmogenic radionuclides for human exposure caused by space radiation [5].

2.2.2 Primordial radionuclides

Naturally occurring radionuclides of terrestrial origin (also known as primordial radionuclides) are found in varying degrees in igneous and sedimentary rock in general, as well as in all media in the environment, including the human body. Only radionuclides with half-lives comparable

to the earth's age, as well as their decay products, are found in significant quantities in these materials. These radionuclides migrate from rocks into soil, water, and even the atmosphere. These radionuclides have also been redistributed by human activities such as uranium mining [3, 5]. The naturally occurring radionuclides can be divided into those that occur singly and those that are components of the three chains of radioactive elements: the uranium series, which originates with ^{238}U; the thorium series, which originates with ^{232}Th; the actinium series, which originates with ^{235}U [12]. Uranium (^{238}U), thorium (^{232}Th) with their decay series, and the potassium isotope ^{40}K in significant quantities are examples of primordial radionuclides. The human body is primarily exposed to gamma radiation from radionuclides in the ^{238}U and ^{232}Th series, as well as ^{40}K. These radionuclides are also present in the body and provide alpha and beta particles, as well as gamma rays, to the various organs. The radon gases (and their decay products) that a person constantly inhales are the most significant. Radon levels are determined by the soil's uranium and thorium content, which varies greatly around the world [3, 5]. The primary goal of this research is to assess their activity levels and health hazard indices in environmental samples.

Uranium-238 decay series

Uranium is found in all rock and soils. Because uranium occurs in soils and fertilizers, the element is present in food and human tissues [12]. Uranium is a naturally radioactive element that is made up of three long-lived isotopes: ^{234}U, ^{235}U, and ^{238}U [13]. The amount of ^{238}U series in the earth's crust is determined by the type of rock and geological formations. In reference to igneous and sedimentary rocks, the average uranium content in the Earth's crust is 2 to 4 ppm. On average, the relative abundance of ^{238}U is 99.274%, the equilibrium concentration of granddaughter ^{238}U is 0.0054%, and the relative abundance of ^{235}U is 0.7205%. As a result of its relative abundance and significant contribution to natural pollution in the environment, we deal with ^{238}U and its decay products in this thesis [14]. The uranium series refers to the decay of ^{238}U (half-life 4.5×10^9 years) containing alpha emitters. ^{238}U is the longest-living member of the (4n + 2) series (n ranging from 51 to 59), which also includes ^{234}U. It decays through a

complex series to a stable lead isotope (^{206}Pb) [15], as shown in a simplified version in Fig. 2.1.

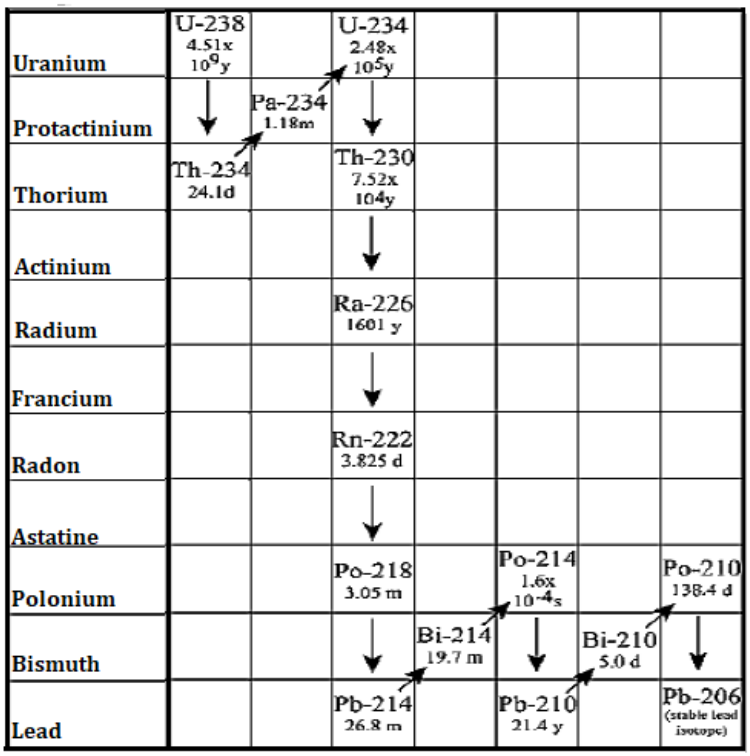

Figure 2.1: Uranium-238 decay series, with the arrows indicating the mode of decay (vertical arrow = alpha particle emission, 45^0 angle arrow = beta particle emission) [17]

The two long-lived progenies of ^{238}U are ^{234}U and ^{230}Th, the decay product of which is known as radium (^{226}Ra). Radon (^{222}Rn), the decay progeny of ^{226}Ra, can cause roughly half of the background radiation dose to humans, primarily through lung deposition. The dose from radon and its progeny varies spatially, depending on ^{226}Ra concentrations in the soil and geosphere [16]. Radon progenies can degrade by emitting alpha particles, beta particles, and gamma rays. Gamma rays emitted by ^{214}Pb and ^{214}Bi are the most important radiation for studying natural radioactivity levels. In undisturbed natural deposits, ^{238}U appears in a secular decay equilibrium (shows the same decay rate) with their 4n + 2 series daughter products [13].

Thorium-232 decay series

^{232}Th concentrations in the earth's crust range from zero to several hundreds of parts per million. Natural thorium is almost entirely composed of ^{232}Th, 1.35×10^{-8}% of ^{228}Th and extremely small amounts of ^{234}Th, ^{230}Th,

^{231}Th and ^{227}Th. ^{232}Th (half-life 14×10^9 years) is the parent of 4n radioactive decay series (n varies from 52 to 58) that contains several radioactive isotopes and contributes to the general background radioactivity. As shown in Fig. 2.2, ^{232}Th and its decay products emit alpha particles, beta particles, and gamma rays before terminating with a stable lead (^{208}Pb) isotope.

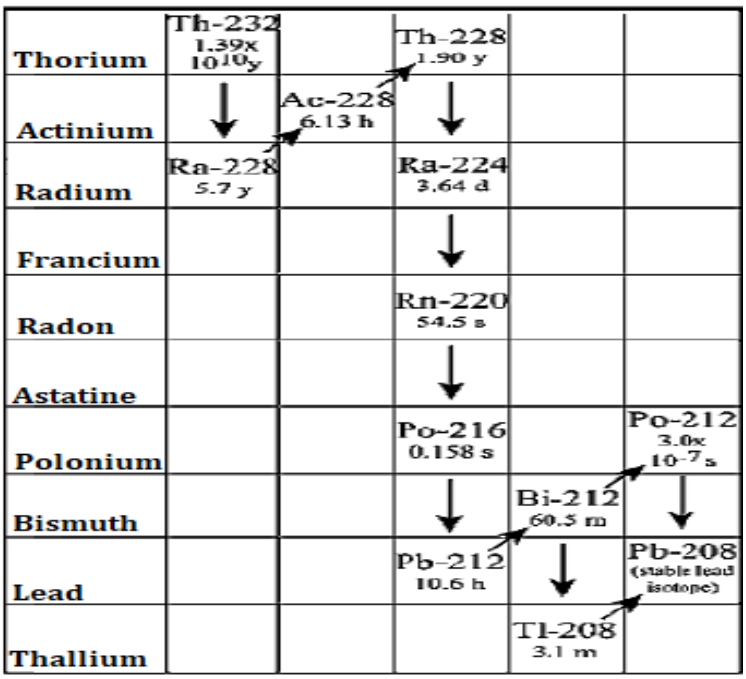

Figure 2.2: Thorium-232 decay series, with the arrows indicating the mode of decay (vertical arrow = alpha particle emission, 45^0 angle arrow = beta particle emission) [17]

When compared to ^{232}Th, all of the daughter products have a short lifetime. ^{232}Th concentrations in the earth's crust range from zero to several hundreds of parts per million [14]. The most common gamma emitters of ^{232}Th progenies are ^{212}Pb, ^{212}Bi, and ^{228}Ac, which are used in this study to determine activity concentration.

Potassium-40 decay

Potassium is found in many rock-forming minerals and is the most common natural gamma ray encountered in nature. Natural potassium is composed of three isotopes (^{39}K, ^{40}K, and ^{41}K), with only ^{40}K (half-life of 1.28×10^9 years) exhibiting natural gamma radioactivity and accounting for 0.012% of all potassium present in the earth's crust. Under most conditions, potassium is soluble and is lost in solution during weathering [14]. The beta and electron capture decay modes of ^{40}K to stable ^{40}Ca (89.28 %) and ^{40}Ar

(10.72 %), respectively, are followed by the emission of 1460.8 keV gamma rays that contributes significantly to natural radioactivity [18]. ^{40}K decays to ^{40}Ca by emitting β^-(electron) and to ^{40}Ar by emitting β^+(positron) as shown in Fig. 2.3.

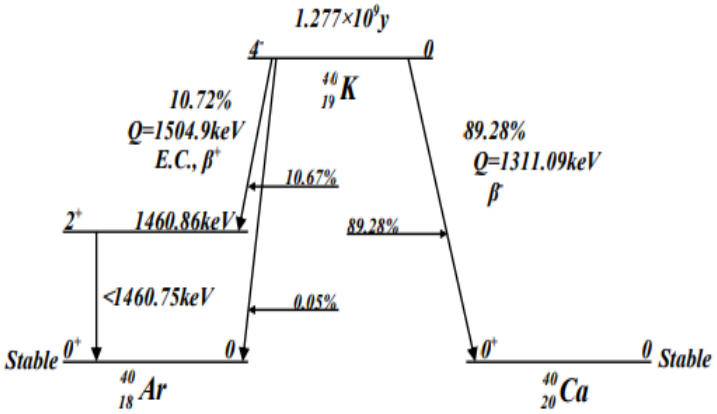

Figure 2.3: Potassium-40 decay scheme [16]

2.3 Radiation detectors

Radiation detectors are used to identify and quantify radionuclides in a variety of matrices. Radiation is a form of energy. This energy can be partially or completely deposited in a suitable medium, producing an effect. Radiation detection and measurement are based on the detection and measurement of its effects in a medium, and the history of radiation detectors is closely related to the discovery of radiation and radiation effects. Ionizing radiation is emitted by radioactive materials that have not been exposed to any external influences. The type of radiation emitted and the energy associated with it are characteristics of the radioactive substance. The goal of many radiation detector applications is to measure the energy distribution of the radiation. The effects discovered in early research work with X-rays and radioactive materials have remained the underlying principles of radiation detection to the present day. Detection instruments have been improved numerous times over the years, thanks to the efforts of numerous investigators [19].

Radiation detection is more than just an indication of the presence of radiation. It must include some measure of radiation, and it may also include information about radiation energy, type, or location. The generation of a signal in radiation-detection materials is a complex process in which energy is transferred from a single particle or quantum of radiation through a cascade of collisions or interactions with electrons and atomic nuclei. This produces a distribution of electrons and holes that serve as information-carrying quanta directly or indirectly to produce a signal that can be collected and quantified by the instrumented readout system. Solid materials used in radiation detectors fall into two broad categories: semiconductor and scintillator. The performance metrics for both semiconductor and scintillator materials are energy resolution (the identification of the nuclear isotope or isotopes giving rise to the radiation), rate and timing (rapid readout of information carriers), spatial resolution (accurate determination of the radiation interaction's location in the detector material), detection efficiency (the fraction of detection events in which the full energy of the incident radiation has been deposited), geometric efficiency (the fraction of radiation quanta emitted by a radiation source that strike an active radiation-detection material), neutron detection (a favorable neutron reaction cross-section is desired to increase the probability of detection) and operational factors (cost and the ease with which detection instrumentation can be designed using a given material) [20].

2.3.1 Scintillator detectors

Scintillators are materials that emit detectable photons in the visible part of the light spectrum after a charged particle passes through them [10]. Scintillators are typically the only viable option for detectors that require large areas or arrays to achieve geometric efficiency. When radiation interacts with scintillator materials, electron-hole pairs are formed, and the electron-hole pairs are then converted into optical photons. These photons then traverse the material before being collected and converted to electrical signals at the material's exterior. The most common detectors used to convert scintillation photons to electronic signals are photomultiplier tubes (PMTs) and photodiodes. A scintillation detector's schematic

diagram is presented in Fig. 2.4.

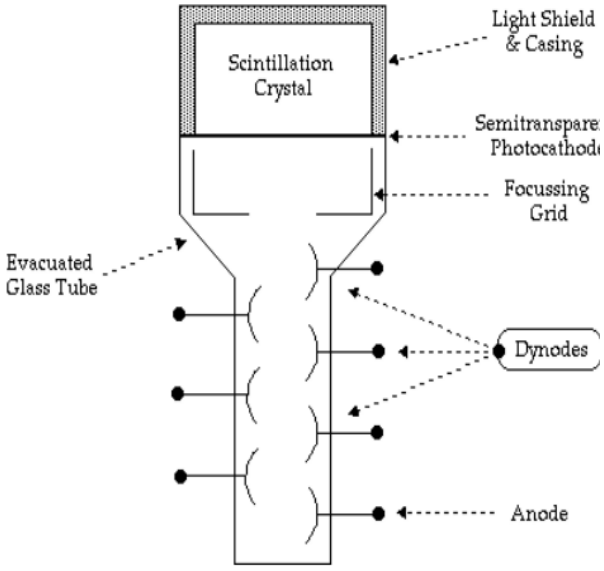

Figure 2.4: A scintillation detector's schematic diagram [21]

Scintillators are typically classified as organic (plastic) or inorganic (crystalline), with distinct scintillation mechanisms. Organic scintillators fluoresce due to molecular transitions, whereas inorganic scintillators scintillate due to electronic transitions within or above the band gap. Organic scintillators have little or no resolution due to their Low-Z content, which prevents complete energy capture, so inorganic scintillators are the best crystal [20]. In 1948, the inorganic scintillator NaI(Tl) was discovered, which revolutionized the field of gamma spectroscopy. Unlike in organic scintillators, gamma photo peaks were easily visible, allowing precise energy determinations. NaI(Tl) is preferred due to its lower cost, larger size, and higher efficiency. Using their crystal lattice structure, inorganic scintillators convert the electron-hole pairs produced by the energy cascade into photons. These luminescence centers are frequently impurities (called activators) deliberately doped into the material, where the crystal band structure is favorably modified to produce a large Stokes shift. In NaI(Tl), the activator is the Tl^{+} ion doped at a concentration of <0.1% [20]. To be a good scintillator, a material should convert as large a fraction as possible of the incident radiation energy into prompt fluorescence, the light yield should be proportional to the deposited energy, the luminescence should be of short duration, the material should be homogeneous and of good optical quality [19].

2.3.2 Semiconductor detectors

Semiconductors, as a class of radiation-detection materials, are commonly used in applications requiring the highest energy resolution because they provide more compact configurations and better energy resolution for gamma-ray spectrometry. Semiconductors, in general, provide far better energy resolution than scintillators, owing to the fact that the information carriers that comprise the signal in semiconductors are electrons and holes directly produced by the energy cascade. For a fixed-energy radiation interaction, essentially all electrons and holes serve as information carriers and yield maximum signal intensity, allowing for improved statistical accuracy and lower energy resolution. The energy required to form an electron-hole pair via the energy cascade is proportional to the band gap, which for semiconductors can be several eV. A larger band gap increases the average energy required to create information carriers, which increases variance. An excessively small band gap, on the other hand, causes thermal excitation and the associated higher conductivity and dark currents that interfere with signal collection. Most band gaps for semiconductors of interest for radiation detectors are in the range of 0.7 to about 3 eV. The final carriers of information are the thermalized electron-hole pairs produced by the cascade. With the application of a strong electric field created by surface electrodes, they are rapidly swept out of the active medium and recorded as an electronic pulse proportional to the number of charge carriers collected and, thus, the energy of the initializing radiation. The disadvantages of semiconductors include higher costs, increased operational complexity, lower efficiency due to small size, and the requirement for high-purity, defect-free crystals to promote complete charge transport over long distances [20]. Silicon and germanium have long been the most widely used semiconductors for radiation detection and thus serve as benchmark materials by which the performance of other semiconductors is judged. Physically they are unique for their relatively high purity and for the fact that they are mono-elemental semiconductors. Silicon has lower performance than germanium due to the former's lower Z value and lower synthesis purity [20]. Because the formation of an electron-hole pair in a semiconductor such as silicon or germanium requires only about 3 eV of energy, these crystals can provide large signals

with very little energy deposition in the medium when used as solid-state ionization chambers. As a result, solid-state devices may be especially advantageous for low-energy applications [10].

Since the 1970s, germanium has been available with sufficient purity (one part in 1012) to enable the construction of relatively large detectors using intrinsic material. This material is known as ”high-purity germanium” (HPGe), and it only needs to be cooled (by liquid nitrogen) when biased. Due to its low band gap of 0.72 eV, HPGe routinely achieves a resolution of 0.2% or less for the benchmark 662 keV gamma ray from ^{137}Cs. This is the best energy resolution achievable by routine materials-based radiation detectors, making HPGe the obvious choice for many high-resolution spectrometry applications. The size of HPGe detectors is commonly measured by comparing the efficiency for full-energy detection of the 1333 keV gamma ray from ^{60}Co with that of a standard 3 in $\times$ 3 in cylindrical NaI(Tl) scintillating detector [20].

To build a semiconductor detector, a connection between n-type (electron donor) and p-type (electron acceptor) semiconductor materials, known as a p-n junction, must be formed. Fig. 2.5 depicts a simplified schematic of a p-n junction with and without external potential.

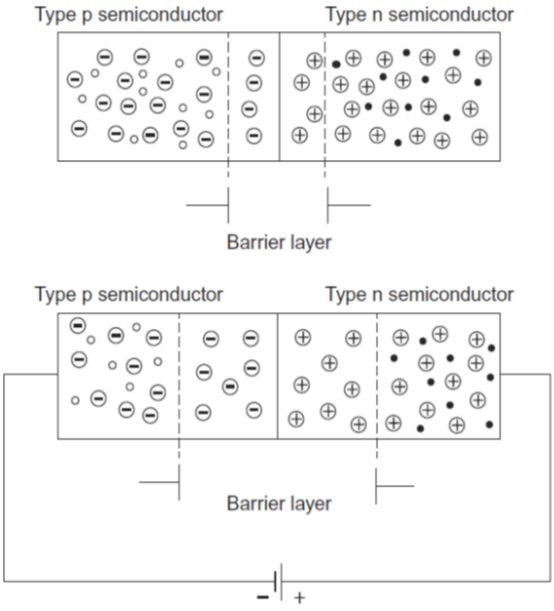

Figure 2.5: P-n junction simplified schematic [9]

Because an n-type semiconductor contains more electrons than a p-type

semiconductor, electron diffusion from n-type to p-type materials is observed after the formation of a p-n junction. This electron diffusion results in positively charged ions in the n-type material and negatively charged ions in the p-type material. This mechanism separates electrical charge, with negative charge concentrated in the p-type semiconductor region and positive charge concentrated in the n-type semiconductor region. An electric field forms between the two types of semiconductors as a result of such charge separation. This field aids in the removal of free charge carriers from the vicinity of the p-n junction. The result is a layer with no free charge carriers, known as a depletion layer (the active volume), which is sensitive to ionizing radiation, particularly X-rays and γ-rays. By applying an external potential across the p-n junction, the size of the depletion layer grows [9].

2.4 Exposure to radiation from natural radionuclides

Natural radiation is the main source of radiation exposure for humans. The total annual dose varies greatly between regions. The distribution of the sources is shown in Fig. 2.6, but the distribution of the sources of exposure varies from area to area and from person to person. It can be seen that more than 80% of the dose is of natural origin, with only about 1% coming from artificial radioactivity [9].

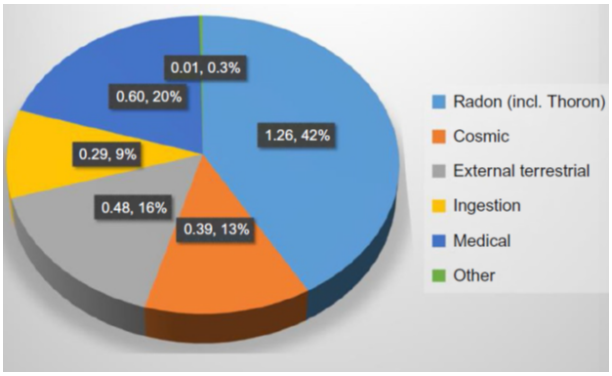

Figure 2.6: Global annual exposure values and exposure source distributions in mSv and percentage of total exposure. Other sources of exposure include fallout from nuclear tests, nuclear accidents, and nuclear power plant releases [9]

.

In nature, there are approximately more than 60 radioactive nuclei. The naturally occurring radioactive nuclei have atomic numbers ranging from Z = 81 to Z = 92 and are distinguished by a significant neutron excess. Nonetheless, the high number of protons in these nuclei causes strong Coulomb repulsion and instability. Such nuclei can decay by emitting one or more α particles in succession. As a result, the resulting daughter nuclei will have an even higher neutron-to-proton ratio and will decay via the emission of β^- particles. The granddaughters could still be unstable and decay by emitting more α particles. This chain of α and β decays will continue until the nucleus reaches the N-Z stability band (Fig. 2.1 and 2.2) [10].

2.4.1 Exposure to external radiation

The dose received from external sources of ionizing radiation originates from cosmic rays and from gamma emitting radionuclides in the earth's crust [12]. Telluric (terrestrial) radiation is primarily caused by the uranium and thorium decay chains, as well as by ^{40}K, which is commonly referred to as NORM. The dose is caused by gamma radiation emitted by soil, rock, and building materials. As a result, the contribution is highly dependent on the concentration of NORM in the ground. Cosmic radiation is primarily composed of high-energy protons (about 90%), which undergo nuclear reactions (spallation reactions) in the upper atmosphere with the atoms and molecules in the air. Different new particles and photons are created in the upper atmosphere, which can reach the Earth's surface and cause the dose. As a result, it is clear that the dose from cosmic radiation is highly dependent on altitude above sea level. The dose, however, is also affected by geographical latitude because the Earth's magnetic field deflects primary cosmic radiation, resulting in higher doses in polar regions [9].

2.4.2 Exposure to internal radiation

Radium-226 and its daughter products are responsible for a major fraction of the dose received by humans from the naturally occurring internal emitters. ^{226}Ra is an alpha emitter that decays, with a half-life of 1622

years, to ^{222}Rn. The decay of radon is followed by the successive disintegration of a number of short-lived alpha and beta-emitting progeny [12]. Internal radiation (without radon) is caused by radionuclides ingested primarily through eating, drinking, and inhaling. Under normal conditions, the uranium and thorium decay chains contribute, but the main sources are potassium, radiocarbon, and, to a lesser extent, tritium. In the human body, the activity of ^{40}K is 4.4 kBq on average, and the activity of ^{14}C is 3.7 kBq. The internal dose from ^{40}K is primarily caused by β decay, because electrons deposit all of their energy within the body, whereas γ-radiation leaves the body almost unattenuated [9].

Radon, a radioactive gas that emanates from rocks and soils and tends to concentrate in enclosed spaces such as inside houses and other buildings, is the source of the majority of internal exposure. Among natural sources of ionizing radiation, radon gas is by far the most significant. It contributes significantly to the ionizing radiation dose received by the general population [22]. According to Fig. 2.6, the primary dose (more than 40%) is caused by radon, which can migrate from the soil or building material to the outdoor or indoor atmosphere and cause internal exposure of the human body. There are three naturally occurring isotopes of radon, that is, ^{222}Rn (radon), ^{220}Rn (thoron), and ^{219}Rn (actinon). The prevalence of the different radon isotopes in the atmosphere is significantly different, due to the difference in half-life. Actinon is not spread in the atmosphere, because it is hardly able to migrate after its formation due to very short lifetime, i.e. $t_{\frac{1}{2}}$ is not exceeding 4 s. The prevalence of thoron ($t_{\frac{1}{2}}$ = 55.6 s) is very small, so it only accounts for 3.3% in the total dose. The contribution of radon ^{222}Rn ($t_{\frac{1}{2}}$ = 3.82 days) to the worldwide annual dose is the highest (38.3%, or 1.15 mSv on average around the globe), therefore radiation protection mainly focuses on radon, unless in specific cases thoron needs to be considered [9].

Radon and its decay products (progeny) are primarily alpha-emitters. The mixture of short-lived radon progeny is a more powerful source of ionizing radiation than radon itself. However, the accumulation of the mixture of the progeny can occur until the radioactive equilibrium with radon is achieved (which can take two to three hours). Irradiation of humans by

radon and its decay products occurs with inhaled air. In contrast to the radon gas, which is inert, the radon progeny, that is radioactive metal isotopes of polonium (Po), lead (Pb), and bismuth (Bi) can be deposited and accumulated in the bronchi and lungs, causing the internal radiation exposure. Thus, the main radiation dose is formed not only by radon but also by its decay products, with radon acting only as a generator and transporter of the potential hazard. In general, the concentration of naturally occurring radionuclides contained in building materials and products during manufacturing, which creates a flow of penetrating ionizing radiation as well as radon exhalation from building products, is an important issue in radiological protection of building occupants [9].

2.5 Health effects of ionizing radiation

Reports of radiation injury began to appear in the literature with astonishing rapidity after the announcement on November 8,1895, of Roentgen's discovery of x-rays. X-ray injuries of 69 cases reported from laboratories and clinics in many countries of the world on the American x-ray Journal, published in 1897. By 1900 the radioactive constituents of radium ore had been sufficiently concentrated that burns were produced on the skins of the Pioneers in radioactivity research. The total number of people who were injured and killed by the use and misuse of x-rays and radium prior to the development proper standards of radiation hygiene will probably never be known, but certainly numbers in the many hundreds. In the 19^{th} centuries, it was suggested that the high incidence of lung cancer among the miners might be explained by their exposure to radioactive substances in the atmosphere of the mine. Studies of the mine air revealed the presence of high concentration of radon [12].

Ionizing radiation causes neutral atoms or molecules to acquire either a positive or negative electrical charge. Alpha, beta, gamma, X, and neutron rays are the most well-known forms of ionizing radiation. Charged-particle radiation, such as alpha or beta rays, has a direct ionizing effect, whereas neutral radiation, such as X, gamma, or neutron rays, has an indirect ionizing effect, which means that these radiations first produce charged particles, which then have the ionizing effect [19].

Ionizing radiation poses well-known health risks to humans. Radon (^{222}Rn) is a noble gas formed from radium (^{226}Ra), which is a byproduct of Uranium decay (^{238}U). According to the findings, the risk of lung cancer increases proportionally with radon exposure. Radon is the second leading cause of lung cancer after smoking. When radon gas is inhaled, densely ionizing alpha particles emitted by radon's deposited short-lived decay products (^{218}Po and ^{214}Po) can interact with biological tissue in the lungs, causing deoxyribonucleic acid (DNA) damage [22].

Radiation particles produce damage on the atomic scale primarily by creating ions and breaking chemical bonds. Ion pairs produced by ionizing radiation eventually produce free radicals, which disrupt cell biochemistry, break chemical bonds, and cause cell damage. Free radicals are highly reactive atoms that scavenge electrons from other atoms or molecules, resulting in a chain reaction that can harm cells and tissues. A direct collision with a radiation particle can also break chemical bonds. Thus, DNA strand, the basic material that controls the structure and function of the cells that make up the human body, or other cellular structures could be damaged directly by a radiation particle or through an interaction with free radicals. Damage, in either case, may result in cell death or mutation. If the cell death count in a specific tissue or organ is high, its function may be disrupted (e.g., skin reddening) or even cease (e.g., necrosis). The short-term function of a tissue or organ, on the other hand, is only relevant for large acute doses. When the cell death count is low, tissue or organ function is unlikely to be an issue; because dead cells cannot reproduce, they cannot mutate, and this leads to cancer. A mutated cell can reproduce and form a carcinogenic mass (tumor), and mutations can occur after either acute or chronic exposure. Radiation exposure causes two types of health effects: deterministic effects and stochastic effects [23].

2.5.1 Deterministic effects

Deterministic effects are also called non-stochastic effect. These effects depend on time of exposure, doses, type of Radiation. It has a threshold of doses below which the effect does not occur, and the threshold may be vary from person to person. All early effect and most tissue late effect is deterministic [24]. Deterministic effects are observable at relatively high

doses (approximately greater than 1 Sv) and include radiation burns, radiation deceased, etc., and as the dose is increased, the severity of the effect increases [9]. Deterministic effect includes acute effect and chronic effect. Acute radiation effect is not dangerous, it occurred when the radiation dose is large, and dose have been delivered in short time. These effect causes just after exposure or within 24 hours to exposure. These are easy to cure and control. Mainly nausea, vomiting, headache, fever, skin and tissue burns are examples of acute radiation sickness. Chronic radiation sickness occurs after a month or year of exposure in high amount. These effects are dangerous and difficult to cure and may lead to death [24].

2.5.2 Stochastic effects

Stochastic radiation effects are typically associated with those that occur over a long period of time, such as months or years (i.e., are typically chronic instead of acute). Chronic doses are typically in the range of background doses (0.003 Sv or less) and are not always associated with higher doses that could result from a terrorist attack using radiological weapons. However, stochastic health effects are defined here as effects that occur many years after chronic or acute radiological contaminant exposure. Cancers and hereditary effects are two types of stochastic effects. Stochastic effects typically take years to manifest (e.g., cancer appearing 20 years after exposure) [23]. Chronic exposure to low doses of ionizing radiation in humans can result in health effects that appear 5-30 years after exposure. The most serious consequence of such exposure is an increase in the likelihood of contracting malignant diseases by both the person who was exposed and his offspring. The risk increases with dose, and the likelihood of damage appearing is greater when exposure begins at a younger age [25]. Stochastic effect includes somatic effect and Genetic effect. Somatic effect is limited to individual expose and individuals suffer during their lifetime. Leukemia, bone cancer, lung cancer are examples of it. Genetic effects are damage on the genetic material in reproductive cell and by the result of which these effects are transmits from generation to generation. Radiation induced material to an individual gene and D.N.A that can contribute to the birth of defective descendants [24].

2.6 Measurements of naturally occurring radionuclides by Gamma-ray Spectrometry

Gamma-ray spectrometry is an analytical technique for identifying and quantifying gamma-emitting isotopes in a variety of matrices. Measurements are required to ensure that building materials meet the requirements of national and international regulations. Gamma-ray spectrometry is an extremely useful tool for measuring natural radioactivity, which typically consists of multiple radioactive nuclide. Potassium-40 and two natural decay series, namely the Uranium and Thorium series, are the most important in terms of potential radiation risk. Gamma-ray spectrometry is commonly used to determine the activity concentration of a radionuclide in environmental samples such as soil, raw materials, and building products. The ability to measure multiple radionuclides simultaneously and the low sample preparation requirements are the main advantages of this method. This method, however, does not allow for the measurement of radionuclides that are pure alpha or beta emitters [9].

Gamma-ray spectrometry is based on a photon (a gamma-ray) in a radiation detector producing a measurable pulse, either electrical or optical. Regardless of the detector type used, the detector output signal must be converted into a current or voltage pulse with a magnitude proportional to the gamma-ray emission energy produced by the radioactive material being measured. A registered pulse's amplitude must be measured, typically using an analog-to-digital converter (ADC), and the measured pulses are then sorted by amplitude into the so-called channels of a multichannel analyzer (MCA). The MCA requires the same number of channels as the ADC resolution; common values include consecutive nonnegative powers of two (512, 1024, 2048, 4096, 8192, or 16,384 channels) [9]. One significant advantage of gamma spectrometry is that there is usually no chemical pretreatment of the samples. Therefore, the gamma spectrometric analytical process is considered non-destructive [26]. The main components of the gamma-ray spectrometry system are shown in Fig. 2.7, which include a HPGe detector, a high voltage power supply, a preamplifier (which is usually sold as part of the detector), an amplifier, an Analogue to Digital Converter (ADC), and a Multi-Channel Analyzer (MCA).

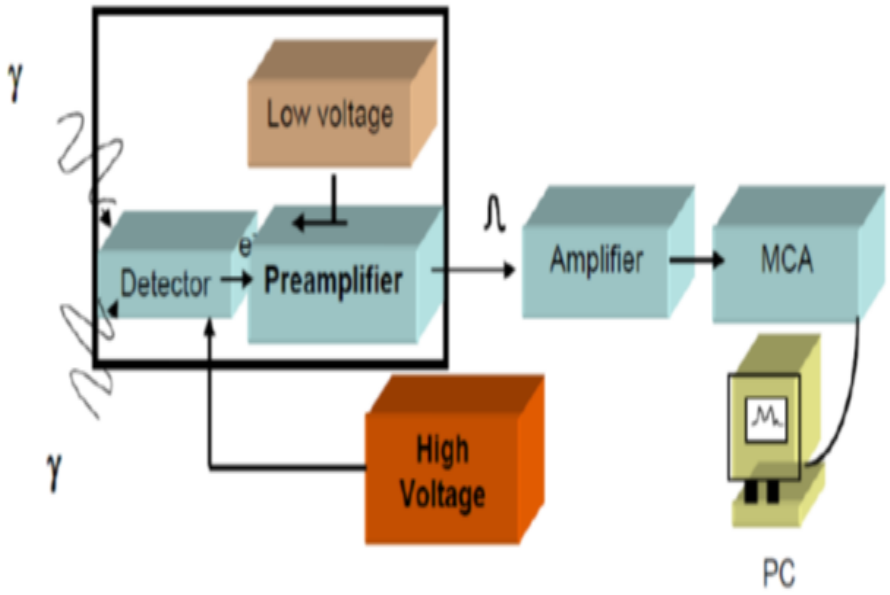

Figure 2.7: Basic components of spectrometry system [27]

.

The electronic system's function is to collect the burst electrons produced by Photon interaction with the detector crystal, and the applied bias voltage sweeps electrons from the crystal; the electron that moves produces a current that forms a signal pulse. A preamplifier increases the pulse size, which is then intensified and shaped by an amplifier. The ADC converts the pulse intensity into numerical values, which are then sent to the MCA. The multichannel analyzer is the heart of most experimental measurements. It performs the essential functions of data collection, visual monitoring, and output, either in the form of final results or data for later analysis [26]. All pulses registered in channels produce a sample spectrum with distinctive peaks (photopeaks) reflecting the energies of gamma rays emitted by radionuclides enclosed in a sample. Fig. 2.8 shows a graphical representation of energy resolution for the HPGe detector at peak energy (Eo) which is at the centroid position of the spectrum.

Each gamma-emitting radionuclide has distinct gamma-ray energy emissions that can be used to both confirm the presence of the radionuclide in a sample and quantify its activity concentration in the sample. Each peak corresponds to the energy of gamma radiation, which reveals the presence of specific radionuclides in the measured sample. The spectrum analysis software available is not always up to the task and sometimes fails to detect radionuclides that are actually present in samples; thus, spectrometer

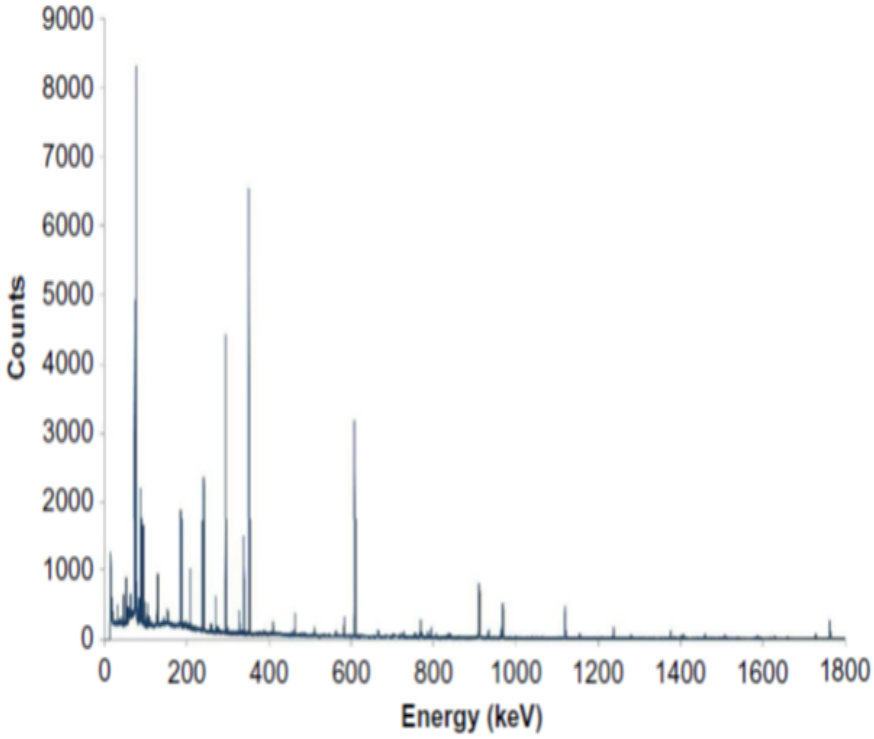

Figure 2.8: A spectrum obtained using high-resolution semiconductor gamma-ray spectrometry [9]

.

calibration is required using a standard sample containing well-known activity concentrations of some radionuclides. Furthermore, results are affected not only by detector types and parameters, but also by electronic components such as amplifier noise, ADC and MCA resolution, and so on. The measurement conditions, most notably sample shape and size (the measurement geometry), self-absorption of gamma rays within the sample, and the radiation background of the gamma-ray, all have an impact on the measurement results [9].

2.6.1 Gamma radiation detection

A gamma ray emitting radionuclide is an excited radionuclide that emits one or more discrete energy gamma rays when it returns to its ground state. Gamma-ray energy is measured in kilo electron volts (keV). One keV is equal to 1.602×10^{-16} J. The deposition of energy in a material is referred to as energy imparted to matter, and it is expressed directly in energy units (J) or absorbed dose, with 1 Gray (Gy) equaling 1 Jkg^{-1} [9]. Because γ-radiation is electromagnetic radiation, photons interact with the material. When gamma rays interact with a detector, they produce a gamma-ray

spectrum. Gamma rays are recorded as a distribution of gamma-ray intensity relative to energy, also known as a gamma-ray spectrum. To analyze a gamma spectrum means to evaluate which radionuclides were present and at what quantity during counting, considering parameters such as sample geometry and counting procedure. The gamma rays interact with the detector by Photo-electric, Compton, and Pair production effects [26].

- If the electron is more strongly bound to a nucleus, the photon's energy causes an electron to be ejected with energy equal to the photon's energy minus its binding energy. This effect is known as the photoelectric effect, and it is what allows us to use Gamma-spectrometry to determine the energy of the γ-radiation and, as a result, the emitting nucleus [9].

- Compton scattering is the scattering of a photon by free or loosely bound electrons. In this case, only a portion of the photon's energy is transferred to the electron, so the resulting electron energy is less than the total of the incident photon's energy [9].

- Finally, when the energy of the γ-radiation exceeds 1.022 MeV (twice the energy equivalent of the electron mass), pair production occurs, and the photon is converted into an electron and a positron (anti-electron). The electron and positron then slowdown in the material, primarily due to ionization. When a positron's kinetic energy is depleted, it annihilates with an electron, producing two 511 keV photons. If these two photons are detected together with the ionization caused by electron and positron slowdown, then the entire energy of the primary γ-radiation is deposited within the detector, resulting in the formation of a single line in the γ-spectrum. This enables detection of the entire γ-energy and its emitting nucleus. If one of the two 511 keV photons escapes the detector, another line 511 keV below the full energy line is formed, which is known as a single escape line. If both 511 keV photons escape the detector, a double escape line at 1022 keV below the full energy line is formed [9].

2.6.2 High Purity Germanium (HPGe) Detector

Germanium semiconductor detectors were first introduced in 1962 and are now the detectors of choice for high energy-resolution γ-ray studies. These detectors directly collect the charges produced by the ionization of the semiconductor material [28]. Germanium detectors are P-I-N semiconductor diodes with an Intrinsic (I) region that is sensitive to ionizing radiation, particularly X-rays and gamma rays. The intrinsic region is determined by the impurity concentration and the applied voltage. An electric field extends across the intrinsic or depleted region when the bias is reversed. When photons interact with the material within a detector's depleted volume, charge carriers (holes and electrons) are produced and swept to the P and N electrodes by the electric field. An integral charge sensitive preamplifier converts this charge, which is proportional to the energy deposited in the detector by the incoming photon, into a voltage pulse. The maximum of each voltage fluctuation represents the total photon gamma energy of that event in kilo electron volts (keV) [26].

High-purity Germanium detectors work in extremely low temperatures to reduce thermally generated electronic noise. These low temperatures are achieved by either cooling with liquid nitrogen (-196 ^{o}C) or, more recently, by electrical cooling, and the need to cool is regarded as a disadvantage of the detector. Because germanium has a low band gap, these detectors must be cooled to keep thermal generation of charge carriers (and thus reverse leakage current) to an acceptable level. Otherwise, the leakage current destroys the detector's energy resolution. A vacuum seal around the detector protects the cooling components from outside temperatures. Lead castles with steel linings reduce the amount of background radiation reaching the detector. Because of their inherent good resolution and linearity, large-volume HPGe detectors have surpassed other detector types for low level gamma ray spectroscopy. The sensitivity of a radiation detector made of HPGe is affected by a number of factors, including detection efficiency, energy resolution, background radiation, sample constituency, sample geometry, and counting time [26].

Detection efficiency

A detector's efficiency (ε) is a measure of how many pulses occur for a given number of gamma rays, i.e., the ratio of the number of events that can be measured in the detector (N) to the total number of photons emitted by the source or sample (N_o).

$$\varepsilon = \frac{N}{N_0} \tag{2.13}$$

The larger the volume of the crystal, the more likely a photon will transfer all of its energy to the germanium detector, and the higher the overall efficiency. The various efficiency definitions commonly used for gamma-ray detectors are as follows:

- Absolute Efficiency is defined as the ratio of counts produced by the detector to gamma rays emitted by the source (in all directions).
- The ratio of the number of pulses produced by the detector to the number of gamma rays striking the detector is known as intrinsic efficiency. It is dependent on the material and sensitive thickness of the detector as well as the source-to-detector distance and the radiation energy.
- Relative efficiency is expressed by comparing the efficiency of two detector. HPGe detectors are almost universally specified in terms of their relative full-energy peak efficiency compared to that of a 3 in. $\times$ 3 in. NaI(Tl).

Energy resolution

Energy resolution is defined as the capability of the detector to distinguish between two photons or particles with close and different energies. It is the identification of the radionuclides giving rise to radiation [29]. The resolution of the HPGe detector is defined as the Full-Width Half Maximum (FWHM) of a single energy peak at a specific energy. The FWHM of a peak in the pulse height spectrum is used to calculate energy spread. The width of the photo peak in relation to the energy of the photo peak is measured by FWHM. The detector's energy resolution describes how useful it is for clearly separating two adjacent energy peaks and thus for unambiguous

nuclide identification. It can be expressed as a percentage or as an absolute value (keV). Using the following equation, the energy resolution (R) of a detector system is calculated from the FWHM of a single peak energy (E_o) [30].

$$R = \frac{FWHM}{E_o} \times 100\% \tag{2.14}$$

Fig. 2.9 shows a graphical representation of energy resolution for the HPGe detector at peak energy (E_o) which is at the centroid position of the spectrum.

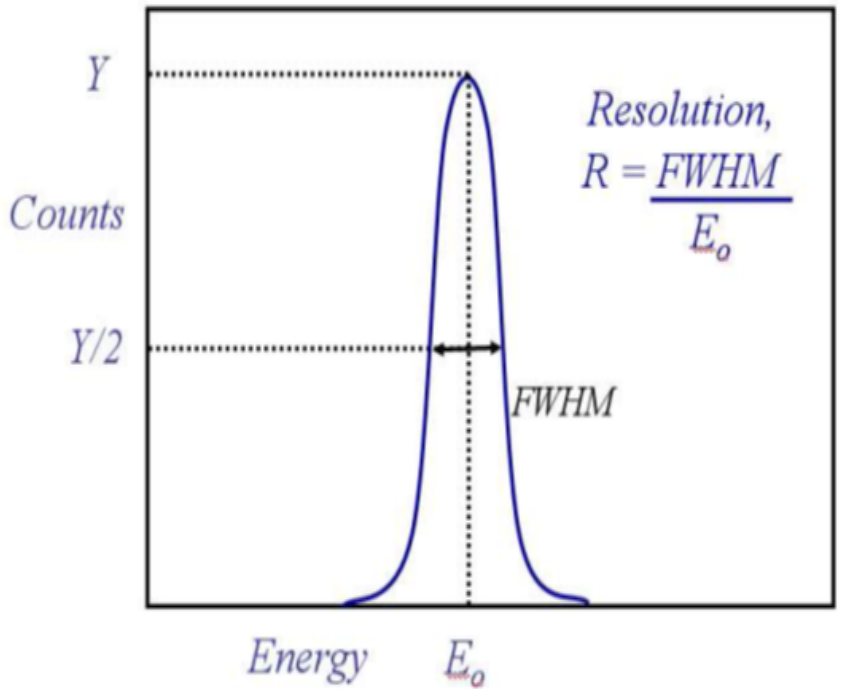

Figure 2.9: HPGe detector energy resolution [27]

.

$$FWHM = \frac{E_B - E_A}{E_o} \times 100\% \tag{2.15}$$

Where E_A is the energy (channel number) at $\frac{Y}{2}$ to the left of E_o, E_B is the energy (channel number) at $\frac{Y}{2}$ to the right of E_o and Y is the maximum height of the spectrum.

Better resolution (lower FWHM value) allows the system to more clearly separate the peaks within a spectrum. In comparison to the NaI (Tl) detector, the HPGe detector has higher resolution and is a better instrument for nuclide identification [26].

Background radiation

Background radiation in gamma spectra can come from either within the sample being counted (Compton produced) or from the environment. The environmental background becomes more significant for extremely weak samples.

Sample constituency

The Compton-produced background will easily outweigh the environmental background if the sample being analyzed contains a high concentration of high-energy gamma-emitting radioisotopes. To separate the unevenly crushed soil particles and reduce radiation self-absorption, samples must be crushed and homogenized by passing them through a 0.425 mm mesh sieve.

Sample geometry

The sample geometry is an often overlooked aspect of HPGe detector sensitivity. For a given sample size (which should be as large as possible for maximum sensitivity), the sample should be distributed in such a way that the distance between the sample volume and the detector itself is minimized.

Counting time

The charge collection time is the limiting factor for the detector, and this parameter is a function of the detector geometry. When photons interact, charge carriers in the form of holes and electrons are created, and the time it takes for these carriers to be swept to the detector's p and n electrodes is the time for full energy collection.

2.7 Previous studies on NORMs dealing with environmental samples

Many previous studies have focused on environmental samples such as soil, construction raw materials, and construction products used around the world because they contain naturally occurring radionuclides. The presence of radionuclides exposes people who live in houses and workers in factories that manufacture building materials to both external and internal exposure. Previous studies are presented here for comparison with this study:

Ahmed H. K. and colleagues (2014) investigated natural radioactivity levels and radiation hazards in Egyptian gypsum materials. Gamma-ray spectrometry was used to determine the activity concentrations, which revealed that the mean values are 499.29 ± 11.53 Bqkg^{-1} for ^{40}K, 91.97 ± 2.61 Bqkg^{-1} for ^{226}Ra, 37.62 ± 1.67 Bqkg^{-1} for ^{238}U and 42.27 ± 2.22 Bqkg^{-1} for ^{232}Th. The activity indexed I_γ for 18, different gypsum samples varied from 0.31 ± 0.03 to 2.3 ± 0.19 and the radium equivalent activity (Raeq), from 38.81 ± 1.68 to 324.7 ± 9.42. These values are lower than the limit of 370 Bqkg^{-1} [31].

Gbadebo A. I. et al., [2021] investigated radionuclide activity concentrations in asbestos and gypsum building materials, as well as their radiological implications in Nigeria. Natural radionuclides ^{238}U, ^{232}Th, and ^{40}K were found in the building materials tested, with activity concentrations ranging from 141.76 to 526.29 Bqkg^{-1}, 2.14 to 7.94 Bqkg^{-1} and 9.89 to 14.23 Bqkg^{-1} for the gypsum samples, respectively. The average concentration obtained for samples is lower than the global average. The estimated radiation hazard indices are also lower than the internationally recommended values [32].

Shala F. et al., [2017] Natural radioactivity in cement and raw materials used in the Albanian cement industry was investigated. The activity concentrations of the natural radionuclides such as ^{226}Ra, ^{232}Th, and ^{40}K range from 9.7 to 14.3 Bqkg^{-1} with mean value 11.8 ± 2.0 Bqkg^{-1}, 3.3 to 7.0 Bqkg^{-1} with mean value 5.8 ± 1.9 Bqkg^{-1}, and 53.7 to 79.8 Bqkg^{-1} with mean value

66.8 ± 11.3 Bqkg^{-1} in gypsum samples, respectively, from 26.4 to 45.6 Bqkg^{-1} with mean value 38.0 ± 8.5 Bqkg^{-1}, 2.3 to 5.0 Bqkg^{-1} with mean value 3.3 ± 1.4 Bqkg^{-1}, and 2.6 to 13.5 Bqkg^{-1} with mean value 6.5 ± 5.2 Bqkg^{-1} in limestone samples, respectively, from 53.1 to 57.3 Bqkg^{-1} with mean value 55.5 ± 2.5 Bqkg^{-1}, 13.7 to 20.0 Bqkg^{-1} with mean value 17.0 ± 2.8 Bqkg^{-1}, and 140.0 to 196.4 Bqkg^{-1} with mean value 160.3 ± 26.4 Bqkg^{-1} in clinker samples, respectively [33].

Turhan S., [2010] Radioactivity levels of limestone and gypsum used as building materials in Turkey were investigated, as well as exposure dose estimation. The measured activity concentrations of the natural radionuclides ^{226}Ra, ^{232}Th, and ^{40}K range from 0.8 to 36.8 Bqkg^{-1} with mean value 7.2 Bqkg^{-1}, 1.3 to 18.2 Bqkg^{-1}, with mean value 3.4 Bqkg^{-1}, and 9.0 to 188.0 Bqkg^{-1} with mean value 40.7 Bqkg^{-1} in raw gypsum samples, respectively, at the same time range from 0.7 to 55.1 Bqkg^{-1} with mean value 19 Bqkg^{-1}, 1.2 to 20.9 Bqkg^{-1}, with mean value 4.3 Bqkg^{-1}, and 10.1 to 258.4 Bqkg^{-1} with mean value 55 Bqkg^{-1} in raw limestone samples, respectively. He demonstrated that the examined gypsum and limestone raw materials pose no excess radiological health risk and are safe for use in building construction [34].

Alzubaidi G. et al. (2016) determined the activity concentrations and radiological parameters of naturally occurring radionuclides ^{226}Ra, ^{232}Th, and ^{40}K in agricultural and virgin soil samples collected at random in Kedah, Malaysia's northwestern state. The mean values of radium equivalent activity, absorbed dose rates, annual effective dose equivalent, and external hazard index in agricultural soils are 458.785 Bqkg^{-1}, 141.62 nGyh^{-1}, 0.169 mSvy^{-1}, and 0.859, respectively, and 214.293 Bqkg^{-1}, 87.47 nGyh^{-1}, 0.106 mSvy^{-1}, and 0.525 in virgin soils, respectively [35].

Thabayneh K. M. and Jazzar M. M. (2012) used gamma spectroscopy to measure the activity concentrations of natural radionuclides ^{226}Ra, ^{232}Th, and ^{40}K in 72 surface soil samples from Tulkarem district in West Back-Palestine (HPGe detector). ^{238}U concentration ranged from 9.7 to 83.5 Bqkg^{-1} with a mean value of 34.5 Bqkg^{-1}, ^{232}Th concentration ranged from 3 to 44.8 Bqkg^{-1} with a mean value of 23.8 Bqkg^{-1}, and ^{40}K concentration ranged from 10.2 to 404 Bqkg^{-1} with a mean value of 120 Bqkg^{-1} [36].

Abiama P. E. et al., (2010) measured the concentration of ^{226}Ra, ^{232}Th, and ^{40}K in soil samples from Awanda, Bikoué, Ngombas in the southwestern region of Cameroon. By using (HPGe) p-type detector coupled to a multi-channel analyzer. The mean concentrations of ^{226}Ra, ^{232}Th, and ^{40}K were 130 ± 10 Bqkg^{-1}, 390 ± 30 Bqkg^{-1} and 850 ± 70 Bqkg^{-1}, respectively [37].

Geremew H. and A. K. Chaubey (2019) investigated the natural radioactivity levels and potential radiation hazards in Floriculture soil in Holeta, Shoa, Ethiopia. The average radioactivity concentrations values of ^{226}Ra, ^{232}Th, and ^{40}K in floriculture soil were found to be 142.29 ± 27.67, 7.82 ± 0.54, and 259.62 ± 44.98 BqKg^{-1} respectively, and in agricultural farmland were also found to be 133.85 ± 20.49, below detection level, and 287.82 ± 35.68 Bqkg^{-1} respectively, and in virgin land 30.51 ± 5.32, 14.52 ± 1.69, 100.29 ± 19.81 Bqkg^{-1} [38].

Issa S. A. M. (2013) investigated the radiological assessment of natural radioactivity levels of agricultural soil samples collected in Dakawia, Egypt. The activity concentrations of ^{226}Ra, ^{232}Th, and ^{40}K in the soil ranged from 5.7 ± 0.3 to 140 ± 7, from 9.0 ± 0.4 to 139 ± 7 and from 22 ± 1 to 319 ± 16 Bqkg^{-1}, respectively. The absorbed dose rate, annual effective dose rate, radium equivalent (Req), excess lifetime cancer risk, hazard indices (Hex and Hin) and annual gonadal dose equivalent were calculated as a result of natural radionuclides concentrations in the soil [39].

Mohebian M., and Pourimani R., (2020) investigated the radiometric properties of virgin and agricultural soil in the vicinity of Iran's Shazand Refinery Complex. The average activity concentrations of ^{226}Ra, ^{232}Th, and ^{40}K and ^{137}Cs in the cultivated (virgin) soil samples were 21.95 ± 0.27 (23.99 ± 0.37), 25.37 ± 0.29 (31.74 ± 0.38), 416.72 ± 1.88 (461.09 ± 2.68) and 5.13 ± 0.08 (5.51 ± 0.14) in Bqkg^{-1}. The excess lifetime cancer risk (ELCR) was obtained for cultivated (virgin) soil as 0.19×10^{-3} (0.22×10^{-3}), which is close to the world average (0.29×10^{-3}) [40].

Nisar A. et al. (2015) investigated natural radioactivity in virgin and agricultural soil in Sungai Petani, Kedah, Malaysia, and its environmental implications. In virgin soils, the mean activity concentrations of ^{226}Ra, ^{232}Th,

and ^{40}K were 51.06 ± 5.83, 78.44 ± 6.42, and 125.66 ± 7.26 Bqkg^{-1}, respectively, while in agricultural soils, they were 80.63 ± 5.78, 116.87 ± 7.87, and 200.66 ± 18.24 Bqkg^{-1}, respectively. They conclude that the corresponding activity concentrations in agricultural soils were higher than those in virgin soils and those reported for other countries of the world. The average values of radium equivalent activity (Raeq), external hazard index (Hex), internal hazard index (Hin), outdoor annual effective doses (Eout), and indoor annual effective doses (Ein) in agricultural soils were 258.38 Bakg^{-1}, 0.708, 0.925, 0.162 mSvy^{-1}, and 0.669 mSvy^{-1}, respectively [41].

Saleh M. A. et al. (2013) studied natural radiation levels and associated dose rates in surface soils in the Pontian district of Johor, Malaysia. They use a high purity germanium (HPGe) detector to measure the activity concentrations of ^{226}Ra, ^{232}Th, and ^{40}K in soil samples. The soil samples' gamma spectrometry results show a range of 2 ± 1 to 113 ± 9 Bqkg^{-1} for ^{232}Th, 3 ± 1 to 68 ± 6 Bqkg^{-1} for ^{226}Ra, and 26 ± 3 to 683 ± 29 Bqkg^{-1} for ^{40}K. The radium equivalent activity (Raeq) and external hazard index (Hex) were 136 Bqkg^{-1} and 0.366, respectively, which were within the recommended levels for the population [42].

The naturally occurring radioactive materials in some Malaysian sand used in building construction were investigated by Ismail A.F. et al. (2009). ^{226}Ra, ^{232}Th, and ^{40}K concentrations were found to be in the ranges of 6.45 to 107.9 Bqkg^{-1}, 7.78 to 96.67 Bqkg^{-1}, and 31.05 to 1105.53 Bqkg^{-1}, respectively. The mean range of gamma level indices was found to be 0.189 to 2.366 mSvy^{-1}, whereas the mean range of annual equivalent dose to dwellers was 0.059 to 0.738 mSvy^{-1}. They conclude that the gamma level index and annual equivalent dose obtained from all studied samples are lower than the recommended limit, despite the presence of high levels of natural radioactivity in some samples [43].

Abel-Ghany H.A. et al. (2009), used high-resolution gamma-ray spectroscopic system to measure the radionuclides content and to calculate some related parameters in three sand samples collected by a local company working in glass industry in Egypt. The concentrations of the radionuclides ^{226}Ra, ^{232}Th, and ^{40}K were calculated using characteristics spectral peaks. ^{238}U activity concentrations were 91.51 ± 4.94, 111.47 ± 6.01 and

81.83 ± 4.41; ^{232}Th activity concentrations were 73.37 ± 3.96, 91.30 ± 4.92, 75.98 ± 4.10; ^{40}K activity concentrations were 572.24 ± 30.89, 723.00 ± 39.03 and 807.13 ± 43.57(Bqkg^{-1}). The calculated Radium-equivalent activities were (Raeq) 240.48 ± 2.98, 297.69 ± 16.07 and 252.62 ± 13.63 Bqkg^{-1}, which were less than the permitted value (370Bqkg^{-1}). In addition, the hazard index (Hin) for the 3 samples were 0.89 ± 0.04, 1.10 ± 0.05 and 0.90 ± 0.04. In air the total absorbed dose rates were 111.69 ± 6.03, 138.32 ± 7.47 and 118.63 ± 6.41(nGyh^{-1}), while the external annual effective dose rates were 0.136 ± 0.007, 0.169 ± 0.009 and 0.145 ± 0.007 (mSvy^{-1}) [44].

Turhan S., [2007] investigated the natural radioactivity and radiological hazards in Turkish cement and its raw materials. He measured activity concentrations of natural radionuclides such as ^{226}Ra, ^{232}Th, and ^{40}K ranging from 2.6 to 48.2 Bqkg^{-1} with mean value 16.5 Bqkg^{-1}, 0.8 to 27.2 Bqkg^{-1}, with mean value 7.7 Bqkg^{-1}, and 4.0 to 354.9 Bqkg^{-1} with mean value 88.1 Bqkg^{-1} in limestone samples, respectively, at the same time range from 8.6 to 90.9 Bqkg^{-1} with mean value 26.7 Bqkg^{-1}, 5.4 to 113.4 Bqkg^{-1}, with mean value 41.8 Bqkg^{-1}, and 316.5 to 1103.6 Bqkg^{-1} with mean value 629.3 Bqkg^{-1} in clay samples, respectively. The calculated radium equivalent activity mean value and the gamma index mean value of these two samples are lower than the world limit set for building materials [45].

Saadi E. et al. (2020) investigated the distribution of natural and anthropogenic radioactivity in various building materials used in Algerian dwellings. They tested 31 samples of various materials (sand, brick, ceramic, cement, clinker, flour, and gypsum) used in Algerian homes with a high-resolution HPGe semiconductor detector. ^{226}Ra, ^{232}Th, and ^{40}K activity concentrations were found to be 16.05 ± 0.53 Bqkg^{-1}, 17.44 ± 0.97 Bqkg^{-1} and 260.31 ± 6.81 Bqkg^{-1}, respectively. These findings were consistent with the global average [46].

Kolo M. T. et al. (2016) used the gamma spectrometric technique to investigate the quantification and radiological risk estimation due to the presence of natural radionuclides in Maiganga coal, Nigeria. The mean activity concentrations of ^{226}Ra, ^{232}Th, and ^{40}K were calculated and found to be 8.18 ± 0.3, 6.97 ± 0.3, and 27.38 ± 0.8 Bqkg^{-1}, respectively. The average estimated radium equivalent activity was 20.26 Bqkg^{-1}, with an external

hazard index of 0.05. Mean values for the internal hazard index and representative gamma index were 0.08 and 0.14, respectively. These values were lower than the precautionary limits established by UNSCEAR [47].

Aslam M. et al., (2012) studied the radiological hazards of naturally occurring radioactive materials in cement industry. The mean values of the total specific activity of ^{226}Ra, ^{232}Th, and ^{40}K are 34.2 ± 11.9, 29.1 ± 3.6 and 295.1 ± 66.9 Bqkg^{-1}, respectively in Portland cement, 28.4 ± 8.7, 11.3 ± 1.7 and 63.1 ± 17.3 Bqkg^{-1}, respectively in lime stone, 8.2 ± 1.9, 16.2 ± 3.9 and 187.7 ± 53.2 Bqkg^{-1}, respectively in gypsum, 34.7 ± 13.1, 41.2 ± 6.7 and 187.6 ± 17.2 Bqkg^{-1}, respectively in clay, 41.1 ± 11.8, 39.3 ± 6.9 and 195.1 ± 29.2 Bqkg^{-1}, respectively in latrite and 51.1 ± 18.2, $23.2pm1.2$ and 258.4 ± 15.3 Bqkg^{-1}, respectively in clinker. Radium equivalent activities, external hazard index, internal hazard index, absorbed dose rate in air, and annual effective dose rate were all determined and found to be less than the global limit [48].

Using a gamma-ray spectrometer system, Akkurt I. et al. (2009) investigated the natural radioactivity of coals and its risk assessment. The activity of radionuclides ^{226}Ra, ^{232}Th, and ^{40}K in coals ranged from 35.95 to 110.37, 15.63 to 22.56, and 135.59 to 321.90 Bqkg^{-1}, respectively. They calculated the radium equivalent (Raeq), external hazard index (Hex), absorbed dose (D), and effective dose rate (EDR) to estimate the health effect caused by the activity of those radionuclides [49].

Khan K., Khan H. M. (2001) studied natural gamma-emiting radionuclides in Pakistani Portland cement using a high-purity germanium (HPGe) detector. The range of the total specific activity (minimum and maximum values) due to all the three radionuclides (^{40}K, ^{226}Ra and ^{232}Th) were found to be 187.8 ± 63.5 to 573.2 ± 73.1 Bqkg^{-1} (Portland cement); 54.5 ± 16.1 to 183.9 ± 31.4 Bqkg^{-1} (limestone); 87.1 ± 30.7 to 297.1 ± 64.4 Bqkg^{-1} (gypsum); 696.4 ± 79.1 to 1043.9 ± 85.0 Bqkg^{-1} (slate); and 490.9 ± 54.5 to 570.2 ± 59.8 Bqkg^{-1} (laterite) [50].

Chapter 3
Materials and Methods of the Study

3.1 Description of the research area

The study area is located in the Amhara region's East Gojjam zone, one of eleven zones. It is bounded on the south by the Oromia Region, on the west by West Gojjam, on the north by South Gondar, and on the east by South Wollo; the northern, eastern, and southern boundaries are defined by the bend of the Abay River. The samples for this study were collected from Dejen district, which is one of eighteen districts in East Gojjam Zone, Amhara region, Ethiopia, and is located in the Zone's eastern part. Dejen district shown in Fig. 3.1 is bounded on the south by the Abay River, which separates it from Oromia Region, on the west by Awabel, on the northwest by Debay Telatgen, on the north by Enemay, and on the east by Shebel Berenta district.

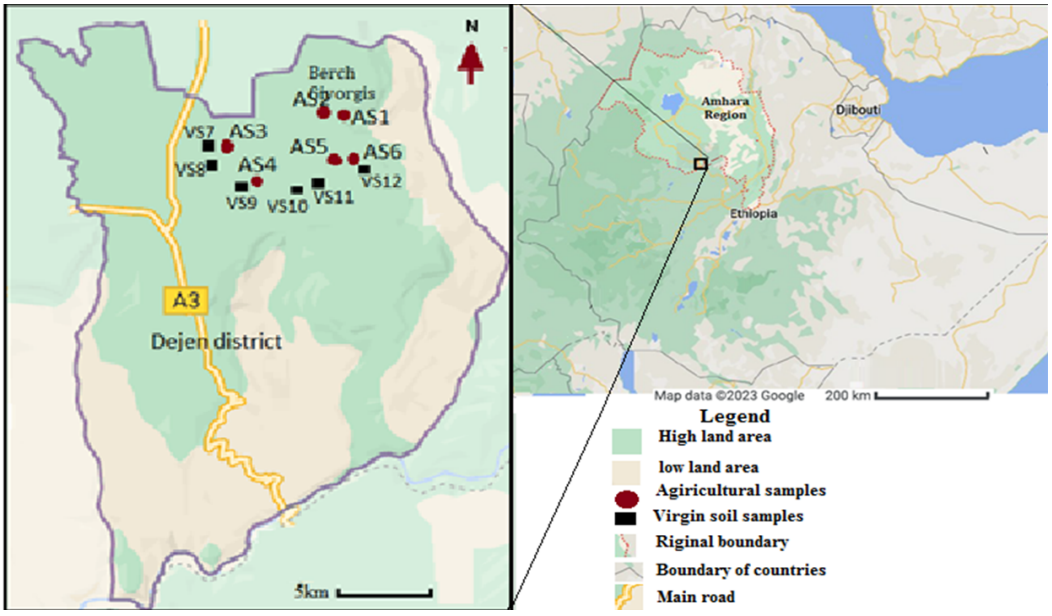

Figure 3.1: Map of Dejen district in east Gojjam, Ethiopia- study area (taken from Google map)

According to Ethiopian population statistics as of 5 August 2012, the district territory (area) spans 620.97 km^2 and has a population of 111, 544 people. The rural villages of the district's societies are based solely on agricultural activities. Local farmers have primarily grown teff with fertilizer, as well as cereal crops with or without fertilizer on occasion. Dejen, the town of the Dejen district, is located on the rim of the Abay Canyon, 230 kilometers north of Addis Ababa, Ethiopia's capital city. It is located at $10^0 10'$ N and $38^0 8'$ E, with an elevation of 2421 to 2490 meters above sea level. The majority of the villages in the Dejen district are located in or near the Abay gorge. The Dejen district, particularly the Abay gorge, provides the majority of raw materials used in construction to produce gypsum powder and cement. As a result, there are six gypsum powder factories and two cement factories in Dejen town.

3.2 Sample collection and preparation

The goal of environmental sampling and analysis is to collect data that describes a specific site at a specific point in time so that an evaluation can be made as a basis for potential action. The collection of valid samples is the critical first step in this process. Sampling should be done with the same care as analysis, and both should be done with the appropriate rigor for the project. To be meaningful, data must be collected with a clear purpose and an understanding of the problem to be solved as well as the physical conditions that exist.

The majority of gypsum products used in Gojjam, Amhara Region, Ethiopia were obtained by digging out an area of ground where the gypsum raw materials are found in Abay gorge in the Dejen district. In this study, five factories in Dejen town, four of which were privately owned and one of which was owned by a regional state company, produced raw gypsum and final gypsum powders. Sand, limestone, clay, gypsum, pumice, and coal are the raw materials used in the majority of Ethiopian cement factories. Except for the coal sample, which is brought from Sudan, all of the raw building materials found in the study area, Dejen district, are collected from Abay gorge and other sites in the district. All village dwellers in the study area (Dejen district) engage in agricultural activities and produce

Teff and other cereals using artificial fertilizers. This study chose one of the villages (Berch Giyorgis) with a high population density, and soil samples were collected from agricultural and virgin land.

3.2.1 Collection of samples

In this study, natural radionuclides were measured in 34 samples, with an average of 10 raw gypsum samples, 12 raw materials used in cement production samples, and 12 soil samples. A total of twenty-two samples were collected from the land store, ten raw gypsum samples from each factory store as shown in Fig. 3.2 in Lalibela gypsum factory store, and twelve raw material samples for cement production from cement factory stores in pairs: two for each sample of sand, limestone, clay, gypsum, pumice, and coal. Twelve soil samples, each weighing about one kilogram, were chosen at random from twelve different sampling points, six of which were agricultural land and six of which were virgin land. The first and second sampling points, then the second and third, and so on, were approximately half a kilometer apart, with depths ranging from 15 to 30 cm. All samples were collected over the course of one month, from March 1 to March 30, 2021. To avoid contamination of the samples during transportation from the study area to Addis Ababa University, where sample preparation takes place, the samples are placed in a polythene bag with labels and sealed.

Figure 3.2: Raw gypsum in Lalibela gypsum factory store

3.2.2 Preparation of samples

Sample preparation is recognized as a major source of errors that, if not done correctly, can have an impact on the final results. As a result, each sample was carefully examined to avoid cross-contamination with themselves and the environment. Following collection, all samples used in this study were spread out on plastic sheets and air-dried at room temperature for three days, as shown in Fig. 3.3 for gypsum powder and Fig. 3.4 for soil sample after being crushed into small pieces and fine powder with a hand mill.

Figure 3.3: Gypsum powder samples during air drying at room temperature

To obtain a homogeneous sample, the fine powder was converted to grain size by passing it through 0.425 mm sieves (mesh). The raw gypsum samples were also dried for 19 hours in a 100 ^{0}C oven to ensure that all humidity was removed. Similarly, agricultural soil samples were dried in an oven for 17 hours at 100 ^{0}C and virgin soil samples for 6 hours at 150 ^{0}C. The raw material samples used in cement production were also oven dried for 16 hours at 100 ^{0}C. This was done on purpose because it is used to ensure that all humidity is removed.

The prepared samples were sealed in polyethylene bags until the Marinelli cups were adjusted by Ethiopian Radiation Protection Authority (ERPA) laboratory as presented in Fig. 3.5.

Figure 3.4: Crushed soil samples during air drying at room temperature

Figure 3.5: Prepared samples sealed in polyethylene bags

The Marinelli cups had previously been cleaned, washed with purified water, and dehydrated to avoid contamination. The 500 g samples were packed and securely fastened to prevent radon-222 from escaping from the cylindrical Marinelli cups that correspond to the geometry of the detector to be used for gamma spectrometric analysis at the Ethiopian Radiation Protection Authority (ERPA) laboratory. Before measurements, the closed Marinelli cups were kept for at least thirty days, which was enough time to achieve a state of secular radioactive equilibrium for uranium-238 and

thorium-232 with their decay daughters [51, 52]. Finally all of the samples were placed and sealed in Marinelli cups until measurement takes place in the laboratory as shown in Fig. 3.6.

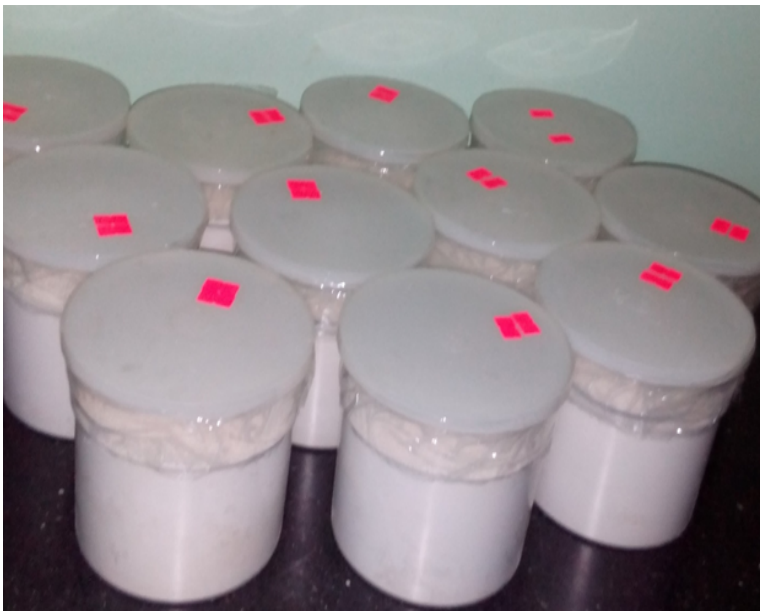

Figure 3.6: Prepared samples sealed in Marinelli cups in ERPA laboratory

3.3 Operational Property of HPGe Detector

High purity germanium detectors are also known as 'intrinsic' germanium detectors. Unlike NaI detectors, semiconductor materials such as HPGe detectors directly convert photons into charge carriers [53]. The P-type coaxial HPGe detectors used in this study have a useful response range for γ-ray energies ranging from 10 keV to 2 MeV. They also have high spectral quality, excellent peak symmetry, and low noise operation [52]. HPGe detectors use liquid nitrogen to operate at low temperatures and with a reverse bias voltage of up to 4000 V. These conditions must be met in order to achieve the best detection efficiency and energy resolution. HPGe detectors for gamma-ray detection must be cooled to temperatures below 120 K, which can be accomplished with liquid nitrogen. Liquid nitrogen as a coolant for HPGe detectors reduces electrical noise caused by the thermal excitation of electrons across the energy gap in the crystals, preserving the excellent energy resolution of HPGe detectors [54]. A large reverse bias voltage applied to a detector has two effects: it changes the drift velocity of the charge carriers and it increases the size of the depletion region

in the crystal [52, 53]. By increasing the bias voltage, the drift velocity increases until it reaches saturation. In a HPGe detector, the saturated velocity of the charge carriers is fast (10^7 cm/sec), which reduces the time required to collect the charge carriers [52]. The size of the depletion region is affected by the second effect of applying a high-bias voltage to the detector. It increases as the magnitude of the electric field increases; the efficiency of the charge collection and the dimensions of the depletion region leads to an increase in the sensitive volume of the detector [53]. A HPGe crystal has a net impurity level of around 1:1010 atoms/cc. With moderate reverse bias (typically a few thousand volts), the entire volume of the detector crystal between the electrodes becomes depleted and an electric field extends across this active region [55].

3.3.1 Calibration of HPGe Detector

Calibration of the HPGe detector is required to convert measurement results (e.g., counts/s) into activity or activity concentration. In most cases, a linear relationship exists between the measurement result and the activity (concentration). The proportionality factor is called efficiency which depends on the geometry of the measurement and the sample properties such as density and composition. Typically, the efficiency of the photopeak as a function of energy (efficiency curve) is determined for a specific geometry and sample properties for semiconductor detectors. Calibration of semiconductor spectrometry can be accomplished through the use of a known activity reference source or through a calculation based on detector characteristics as well as the anticipated measurement geometry and sample properties [9]. A gamma spectrometry system must be calibrated in terms of both energy and efficiency in order to produce meaningful results such as isotope identification, qualitative and quantitative analysis. Calibration is typically performed with known activity standard sources and reference material. In this study, the energy and efficiency calibration of a HPGe detector was carried out using full energy peaks from three standard sources of ^{241}Am, ^{137}Cs, and ^{60}Co.

Energy calibration

The performance of the HPGe detector used was characterized by the energy calibration and its absolute full energy peak detection efficiency. The

goal of energy calibration is to establish a relationship between a spectral peak position and the corresponding gamma-ray energy. The germanium detector system's energy calibration was performed by comparing standard sources of known radionuclides with well-defined energies to the energy of interest. An essential requirement for the measurement of the gamma emitter is the exact identify of photopeaks present in a spectrum produced by the detector system. The gamma-ray energies measured are only used to identify the nuclide in the spectra. Fig. 3.7 depicts the energy calibration curve between energy and channel numbers (counts per second) for a 77% efficiency HPGe detector using a standard sources containing well-known activity concentrations of some radionuclides.

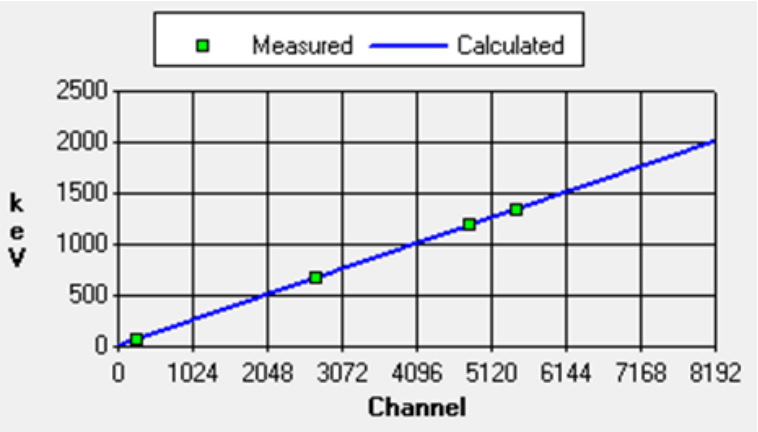

Figure 3.7: Energy calibration curve of HPGe detector using ^{60}Co standard source in this study

Efficiency calibration

A known activity standard source is used to calibrate the efficiency of a HPGe detector. To calculate the efficiency of calibration sample counting geometry, calibration method, calibration sources, and analytical efficiency expression should all be taken into account. To quantify the present radionuclide in a sample, the system's efficiency must be precise. This calibration must be performed over a large area because the accuracy of all quantity results is dependent on it. In order to determine efficiency calibration, all system settings and adjustments must be repeated many times. A slight change in the settings of the system components may give a direct effect on the efficiency measurement. Fig. 3.8 depicts the efficiency calibration curve between efficiency and energy for a (HPGe) detector using a standard sources containing well-known activity concentrations of some

radionuclides.

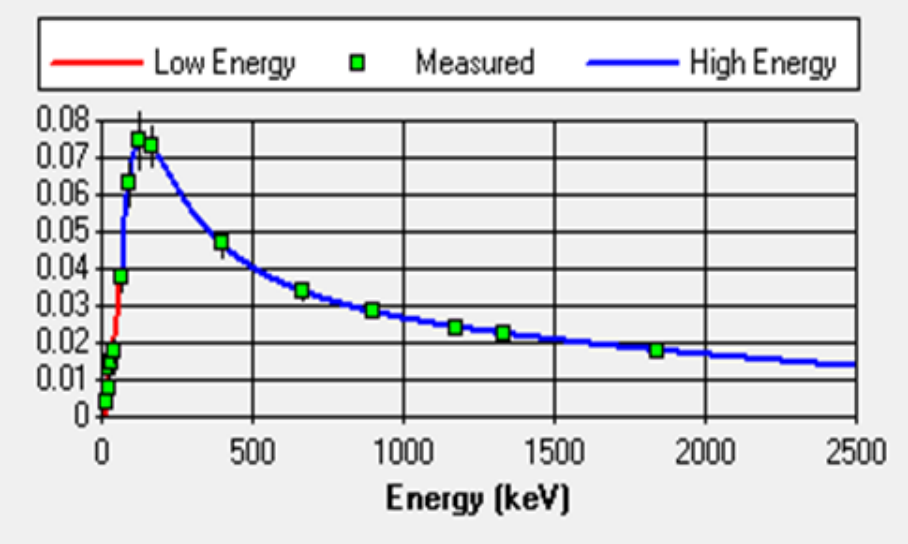

Figure 3.8: Efficiency calibration curve of HPGe detector using standard source in this study

Following standardization, the full energy peak absolute efficiency (ε) of the detector was calculated using the same experimental setup as in Eq. 3.1:

$$\varepsilon = \frac{N_{net}}{A_c \times P_\gamma \times m \times t} \tag{3.1}$$

Where N_{net} is the net peak area, A_c is the workout activity concentration for a certified radionuclide, P_γ is the absolute gamma-ray release probability, m (kg) is the mass of the sample, and t is the counting time.

3.3.2 Experimental setup of HPGe Detector

The measurements of activity concentration of ^{238}U (^{226}Ra), ^{232}Th, and ^{40}K in raw gypsum, soil samples, and raw materials for cement production samples were then carried out by means of a p-type high-purity germanium (HPGe) coaxial detector at the Ethiopian Radiation Protection Authority (ERPA) laboratory. The detector has a relative efficiency of 77% and an 8192-channel multichannel analyzer for data acquisition with an energy resolution of 1.8 keV Full Width at Half Maximum (FWHM) for the 1.332 MeV gamma-ray line of a standard source. The experimental setup of a HPGe detector in the Ethiopian Radiation Protection Authority laboratory is depicted in Fig. 3.9.

Figure 3.9: Experimental setup of a HPGe detector at ERPA laboratory

The gamma rays produced by out-of-the-examine samples were investigated using the Genie-2000 software. The detector is surrounded by lead of 10 mm thickness, which is used to reduce soft cosmic ray components to extremely small amounts, cadmium of 2 mm thickness, which is used to suck up thermal neutrons generated by a cosmic ray interaction, and copper of 2.5 mm thickness, which is used to overpower the X-ray produced by the lead by its interaction with external radiation. The dispersed radiation from the protecting substances is managed by placing the detector in the middle of the protecting substances.

Sample analysis

The samples were placed directly over the front face of the detector for measurement. The acquisition time for all samples studied ranges from 25,200 to 57,500 seconds. The sampling geometry and standard sources used for efficiency calibration were kept constant. The background radiation of the counting room was measured for an empty Marinelli beaker under similar conditions to the real samples and then subtracted from the sample count to obtain the remaining counts [56]. These data were analyzed under the assumption of secular equilibrium of the parent radionuclides with shorter-lived daughter radionuclides within the studied

samples. The spectrum for each gamma emitter of short-lived daughter radionuclides obtained from primordial radionuclides in one of the studied samples that is agricultural soil sample (AS_6) is shown in Fig. 3.10.

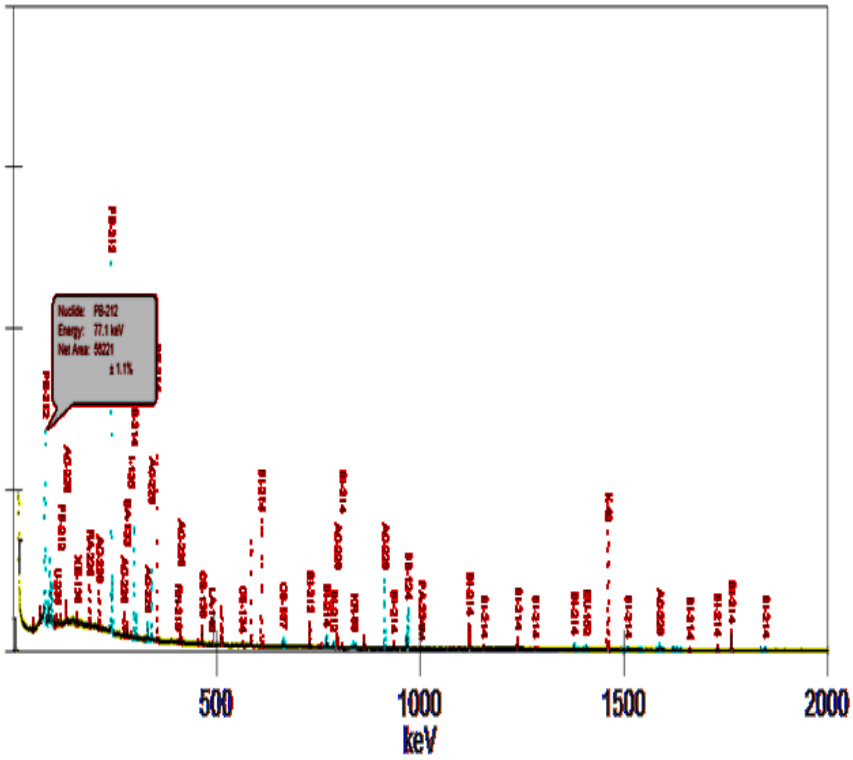

Figure 3.10: Gamma-ray spectrum of specific activity for ^{226}Ra, ^{232}Th, and ^{40}K in agricultural soil sample (AS_6)

The activity concentration of the various radioactive elements detected from samples studied in this thesis was calculated using the gamma energy lines of their progeny elements. The 295.21 (19.20%) keV and 351.92 (37.20%) keV gamma lines from ^{214}Pb, 609.31 (46.30%), 1120.29 (15.10%), and 1764.49 (15.80%) keV gamma lines from ^{214}Bi were used to determine ^{238}U (^{226}Ra) activity concentration. To determine ^{232}Th activity concentration, gamma lines of 77.11 (17.50%) keV and 238.63 (44.60%) keV from ^{212}Pb, 911.21 (26.60%) keV, and 968.97 (16.20%) keV from ^{228}Ac were used. Its gamma line at 1460.81 (10.67%) keV is used for ^{40}K. The experimental setup declares nearly 99% identification confidence in radionuclides and their energy peaks.

Detection Limits

The detection capabilities of measuring and analyzing radioactivity levels differ depending on the instrumentation and analytical techniques used.

The detection limit above which counts are statistically significant for the measurement must be determined for the low-level counting system. Currie is the first to explore the detection limit concept in 1968. When there is real activity, the Detection Limit (DL) is a level at which true net counts are detected above the acceptable level with a given probability. The detection limit can be expressed mathematically as follows [57]:

$$DL = (2.77 + 3.29\sqrt{BG}) \times \frac{A_c}{N_{net}} \tag{3.2}$$

where A_c is the activity concentration in Bqkg^{-1}, N_{net} is the net area under the peak and BG is the corresponding net peak area in the background spectrum when a blank sample is used which can be calculated from the spectrum as:

$$BG = N_g - N_{net} \tag{3.3}$$

Where N_g is the gross measured count rate (the net peak area in the spectrum of the sample).

The minimum detection activity (MDA), a performance criterion for gamma-ray spectroscopy methods, can be defined qualitatively as the smallest amount of activity concentration of radioactive nuclide that can be determined reliably for the specific measurement. The detection limit (DL) in Eq. 3.2 can be used to calculate the minimum detectable amount of activity using the following expression [58]:

$$MDA = \frac{DL}{\varepsilon P_\gamma t} \tag{3.4}$$

where P_γ = Gamma emission probability, ε = Absolute efficiency of the detector, and t = the counting time in seconds. The minimum detectable activity is in units of Bqkg^{-1}.

3.4 Assessment of radiation risk indices

The process of estimating the nature and probability of adverse health effects in humans who may be exposed to environmental contaminants is known as human health risk assessment [59]. The risk of radionuclides in humans is assessed using various estimating parameters. The goal of exposure assessment is to quantify or estimate the intensity, frequency, and duration of human exposure to a contaminant in the environment. The activity concentrations of radionuclides in studied samples were measured to assess exposure in this study. The biological effect of radiation is determined by the amount of energy deposited in an organism, the type of radiation, and the manner in which the energy is deposited along the radiation's path.

3.4.1 Activity concentration

The determination of activity concentrations in samples comprises the preparation of the sample, the measurement, and the calculation of activity concentration from the measurement results. Activity (A) of a nuclide is the number of radioactive decay per unit of time, and its unit is Becquerel (1 Bq = 1 disintegration per second). The activity per unit mass (activity concentration) in Bqkg^{-1} of the detected radioisotopes in the studied samples was calculated using the formula shown below [60].

$$A_c = \frac{N_{net}}{\varepsilon \times P_\gamma \times m \times t} \tag{3.5}$$

Where A_c is the activity concentration, N_{net} is the net count rate (cps) (measured count rate minus background count rate), ε is the efficiency of the detector, p_γ indicates the probability of specific energy photon emission per decay, m is the mass of the sample and t is the counting time.

3.4.2 Absorbed dose rate

When ionizing radiation penetrates the human body or an object, it deposits energy. The absorbed dose refers to the amount of energy actually absorbed by any material from radionuclides and is also used for any radiation type. The gray is the unit used to measure an absorbed dose. One

Gray (Gy) is equal to one joule of energy deposited in one kg of material (1 Gy = 1 Jkg^{-1}). The absorbed dose rate is the rate at which an absorbed dose is received (Gys^{-1}). The absorbed dose rate (ADR) for each of the considered samples measured is the sum of the dose rates contributed by both series of ^{238}U and ^{232}Th radioisotopes, as well as ^{40}K radioisotopes. The absorbed dose rate in the outdoor air at one meter above ground in measured samples of natural radioisotopes was calculated using Eq. 3.6 based on [5] if the naturally existing radioisotopes are homogeneously dispersed.

$$ADR(nGyh^{-1}) = 0.462A_{Ra} + 0.604A_{Th} + 0.0417A_K \tag{3.6}$$

Where 0.462, 0.604, and 0.0417 $nGyh^{-1}$ per $Bqkg^{-1}$ are the dose conversion factors [61], and A_{Ra}, A_{Th} and A_K are the activity concentrations ($Bqkg^{-1}$) of ^{226}Ra, ^{232}Th, and ^{40}K, respectively.

The absorbed dose rate can also be calculated in indoor air by the following formula [5].

$$ADR(nGyh^{-1}) = 0.92A_{Ra} + 1.10A_{Th} + 0.08A_K \tag{3.7}$$

Where the specific dose rates 0.92 $nGyh^{-1}$ per $Bqkg^{-1}$ for ^{226}Ra, 1.1 $nGyh^{-1}$ per $Bqkg^{-1}$ for ^{232}Th, 0.08 $nGyh^{-1}$ per $Bqkg^{-1}$ for ^{40}K.

3.4.3 Annual effective dose rate

The annual effective dose rate (AEDR) due to gamma-ray emission from radioisotopes in the studied samples describes the health effects of the absorbed dose over a year (365 $\times$ 24 h = 8760 hy^{-1}). In order to estimate the annual effective dose rate, the conversion coefficient from the absorbed dose to the effective dose received by an adult must be considered. AEDR in $mSvy^{-1}$ is computed by the conversion coefficient (0.7 $SvGy^{-1}$), which translates the absorbed dose rate to the effective dose rate, and the occupancy factor (0.8), with the residents having to spend 80% of their time within homes. Consequently, the AEDR within homes is determined as follows [5, 62]:

$$AEDR = ADR(nGyh^{-1}) \times (0.7mSvnGy^{-1}) \times 0.8 \times (8760hy^{-1}) \times 10^{-6} \quad (3.8)$$

The outdoor annual effective dose equivalent using the outdoor occupancy factor (0.2) is given by the following equation:

$$AEDR = ADR(nGyh^{-1}) \times (0.7mSvnGy^{-1}) \times 0.2 \times (8760hy^{-1}) \times 10^{-6} \quad (3.9)$$

The world average annual effective dose equivalent to outdoor or indoor terrestrial gamma radiation is 0.460 mSvy^{-1} [5].

3.4.4 Radium equivalent activity

To represent the activity concentrations of natural radionuclides by a single quantity, which takes into account the radiation hazards associated with them, a common radiological index has been introduced. In the studied samples, the distribution of natural radionuclides is not uniform, and thus the actual activity level of ^{226}Ra, ^{232}Th, and ^{40}K can be calculated by means of a common radiological index called the radium equivalent activity (Ra$_{eq}$). It is the sum of the activities of ^{226}Ra, ^{232}Th, and ^{40}K radioactive elements based on the assumption that 370 Bqkg^{-1} of ^{226}Ra, 259 Bqkg^{-1} of ^{232}Th, and 4810 Bqkg^{-1} of ^{40}K produce the same gamma-ray dose rate [5]. The following equation [62] calculates the specific activity of these radionuclides as a single quantity and their gamma-ray radiation hazards as radium equivalent activity in Bqkg^{-1}.

$$Ra_{eq} = (\frac{A_{Ra}}{370} + \frac{A_{Th}}{259} + \frac{A_K}{4810}) \times 370 \quad (3.10)$$

which is equivalent to

$$Ra_{eq} = A_{Ra} + 1.43A_{Th} + 0.077A_K \quad (3.11)$$

The published maximal admissible (permissible) radium equivalent activity is 370 Bqkg^{-1} which is equivalent to 1.5 mSvy^{-1} [61].

3.4.5 External radiation hazard index

The external hazard index is an evaluation of the hazard of natural gamma radiation. The external radiation hazard index (H_{ex}) is used to estimate the radiological suitability of the studied samples in this research, and its amount needs to be lower than one in order for the radiation hazard negligible. This means that the maximum value of H_{ex} equal to unity corresponds to the upper limit of Radium Equivalent Activity of 370 Bqkg^{-1} (Beretka and Mathew, 1985). The H_{ex} was calculated using the formula [63]:

$$H_{ex} = \frac{A_{Ra}}{370} + \frac{A_{Th}}{259} + \frac{A_K}{4810} \tag{3.12}$$

3.4.6 Internal radiation hazard index

The internal hazard index (H_{in}) should be computed to evaluate the internal hazard caused by the radioactive elements found in the samples. H_{in} was used to calculate the internal exposure to respiratory organs caused by the inhalation of alpha particles emitted from the inert gas ^{222}Rn and its short-lived daughter products. The following equation [63] was used to compute it.

$$H_{in} = \frac{A_{Ra}}{185} + \frac{A_{Th}}{259} + \frac{A_K}{4810} \tag{3.13}$$

The value of H_{in} should be less than unity to provide safe levels of radon and its short-lived daughters for the respiratory organs of individuals living in the dwellings.

3.4.7 Activity concentration index

The activity concentration index (I_γ) is a screening tool popularly utilized to judge the gamma radiation dose that a person might accept from ^{226}Ra, ^{232}Th, and ^{40}K found in the assessed samples. In this work, the European Commission [62], suggestion is used to calculate the gamma hazard index.

$$I_\gamma = \frac{A_{Ra}}{150} + \frac{A_{Th}}{100} + \frac{A_K}{1500} \tag{3.14}$$

Where A_{Ra}, A_{Th}, and A_K are as before specified. $I_\gamma \leq 1$ corresponds to a dose creation of 1 mSvy^{-1}, while $I_\gamma \leq 0.5$ corresponds to 0.3 mSvy^{-1}.

3.4.8 Alpha index

The alpha index (I_α) is used to estimate the excess alpha radiation caused by breathing-in alpha emitters obtained from radionuclides found in the examined samples. The next formula is applied to calculate the I_α.

$$I_\alpha = \frac{A_{Ra}}{200} \leq 1 \tag{3.15}$$

The suggested exemption and higher amount of ^{226}Ra activity concentrations in examined samples are 100 and 200 Bqkg^{-1}, respectively, as recommended by ICRP [64]. The suggested higher boundary concentration of ^{226}Ra is 200 Bqkg^{-1}, for which I_α = 1.

3.4.9 Excess lifetime cancer risk

The excess lifetime cancer risk (ELCR) asserts the chance of getting cancer as a result of gamma irradiation exposure during a person's lifetime obtained from radionuclides in the assessed samples. Excess lifetime cancer risk can be calculated using the annual effective dose rate, duration of life (DL), which is estimated to be 70 years, and risk factor (RF) with a value of 0.05 Sv^{-1} by the relation 3.16 [65].

$$ELCR = AEDR \times DL \times RF \tag{3.16}$$

3.4.10 Annual gonadal dose equivalent

UNSCEAR is interested in organs such as the thyroid, lungs, bone marrow, bone surface cells, gonads, and female breasts [66]. Therefore, the annual gonadal dose equivalent (AGDE) in units of μSvy^{-1} because of radioactive element specific activities in the explored samples was estimated by the formula [46].

$$AGDE = 3.09A_{Ra} + 4.18A_{Th} + 0.314A_K \tag{3.17}$$

Chapter 4
Results and Discussion

4.1 Activity Concentrations in Raw Gypsum Samples

4.1.1 Results

The specific activities and the average specific activity values of the natural gypsum samples studied using the gamma spectroscopy technique are shown in Table 4.1. The radioisotopes discovered are the decomposition sequences of ^{238}U, ^{232}Th, and the individually occurring ^{40}K, all of which are natural radioisotopes. According to the results, the specific activity for the studied samples varies for each of the natural gypsum because radioactivity varies greatly over a distance of some meters and at geological locations. The acquired values of the specific activities in the gypsum raw samples vary from 1.47 $\pm$ 0.26 to 2.42 $\pm$ 0.37 Bqkg^{-1} in samples GR_5 and GR_{10}, respectively, with an average value of 1.90 $\pm$ 0.33 Bqkg^{-1} for ^{238}U, 1.10 $\pm$ 0.26 to 2.60 $\pm$ 0.48 Bqkg^{-1} in GR_1 and GR_3 samples with an average value of 1.99 $\pm$ 0.39 Bqkg^{-1} for ^{232}Th and 4.27 $\pm$ 1.92 to 44.53 $\pm$ 2.84 Bqkg^{-1} in samples GR_2 and GR_3, with an average value of 28.16 $\pm$ 2.57 Bqkg^{-1} for ^{40}K, respectively. Because potassium is the most abundant radioisotope in the study area, activity concentrations of ^{238}U, ^{232}Th, and ^{40}K in raw gypsum show high variability, and ^{40}K has higher specific activity compared to ^{238}U and ^{232}Th (Table 4.1). The average values obtained for the radionuclides identified are lower than the globally recommended values. In addition, the results obtained are consistent with literature reports on building materials [67].

Fig. 4.1 depicts a graphical representation of specific activities of ^{238}U, ^{232}Th, and ^{40}K.

Table 4.1: Average activity concentrations for ^{238}U, ^{232}Th and ^{40}K in gypsum raw (GR) samples

sample code	^{238}U (Bq kg^{-1})	^{232}Th	^{40}K (Bq kg^{-1})
GR_1	2.15 ± 0.30	1.10 ± 0.26	10.70 ± 2.65
GR_2	1.96 ± 0.35	1.95 ± 0.27	4.27 ± 1.92
GR_3	1.80 ± 0.28	2.60 ± 0.48	44.53 ± 2.84
GR_4	1.54 ± 0.31	2.01 ± 0.44	29.36 ± 2.35
GR_5	1.47 ± 0.26	1.85 ± 0.40	28.31 ± 2.21
GR_6	1.95 ± 0.34	1.99 ± 0.43	38.02 ± 2.97
GR_7	1.78 ± 0.33	2.35 ± 0.45	36.41 ± 2.60
GR_8	1.79 ± 0.34	1.84 ± 0.45	31.26 ± 2.85
GR_9	2.12 ± 0.38	2.11 ± 0.41	27.77 ± 2.53
GR_{10}	2.42 ± 0.37	2.09 ± 0.29	31.01 ± 2.75
Range	1.47 ± 0.26 - 2.42 ± 0.37	1.10 ± 0.26 - 2.60 ± 0.48	4.27 ± 1.92 - 44.53 ± 2.84
Average	1.90 ± 0.33	1.99 ± 0.39	28.16 ± 2.57

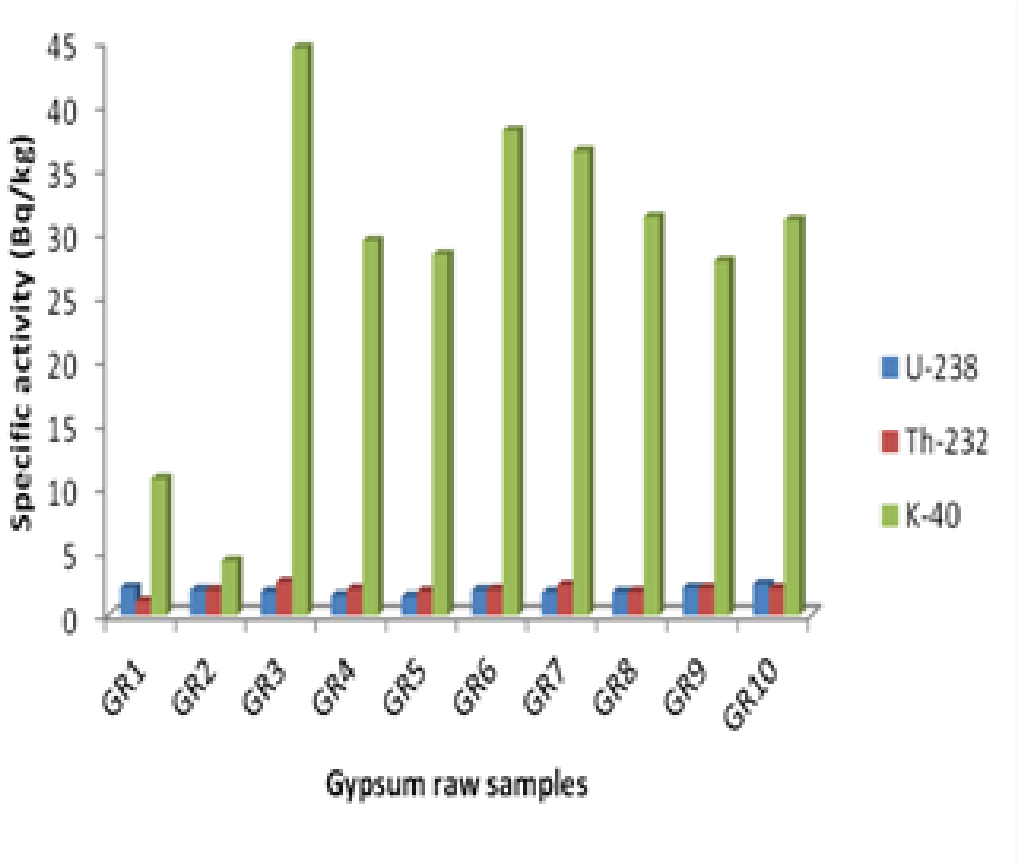

Figure 4.1: Graphical representation of specific activities of ^{238}U, ^{232}Th, and ^{40}K in gypsum raw samples

Comparison of activity concentration with Other Measurements in raw gypsum Samples

Table 4.2 compares the average specific activities of ^{238}U, ^{232}Th, and ^{40}K in the current study to those performed by other countries. It demonstrates

that the average specific activities in current work are lower than those performed by other countries, whereas the value of ^{232}Th in Ethiopia is higher than that of Kuwait, and the value of ^{40}K in Ethiopia is also higher than that of Italy and Kuwait, as shown in Table 4.2. This high variability in average activity concentrations of ^{238}U, ^{232}Th, and ^{40}K compared to other countries (Table 4.2) is primarily due to different geological areas and the availability of various types of raw gypsum.

Table 4.2: Comparison of mean activity concentrations (Bqkg^{-1}) of ^{238}U (^{226}Ra), ^{232}Th, and ^{40}K in Ethiopian raw gypsum samples with results reported in other countries

Country	^{238}U (^{226}Ra)	^{232}Th	^{40}K	References
Ethiopia	1.90 ± 0.33	1.99 ± 0.39	28.16 ± 2.57	Present work
Egypt	31.7 ± 4.6	52.2 ± 2.8	88.7 ± 4.4	[68]
Egypt	91.97 ± 2.61	42.27 ± 2.22	499.29 ± 11.53	[31]
Egypt	31.7 ± 4.6	55 ± 2.7	116	[69]
Saudi Arabia	33.28 ± 4.7	47.2 ± 2.8	88 ± 4.4	[69]
Italy	6.0 ± 5.0	2.0 ± 2.0	12 ± 11	[69]
Bangladesh	254 ± 28	21.4 ± 2.8	294.3 ± 27.7	[69]
Kuwait	2.81 ± 0.4	0.55 ± 0.1	17.4	[69]
Albania	11.8 ± 2.0	5.8 ± 1.9	68.8 ± 11.3	[33]
Turkey	8 ± 3	11 ± 7	35 ± 5	[33]
Turkey	10.8 ± 12.2	3.6 ± 2.7	44.5 ± 23.2	[33]
Pakistan	8.2 ± 1.9	16.2 ± 3.9	187.7 ± 53.2	[33]
Saudi Arabia	7.7 ± 0.1	3.3 ± 0.1	173 ± 2.4	[70]
Egypt	105 ± 6	45 ± 15	500 ± 141	[70]
Pakistan	6.2 ± 1.6	13.3 ± 2.8	173 ± 50.3	[70]
Qatar	11.5 ± 0.2	2.5 ± 0.1	72 ± 3	[70]

4.1.2 Radiological Parameters for raw gypsum Samples

The particular radioisotopes ^{238}U, ^{232}Th, and ^{40}K emit gamma-ray radiation, which is the cause of radiological risk, were estimated using, different indices. The radiological variables calculated due to the specific activities of the recognized radioisotopes in the studied samples is absorbed dose rate. The calculated ADR values changed from 2.10 ± 0.41 to 4.26 ± 0.54 nGyh^{-1} in GR_1 and GR_3 samples, respectively, with an average value of 3.25 ± 0.49 nGyh^{-1} in gypsum raw samples as presented in Table 4.3. Fig. 4.2 depicts the ADR results graphically. The calculated mean value of ADR is far less than the global mean value of 55 nGyh^{-1} [5].

The health effects of the absorbed dose in a year from gamma radiation emitted from obtained radionuclides is estimated by annual effective dose rate. The obtained indoor AEDR ranged from 0.01 ± 0.002 to 0.021 ± 0.003

mSvy^{-1} in GR_1 and GR_3, respectively, with an average value of 0.02 $\pm$ 0.003 mSvy^{-1} for the gypsum raw samples. Table 4.3 shows the calculated results of indoor AEDR, and Fig. 4.3 shows a graphical representation of it. The average calculated AEDR result for both raw gypsum samples is far less than 1 mSvy^{-1} which is the global indoor mean annual effective dose.

Table 4.3 shows the calculated radium equivalent activity for all raw gypsum samples studied, and Fig. 4.4 shows it graphically. The values vary from 4.47 $\pm$ 0.86 to 8.95 $\pm$ 1.19 Bqkg^{-1} in GR_1 and GR_3, with an average result of 6.91 $\pm$ 1.08 Bqkg^{-1} for studied samples, respectively. The average result shows that the radiation dose provided to factory workers and residents where natural gypsum powder is used as building material is insignificant, as the result is much less than 370 Bqkg^{-1}, which is equivalent to 1.5 mSvy^{-1}, the maximum recommended value for building materials [25].

Table 4.3: Radiological parameters (estimated for gypsum raw (GR) samples)

sample code	Ra_{eq} (Bq kg^{-1})	ADR (nGyh^{-1})	AEDR (mSvy^{-1})
GR_1	4.47 $\pm$ 0.86	2.10 $\pm$ 0.41	0.01 $\pm$ 0.002
GR_2	5.08 $\pm$ 0.88	2.26 $\pm$ 0.40	0.011$\pm$ 0.002
GR_3	8.95 $\pm$ 1.19	4.26 $\pm$ 0.54	0.021 $\pm$ 0.003
GR_4	6.68 $\pm$ 1.12	3.15 $\pm$ 0.51	0.016 $\pm$ 0.003
GR_5	6.30 $\pm$ 1.00	2.98 $\pm$ 0.45	0.015 $\pm$ 0.002
GR_6	7.72 $\pm$ 1.18	3.69 $\pm$ 0.54	0.018 $\pm$ 0.003
GR_7	7.94 $\pm$ 1.18	3.76 $\pm$ 0.53	0.019 $\pm$ 0.003
GR_8	6.83 $\pm$ 1.20	3.24 $\pm$ 0.55	0.016 $\pm$ 0.003
GR_9	7.28 $\pm$ 1.16	3.41 $\pm$ 0.53	0.017 $\pm$ 0.003
GR_{10}	7.80 $\pm$ 1.00	3.68 $\pm$ 0.46	0.018 $\pm$ 0.002
Range	4.47 $\pm$ 0.86 - 8.95 $\pm$ 1.19	2.10 $\pm$ 0.41 - 4.26 $\pm$ 0.54	0.01 $\pm$ 0.002 - 0.021 $\pm$ 0.003
Mean	6.91 $\pm$ 1.08	3.25 $\pm$ 0.49	0.02 $\pm$ 0.003

The external and internal health hazard indices have a maximum value of unity, as world standard value, for the sum total of the three radioactive materials found in the examined samples. Table 4.4 displays the calculated values of H_{ex} and H_{in}, which are graphically depicted in Fig. 4.5. The calculated results vary from 0.012 $\pm$ 0.002 to 0.024 $\pm$ 0.003 in GR_1 and GR_3, respectively, with an average value of 0.02 $\pm$ 0.003 for H_{ex} and from 0.018 $\pm$ 0.003 to 0.029 $\pm$ 0.004 in GR_1 and GR_3, respectively, with an average value of 0.024 $\pm$ 0.004 for H_{in}. Thus, the use of gypsum powder obtained from the studied samples is safe because the calculated values of H_{ex} and H_{in} are

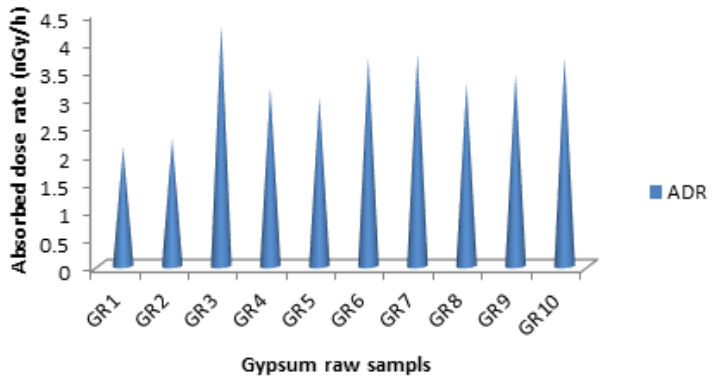

Figure 4.2: Absorbed dose rate ($nGyh^{-1}$) for gypsum raw samples

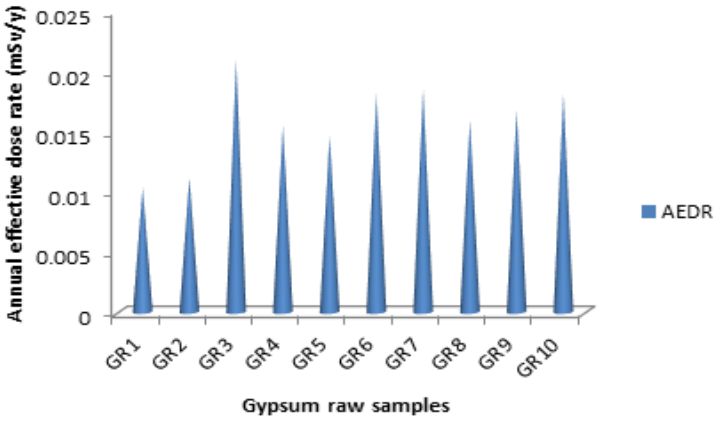

Figure 4.3: Bar diagram showing the calculated values of annual effective dose rate ($mSvy^{-1}$) for gypsum raw samples

much less than one, which is the allowed upper limit of radiation hazard [71].

The range and average obtained values of gamma index derived from the activity concentrations of radium, thorium, and potassium in various gypsum raw samples are presented in Table 4.4, and its pictorial illustration is shown in Fig. 4.5. The calculated values of I_γ range from 0.03 ± 0.007 to 0.06 ± 0.008 in GR_5 and GR_7, with an average value of 0.05 ± 0.008, respectively. The average value is far less than the criterion of the unit, corresponding to an effective dose of 1 $mSvy^{-1}$ for building materials, indicating that the studied samples are safe for use in construction.

Table 4.4 shows the range and mean calculated values of alpha index derived from the activity concentrations of radium in various gypsum raw samples, and Fig. 4.5 shows a graphical representation. The calculated

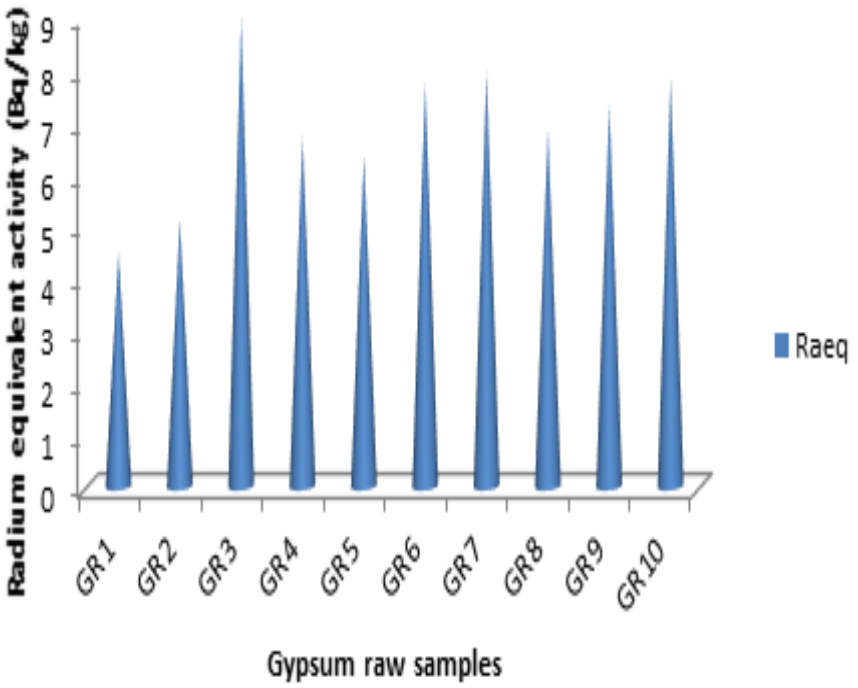

Figure 4.4: Bar diagram showing the calculated values of radium equivalent activity (Bqkg^{-1}) for gypsum raw samples

results of I_α varied from 0.007 $\pm$ 0.001 to 0.012 $\pm$ 0.002 in GR_5 and GR_{10}, with an average value of 0.01 $\pm$ 0.002, respectively. It is observed that the calculated average values of I_α are much lower than the recommended upper value, indicating that it is safe to use gypsum powder obtained from gypsum raw in the construction of dwellings.

Table 4.4: The radiological hazard indices calculated for each gypsum raw (GR) sample

sample code	H_{ex}	H_{in}	I_γ	I_α
GR_1	0.012 $\pm$ 0.002	0.018 $\pm$ 0.003	0.033 $\pm$ 0.006	0.011 $\pm$ 0.0
GR_2	0.014 $\pm$ 0.002	0.019 $\pm$ 0.003	0.035 $\pm$ 0.006	0.010 $\pm$ 0.002
GR_3	0.024 $\pm$ 0.003	0.029 $\pm$ 0.004	0.057 $\pm$ 0.009	0.009 $\pm$ 0.001
GR_4	0.018 $\pm$ 0.003	0.025 $\pm$ 0.004	0.050 $\pm$ 0.008	0.008 $\pm$ 0.002
GR_5	0.017 $\pm$ 0.003	0.021 $\pm$ 0.003	0.030 $\pm$ 0.007	0.007 $\pm$ 0.001
GR_6	0.021 $\pm$ 0.003	0.026 $\pm$ 0.004	0.058 $\pm$ 0.009	0.010 $\pm$ 0.002
GR_7	0.022 $\pm$ 0.003	0.026 $\pm$ 0.004	0.060 $\pm$ 0.008	0.009 $\pm$ 0.002
GR_8	0.018 $\pm$ 0.003	0.023 $\pm$ 0.004	0.051 $\pm$ 0.009	0.009 $\pm$ 0.002
GR_9	0.020 $\pm$ 0.003	0.025 $\pm$ 0.004	0.054 $\pm$ 0.009	0.011 $\pm$ 0.002
GR_{10}	0.021 $\pm$ 0.003	0.028 $\pm$ 0.004	0.058 $\pm$ 0.007	0.012 $\pm$ 0.002
Range	0.012 $\pm$ 0.002 - 0.024 $\pm$0.003	0.018 $\pm$ 0.003 - 0.029 $\pm$ 0.004	0.030 $\pm$ 0.007 - 0.060 $\pm$ 0.008	0.007$\pm$ 0.001 - 0.012 $\pm$ 0.002
Mean	0.02 $\pm$ 0.003	0.024 $\pm$ 0.004	0.05 $\pm$ 0.008	0.01 $\pm$ 0.002

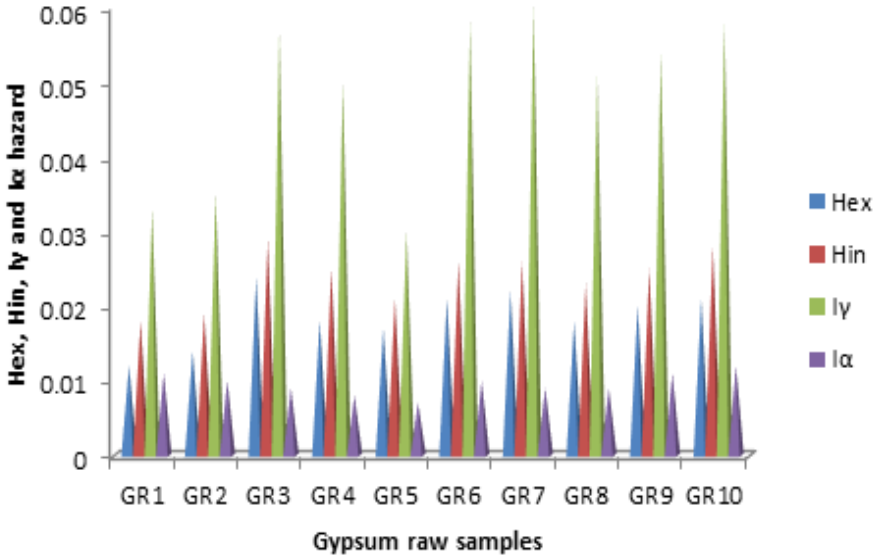

Figure 4.5: External and internal hazard indices, as well as gamma and alpha indices, are graphically represented in raw gypsum samples

The mean value of Ra_{eq} for all raw gypsum is far less than the work of other countries, as given in Table 4.5. When the mean value of absorbed dose rate is compared to the mean value of other works (Table 4.5), it is significantly lower. Similarly, when the mean value of annual effective dose rate is compared with other country's studies, it is much less than other work (Table 4.5).

Table 4.5: Comparison of the average values of Ra_{eq} in $Bqkg^{-1}$, ADR in $nGyh^{-1}$ and AEDR in $mSvy^{-1}$ to other work

Country	Ra_{eq}	ADR	AEDR	References
Ethiopia	6.91 ± 1.08	3.25 ± 0.49	0.02 ± 0.003	Present work
Saudi Arabia	122.71	54.27	not available	[69]
Egypt	190.87 ± 5.34	89.56 ± 2.61	0.44 ± 0.04	[31]
Turkey	104.2	105.82	not available	[71]
Turkey	15.1 ± 2.4	13.6 ± 2.1	0.07 ± 0.01	[34]
Algeria	34.03	15.91	not available	[69]
Nigeria	42.09 ± 1.34	38.83 ± 1.18	0.19 ± 0.01	[32]

Table 4.5 compares the mean value of H_{ex} and H_{in} of this work to that of other countries' studies, but this value is lower than other studies. Table 4.6 compares the mean value of the gamma hazard index in this study with other countries, and it is less than in other studies.

Table 4.6: Comparison of the average values of H_{ex}, H_{in} and I_{γ} to other work

Country	H_{ex}	H_{in}	I_{γ}	References
Ethiopia	0.02 ± 0.003	0.024 ± 0.004	0.05 ± 0.008	Present work
Saudi Arabia	0.24	not available	not available	[69]
Egypt	0.37 ± 0.04	0.47 ± 0.05	1.37 ± 0.16	[31]
Turkey	0.2	0.3	not available	[71]
Turkey	not available	0.06 ± 0.01	not available	[34]
Algeria	0.09	0.12	0.13	[69]
Nigeria	not available	not available	0.15	[32]

4.1.3 Discussion

Radioactivity is a component of the natural environment that contains radioactive elements. The so-called natural radioactive elements, as well as the radioisotopes into which they decay, emit radiation. Thus, humans are constantly exposed to radiation, either willingly or unwittingly, from radioactive elements produced by cosmic ray interaction in the atmosphere and those from naturally occurring substances that are primarily dispersed in the ecosystem. Natural radioactive elements such as ^{40}K and the ^{238}U and ^{232}Th series are found in building materials derived from rock and soil [5].

Internal and external radiation exposure from natural radionuclides have been distinguished. The release of penetrating gamma rays from radioactive nuclides causes external exposure. Breathing in radon gas produced by the uranium-238 decay series and its short-lived decay products exposes people internally. Radon-222 levels vary dramatically depending on the underlying regional geology, soil porosity, building materials, long-term temperature shifts, and family lifestyle. Radon-222 and its decay products are constituents of soil gas and its surroundings, and they seep into buildings, where their concentrations tend to be higher than outside. Because people spend more than 80% of their time at home, the inside and outside radiation subjection caused by radioisotopes in building materials create extended subjection circumstances [5, 72]. As soon as radon-222 enters the body, some of its impermanent disintegrations are retained in the lungs and irradiate cells in the respiratory tract, allowing the amount in the lung to grow into lung cancer [2, 5].

Gypsum rocks were formed over geological time by the evaporation of seawater and were frequently laid down in beds with thicknesses ranging from a few centimeters to several tens of meters. Natural gypsum does not normally form above the ground in moist areas because it is slightly soluble in water, but it may form below the ground where it is not influenced by the water table. It can grow above the ground in dried areas, sometimes in the form of gypsum sand. The presence of natural gypsum above or below the earth's surface is usually indicated by changes in vegetation, and some plants thrive in gypsum-rich soil. Natural gypsum is typically white or colourless; however, grey and other colours are occasionally permitted [73]. Natural gypsum powder has been the substance of choice in building manufacturing for centuries due to rapid constructional and fundamental growth by administration, discrete and personal districts at all levels [74].

Raw gypsum extracted from rocks contains varying levels of naturally occurring radioactive elements. Various types of literature show that gypsum raw contains natural radioactive elements such as radium-226, just like other construction materials, but it also provides significant practical and economic benefits. Despite this, its use would increase radiation levels in society, primarily among gypsum factory workers and home decorators. Because workers and residents waited for extended periods of time indoors, they were constantly exposed to radioactive elements emitted by gypsum powders used to decorate buildings, which could lead to health complications. However, the radiation levels for workers in the gypsum factory and dwellers in gypsum-decorated buildings varied as a result of the amount of gypsum used in the construction, the arrangement of the construction, the size of the interior of the building, and the hours spent waiting in the home [32, 75, 76]. However, no comprehensive research has been conducted on the contribution of raw gypsum to background radiation in Ethiopia. As a result, the focus of this work is on evaluating, comparing, and contrasting the activity concentration of ten natural gypsum samples obtained from various sites in the Abay gorge, Dejen district, used by five factories producing gypsum powder in Dejen town, Amhara Region, Ethiopia. This will help to determine the obtained radionuclides and their concentrations while also determining the radiation risk to humans

from raw gypsum samples in the work. The potential radiation risk associated with raw gypsum was assessed by calculating the absorbed dose rate, annual effective dose rate, radium equivalent activity, external and internal hazard indices, and gamma radiation hazard level index, as shown in Table 4.3. The obtained results were related to the suggested standards for evaluating the radioactivity risks to a person due to construction resources (raw gypsum), as well as the analogous results of the building materials from various works completed using a similar method.

4.2 Activity Concentrations in Raw Materials Used for Cement Production

4.2.1 Results

Table 4.7 show the results for the average activity concentrations of ^{226}Ra, ^{232}Th, and ^{40}K obtained in the analyzed raw materials used for cement production. The radioactive isotopes discovered are the daughter products of ^{226}Ra, ^{232}Th, and singly occurring ^{40}K. The average result of the activity concentrations of ^{226}Ra, ^{232}Th, and ^{40}K computed in the sand sample are 9.56 $\pm$ 0.75, 21.99 $\pm$ 1.77 and 8.11 $\pm$ 1.48 Bqkg^{-1}, respectively; in limestone is found to be 10.02 $\pm$ 0.77, 3.06 $\pm$ 0.42 and 3.18 $\pm$ 1.32 Bqkg^{-1}, respectively; in clay is found to be 37.33 $\pm$ 2.56, 71.06 $\pm$ 5.45 and 208.66 $\pm$ 9.69 Bqkg^{-1}, respectively; in gypsum it is 5.18 $\pm$ 0.55, 4.95 $\pm$ 0.61 and 54.36 $\pm$ 3.40 Bqkg^{-1}, respectively; in pumice it is 5.54 $\pm$ 0.54, 14.45 $\pm$ 1.23 and 146.76 $\pm$ 6.99 Bqkg^{-1}, respectively; and in coal it is 16.34 $\pm$ 1.28, 12.54 $\pm$ 1.26 Bqkg^{-1}, respectively. The mean activity concentration of ^{40}K in coal is below the detector's detection limit. The average activity of ^{226}Ra, ^{232}Th, and ^{40}K was found to be lowest in limestone and gypsum samples, respectively, and highest in clay. Except for the values in clay for radium and thorium, the average results of ^{226}Ra, ^{232}Th, and ^{40}K activity concentrations of obtained in the examined samples are markedly smaller than the world average results in the crust of the earth (35, 30 and 400 Bqkg^{-1}, respectively) [5].

Because of the different physical characteristics, different geological areas and the availability of various types raw materials, the radionuclide activity concentrations obtained in the examined raw materials shows high

Table 4.7: Activity concentration values of ^{226}Ra, ^{232}Th, and ^{40}K in Bqkg^{-1} for Sand (S), Limestone (LS), Clay (C), Gypsum (G), pumice (P) and Coal (CA) samples

sample code	^{226}Ra (Bq kg^{-1})	^{232}Th (Bq kg^{-1})	^{40}K (Bq kg^{-1})
S_1	9.64 ± 0.75	22.13 ± 1.78	6.90 ± 1.41
S_2	9.48 ± 0.75	21.84 ± 1.76	9.32 ± 1.54
Mean	9.56 ± 0.75	21.99 ± 1.77	8.11 ± 1.48
LS_3	10.03 ± 0.77	3.14 ± 0.41	2.58 ± 1.28
LS_4	10.01 ± 0.76	2.97 ± 0.42	3.78 ± 1.36
Mean	10.02 ± 0.77	3.06 ± 0.42	3.18 ± 1.32
C_5	37.43 ± 2.57	70.01 ± 5.37	208.53 ± 9.68
C_6	37.23 ± 2.55	72.08 ± 5.53	208.78 ± 9.70
Mean	37.33 ± 2.56	71.06 ± 5.45	208.66 ± 9.69
G_7	4.90 ± 0.49	4.91 ± 0.57	48.65 ± 2.97
G_8	5.45 ± 0.61	4.99 ± 0.65	60.07 ± 3.82
Mean	5.18 ± 0.55	4.95 ± 0.61	54.36 ± 3.40
P_9	6.00 ± 0.57	15.31 ± 1.30	152.18 ± 7.22
P_{10}	5.07 ± 0.50	13.58 ± 1.15	141.34 ± 6.76
Mean	5.54 ± 0.54	14.45 ± 1.23	146.76 ± 6.99
CA_{11}	15.88 ± 1.29	12.34 ± 1.26	Not detected
CA_{12}	16.79 ± 1.26	12.74 ± 1.26	Not detected
Mean	16.34 ± 1.28	12.54 ± 1.26	Not detected
Total mean	13.99 ± 1.07	21.34 ± 1.79	84.21 ± 4.57
Range	4.90 ± 0.49 - 37.43 ± 2.57	2.97 ± 0.42 - 72.08 ± 5.53	2.58 ± 1.28 - 208.78 ± 9.70

variability (Table 4.7). The studied samples will have a specific dose that is closely related to the geological processes, types of mineral crystallization, mineralogical composition, and possibly uneven distribution of these radionuclides in the different sampled media.

Comparison with other studies

Table 4.8 compares the mean activity concentrations of radioisotopes in the samples studied to the values studied in other countries. Table 4.8 shows that the activity concentration of ^{226}Ra and ^{232}Th in the sand is lower in Bangladesh and Saudi Arabia but higher in Kuwait, while its value in ^{226}Ra is comparable to Egypt but higher in ^{232}Th. The value of ^{40}K in the sand is lower than in previous studies. The activity concentration of ^{226}Ra, ^{232}Th, and ^{40}K computed in limestone are lower than in Pakistan, Greece, and Egypt, while the value of ^{226}Ra is greater than in Greece. The activity concentration of ^{226}Ra, ^{232}Th, and ^{40}K measured in clay are higher than in Turkey, Pakistan, Saudi Arabia and Egypt, while the value of ^{40}K is lower than in Turkey. The specific activity of ^{226}Ra, ^{232}Th, and ^{40}K computed in

gypsum is lower than in Albania, Pakistan, Saudi Arabia, and Egypt, while the value of ^{232}Th is higher than in Saudi Arabia. The specific activity of ^{226}Ra and ^{232}Th measured in coal is less than in China, Greece, and Spin, but the values of ^{226}Ra and ^{232}Th are greater than in Nigeria. Generally, the clay samples have high mean activity concentration of ^{226}Ra, ^{232}Th, and ^{40}K in this study and other similar studies as presented in Table 4.8. This comparison of activity concentrations (Table 4.8) reveals significant variability due to differences in geological areas and the availability of various types of raw materials.

Table 4.8: Comparison of mean activity concentrations in (Bqkg^{-1}) of ^{226}Ra, ^{232}Th, and ^{40}K in studied samples with other countries' results

Country	Sample	^{226}Ra	^{232}Th	^{40}K	References
Ethiopia	Sand	9.56 ± 0.75	21.99 ± 1.77	8.11 ± 1.48	Present work
Ethiopia	Limestone	10.02 ± 0.77	3.06 ± 0.42	3.18 ± 1.32	Present work
Ethiopia	Clay	37.33 ± 2.56	71.06 ± 5.45	208.66 ± 9.69	Present work
Ethiopia	Gypsum	5.18 ± 0.55	4.95 ± 0.61	54.36 ± 3.40	Present work
Ethiopia	Pumice	5.54 ± 0.54	14.45 ± 1.23	146.76 ± 6.99	Present work
Ethiopia	Coal	16.34 ± 1.28	12.54 ± 1.26	Not detected	Present work
Egypt	Sand	9.2 ± 2.5	3.3 ± 1.3	47.3 ± 9	[77]
Bangladesh	Sand	14.1 ± 2.3	25.0 ± 4.3	158.4 ± 31.4	[78]
Kuwait	Sand	7.4 ± 0.6	7.2 ± 0.3	360 ± 14	[79]
S. Arabia	Sand	12.3 ± 2.3	24.2 ± 1.3	195 ± 4	[69]
Pakistan	Limestone	21.9 ± 7.6	8.6 ± 1.6	73.8 ± 21.9	[50]
Greece	Limestone	6.0 ± 0.4	6.6 ± 1.0	101.6 ± 9	[80]
Egypt	Limestone	19.7 ± 2.9	39.0 ± 2.0	61.2 ± 3.1	[81]
Pakistan	Limestone	28.4 ± 8.7	11.3 ± 1.7	63.1 ± 17.3	[48]
Turkey	Clay	26.7 ± 20.0	41.8 ± 27.7	629.3 ± 232.1	[45]
Egypt	Clay	33.7 ± 4.4	68.9 ± 3.5	130.7 ± 6.5	[81]
Pakistan	Clay	34.7 ± 13.1	41.2 ± 6.7	187.6 ± 17.2	[48]
S. Arabia	Clay	18.2 ± 0.2	22.4 ± 0.3	127 ± 1.8	[70]
Albania	Gypsum	11.8 ± 2.0	5.8 ± 1.9	66.8 ± 11.3	[33]
Egypt	Gypsum	31.7 ± 4.7	55.2 ± 2.8	88.7 ± 4.4	[81]
Pakistan	Gypsum	8.2 ± 1.9	16.2 ± 3.9	187.7 ± 53.2	[48]
S. Arabia	Gypsum	7.7 ± 0.1	3.3 ± 0.1	173 ± 2.4	[70]
Nigeria	Coal	8.18 ± 0.3	9.97 ± 0.3	27.38 ± 0.8	[47]
China	Coal	17	20	24	[82]
Greece	Coal	133	18	108	[83]
Spain	Coal	64	18	104	[84]

4.2.2 Radiological Parameters in raw materials used for cement production

The radionuclides obtained in the studied samples are ^{226}Ra, ^{232}Th, and ^{40}K emits gamma radiation, which is the cause of radiation hazards, were calculated using different indices.

In this study, the absorbed dose rate range and total mean values for raw building materials were 12.78 to 130.29 nGyh^{-1} and 41.96 nGyh^{-1}, respectively (Table 4.9). The limestone sample yields the lowest value and the clay sample yields the highest value. The global average indoor D_R range from 20 to 200 nGyh^{-1}, with a population-weighted average value 84 nGyh^{-1} [5]. As a result, the values discovered in this study are lower than the global average.

The range and total mean values of AEDR for raw building materials were 0.063 to 0.639 mSvy^{-1} and 0.206 mSvy^{-1}, respectively (Table 4.9). Except for the clay sample (0.634 mSvy^{-1}) the mean values of all samples are less than the exemption dose criterion of 0.3 mSvy^{-1}.

Table 4.9 displays the calculated AGDE values; the range and total mean values were 44.54 to 481.89 μSvy^{-1} and 154.47 μSvy^{-1}, respectively, which were lower than the standard mean value of 300 Svy^{-1} [85].

Table 4.9 shows the total mean value and range of the radium equivalent, which are 49.91 Bqkg^{-1} and 14.55 (limestone) to 156.38 Bqkg^{-1} (clay). These values are well below the permissible limit of 370 Bqkg^{-1} [86]. As a result, the use of these materials in construction is thought to be safe for human habitation.

The estimated values of H_{ex} and H_{in} in the studied raw materials are ranged from 0.040 to 0.422 and 0.062 to 0.522, respectively, with total mean values of 0.135 and 0.173. As shown in Table 4.10, the H_{ex} and H_{in} values for all studied samples are less than the recommended upper level of unity, indicating the raw materials in the studied area can be used safely as building materials.

According to Table 4.10, the I_γ in raw materials varies from 0.049 (limestone) to 0.554 (clay), with a mean value of 0.177. These values were less than one, indicating that the AEDR for radionuclides in raw samples was less than one mSvy^{-1}. As a result, using these raw materials for building construction poses no radiological risk to the general public.

The range and total mean values of ELCR are shown in Table 4.10, which range from 0.221 $\times$ 10^{-3} (limestone) to 2.237 $\times$ 10^{-3} (clay), with a mean

Table 4.9: Calculated received doses and radiological hazard indices in the studied samples

sample code	D_R ($nGyh^{-1}$)	AEDR ($mSvy^{-1}$)	AGDE (μSvy^{-1})	Ra_{eq} ($Bqkg^{-}$)
S_1	33.76	0.166	124.46	41.82
S_2	33.49	0.164	123.51	41.43
Mean	33.63	0.165	123.99	41.63
LS_3	12.89	0.063	44.93	14.72
LS_4	12.78	0.063	44.54	14.55
Mean	12.84	0.063	44.75	14.64
C_5	128.13	0.629	473.78	153.60
C_6	130.24	0.639	481.89	156.38
Mean	129.19	0.634	477.84	154.99
G_7	13.80	0.068	50.94	15.67
G_8	15.31	0.075	56.56	17.22
Mean	14.56	0.072	53.75	16.45
P_9	34.53	0.169	130.33	39.61
P_{10}	30.91	0.152	116.81	35.37
Mean	32.72	0.161	123.57	37.49
CA_{11}	28.18	0.138	100.65	33.53
CA_{12}	29.46	0.143	105.13	35.01
Mean	28.82	0.141	102.89	34.27
Total mean	41.96	0.206	154.47	49.91
Range	12.78 - 130.29	0.063 - 0.639	44.54 - 481.89	14.55 - 156.38

Table 4.10: Calculated radiological hazard indices in the studied samples

sample code	H_{ex}	H_{in}	I_γ	ELCR$\times 10^{-3}$
S_1	0.112	0.138	0.145	0.581
S_2	0.112	0.137	0.144	0.574
Mean	0.112	0.138	0.145	0.58
LS_3	0.040	0.067	0.05	0.221
LS_4	0.040	0.067	0.049	0.221
Mean	0.040	0.067	0.05	0.221
C_5	0.414	0.515	0.545	2.202
C_6	0.422	0.522	0.554	2.237
Mean	0.418	0.519	0.55	2.22
G_7	0.042	0.056	0.057	0.238
G_8	0.047	0.062	0.063	0.263
Mean	0.045	0.059	0.06	0.25
P_9	0.107	0.123	0.148	0.592
P_{10}	0.095	0.108	0.132	0.532
Mean	0.101	0.116	0.140	0.56
CA_{11}	0.091	0.134	0.115	0.483
CA_{12}	0.094	0.139	0.120	0.508
Mean	0.093	0.137	0.118	0.50
Total mean	0.135	0.173	0.177	0.72
Range	0.040 - 0.422	0.062 - 0.522	0.049 - 0.554	0.221 - 2.237

value of 0.72×10^{-3}. The values obtained for limestone and gypsum are lower, while the other results are higher than the world mean value of

0.299×10^{-3} [5].

4.2.3 Correlation studies

Pearson coefficient (R) evaluates the strength and direction of a linear relationship between two variables. Correlation tests were conducted between the activity concentrations to determine the amount of ^{226}Ra, ^{232}Th, and ^{40}K in the analyzed raw materials. The correlation coefficient, R = 0.58, and the relationship of the activity concentrations for (^{226}Ra, ^{40}K) are shown in Fig. 4.6, indicating that they have a good association. Similarly, the correlation coefficient, R = 0.92, for (^{226}Ra, ^{232}Th) is presented in Fig. 4.7, indicating that the radionuclides have a high correlation. The relationship between (^{232}Th, ^{40}K) is depicted in Fig. 4.8, and the correlation coefficient, R = 0.76, indicates a high correlation. The Pearson coefficient suggests a positive association between the radionuclides obtained in the studied samples.

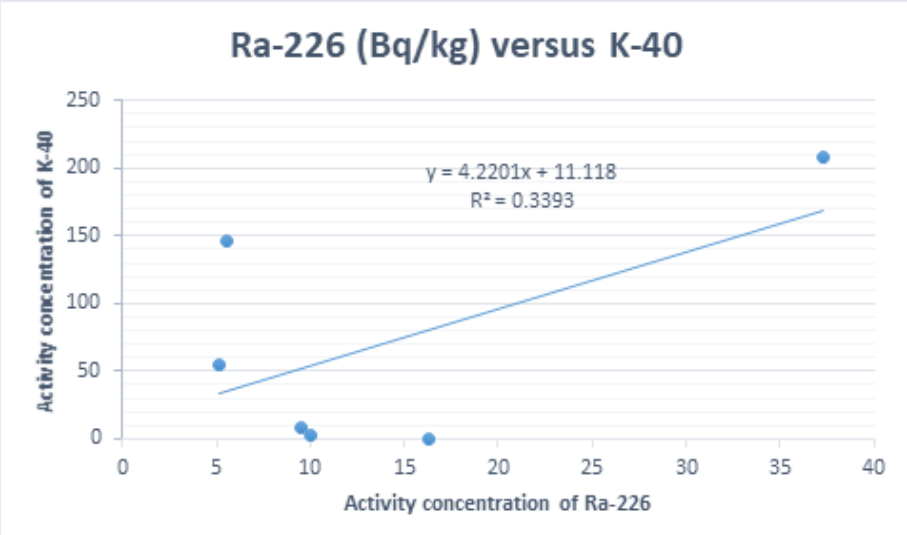

Figure 4.6: Relationship between activity concentrations of ^{226}Ra and ^{40}K in the studied samples

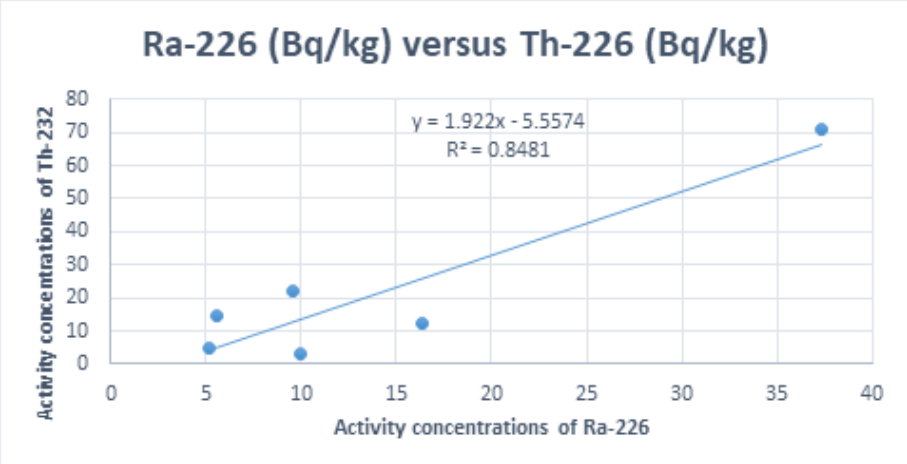

Figure 4.7: Correlation between concentrations of ^{226}Ra and ^{232}Th in cement raw samples

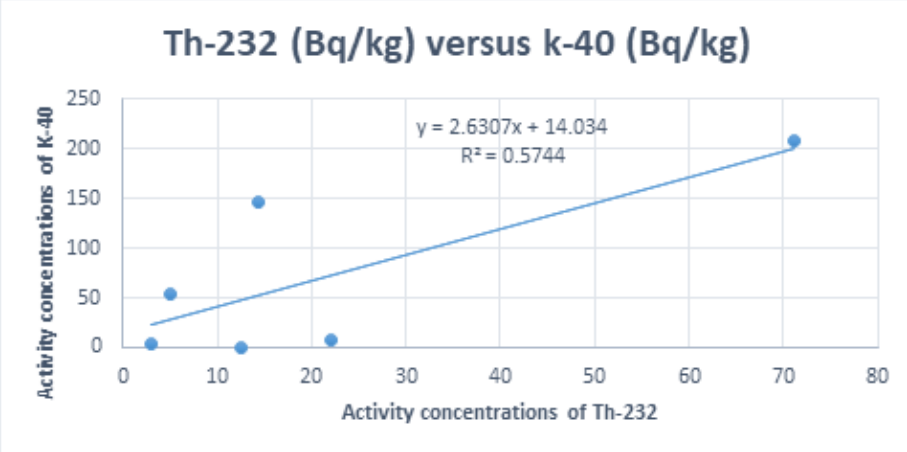

Figure 4.8: Correlation between concentrations of ^{232}Th, and ^{40}K in the analyzed samples

4.2.4 Discussion

The inhabitants are exposed both internally and externally as a result of natural radioactivity in the building components. All raw materials used in construction that are produced from rock and soil, such as sand, limestone, clay, gypsum, pumice, coal, etc., include varying levels of radioactive isotope ^{40}K as well as the naturally occurring radionuclides ^{238}U and ^{232}Th and their decay products. Since the radiologically most significant portion of the ^{238}U series' decay chain begins with ^{226}Ra, references to that segment are frequently made to ^{226}Ra rather than ^{238}U. The Earth's crust is where radionuclides originate, but they also end up in things like food, air, water, building materials, and the human body. The average effective indoor dose caused by gamma rays from building materials is thought to

be 0.4 $mSvy^{-1}$ on a global scale. Internal exposure is brought on by breathing in the radioactive inert gas ^{222}Rn, a daughter product of ^{226}Ra, and its short-lived decay products, whereas external exposure is brought on by direct gamma radiation released from these radionuclides. According to the geographical locations and geochemical properties of the raw materials, the specific activities of natural radionuclides can vary greatly [2, 33]. In order to limit the manufacturing of cement with relatively high radioactive concentrations, it is vital to determine the natural radioactivity level in raw materials in order to comprehend the presence of radionuclides in building materials. Additionally, since people spend about 80% of their time in homes, understanding the level of natural radioactivity in building materials is necessary for developing standards and guidelines for the use and management of these materials in addition to assessing any potential radiological hazards to human health [5].

^{222}Rn in homes is a severe health risk, according to recent studies of those who have been exposed to it [22]. 1.2 $mSvy^{-1}$ of the 2.4 $mSvy^{-1}$ average yearly dose from natural sources is received through breathing, primarily from ^{222}Rn [5]. The greatest health concern brought on by prolonged, high ^{222}Rn exposure is an increased risk of lung cancer, which is influenced by both the ^{222}Rn concentration and the duration of exposure. ^{222}Rn is considered to be responsible for somewhere between 3% and 14% of all lung cancer incidences, depending on the average ^{222}Rn level in a given country. The first places where lung cancer rates rose were uranium mines that were exposed to a lot of radon. Additionally, research conducted in Europe, North America, and China have demonstrated that even low levels of radon, such as those present in households, carry health concerns and significantly contribute to the global prevalence of lung cancer [87].

The activity concentration of gamma-ray emitting nuclides in the studied raw materials was measured using a P-type high purity germanium detector. The findings are used to assess the doses received and prospective radioactive risks related to the use of these materials in buildings by calculating various indices such as radium equivalent activity, excess lifetime cancer risk, external and internal hazard index, indoor absorbed gamma dose rate, and corresponding annual effective dose rate, annual gonadal

dose equivalent, and activity concentration index. There is no standard of reference, and there is a lack of understanding about the presence of radionuclides in various raw materials used in the study area. Consequently, the primary goal of this research is to evaluate the raw materials and determine the activity concentration of radionuclides, as well as their potential health implications. The findings were compared to other country studies and global standard limits.

4.3 Activity Concentrations in Soil Samples

4.3.1 Results

Radioactivity level assessment and interpretation of radiologically related parameters are critical aspects of public awareness and environmental safety. The calculated average specific activity in 12 soil samples resolved by the HPGe detector is shown in Table 4.11. The obtained values of specific activities in agricultural soil samples (AS) in ^{226}Ra, ^{232}Th, and ^{40}K ranged from 29.30 $\pm$ 1.94 to 41.08 $\pm$ 1.40 Bqkg^{-1}, 53.53 $\pm$ 4.13 to 72.76 $\pm$ 5.45 Bqkg^{-1}, and 186.03 $\pm$ 8.40 to 239.94 $\pm$ 10.71 Bqkg^{-1}, respectively, while in virgin soil samples (VS) ranged from 35.10 $\pm$ 2.37 to 41.51 $\pm$ 2.59 Bqkg^{-1}, 51.43 $\pm$ 3.95 to 70.36 $\pm$ 5.42 Bqkg^{-1}, and 218.58 $\pm$ 10.02 to 251.74 $\pm$ 11.25 Bqkg^{-1}, respectively. Table 4.11 shows that the specific activity of ^{40}K in agricultural and virgin soil samples is higher than that of ^{226}Ra and ^{232}Th. This is due to the fact that potassium is the most abundant radioisotope, which means potassium has more concentration compared with radium and thorium in the soil under consideration [36], as well as the study area's excessive use of potassium-containing fertilizer in agricultural land, which increases the activities of ^{40}K. Because thorium is 1.5 times more abundant in the earth's crust than uranium, the specific activity of ^{232}Th in both types of samples is greater than ^{226}Ra [88].

When the concentrations of radium and potassium activity in virgin and agricultural soil samples are compared, the concentrations of radium and potassium in virgin soil are higher than in agricultural soil samples, indicating that radium and potassium can be transported by irrigation.

Table 4.11: Activity concentration values of ^{226}Ra, ^{232}Th, and ^{40}K in Bqkg^{-1} for each agricultural soil sample (AS) and virgin soil sample (VS)

sample code	^{226}Ra	^{232}Th	^{40}K
		Agricultural soil samples	
AS_1	41.08 ± 1.40	70.78 ± 2.52	225.18 ± 5.73
AS_2	29.30 ± 1.94	71.33 ± 5.43	189.46 ± 8.54
AS_3	31.10 ± 2.07	61.45 ± 4.77	230.38 ± 10.33
AS_4	33.05 ± 2.19	72.76 ± 5.45	213.98 ± 9.66
AS_5	30.93 ± 2.06	53.53 ± 4.13	186.03 ± 8.40
AS_6	35.14 ± 2.31	66.29 ± 4.96	239.94 ± 10.71
Range	29.30 ± 1.94 -	53.53 ± 4.13 -	186.03 ± 8.40 -
	41.08 ± 1.40	72.76 ± 5.45	239.94 ± 10.71
Average	33.44 ± 2.01	66.02 ± 4.54	214.16 ± 8.90
		Virgin soil samples	
VS_7	40.42 ± 2.63	68.37 ± 5.11	241.46 ± 10.69
VS_8	38.02 ± 2.49	70.36 ± 5.42	251.74 ± 11.25
VS_9	38.02 ± 2.49	70.36 ± 5.42	251.74 ± 11.25
VS_{10}	35.24 ± 2.33	57.29 ± 4.51	241.62 ± 10.83
VS_{11}	41.51 ± 2.59	52.87 ± 4.13	236.76 ± 10.68
VS_{12}	35.10 ± 2.37	51.43 ± 3.95	218.58 ± 10.02
Range	35.10 ± 2.37 -	51.43 ± 3.95 -	218.58 ± 10.02 -
	41.51 ± 2.59	70.36 ± 5.42	251.74 ± 11.25
Average	38.05 ± 2.48	61.78 ± 4.76	240.32 ± 10.79

Comparison of mean specific activities with other studies

Table 4.12 compares the average specific activities of radioisotopes obtained from agricultural and virgin soil samples to the mean specific activities described in other countries. The average specific activity of thorium in agricultural and virgin soil samples, as well as radium in virgin soil samples, is higher than the world average, whereas radium in agricultural soil samples and potassium in both samples are lower than the world average published by [5] for ^{226}Ra, ^{232}Th, and ^{40}K are 35, 30, and 400 Bqkg^{-1}, respectively.

In these comparisons, the highest values of average specific activity of ^{226}Ra, ^{232}Th, and ^{40}K in agricultural soil samples were found in Ethiopia (shoa), North Malaysia (Kedah), and Pakistan, respectively, whereas in virgin soil samples, it is in Malaysia (Penang), North Malaysia (Kedah), and Pakistan, respectively. This comparison shows that the mean specific activity of natural radionuclides varies in soil samples from various regions around the world, which is due to the geographical and geological conditions of the district, improper fertilizer use in agricultural land [41], and

Table 4.12: Comparison of mean activity concentrations of ^{226}Ra, ^{232}Th, and ^{40}K in Bqkg^{-1} in agricultural and virgin soil samples with other countries' results

Country	^{226}Ra	^{232}Th	^{40}K	References
		Agricultural soil samples		
Ethiopia (Dejen)	33.44 ± 2.01	66.02 ± 4.54	214.16 ± 8.90	Present work
Egypt	43	54	183	[39]
India	64	93	124	[89]
Ethiopia(Shoa)	133.85 ± 14.36	Not detected	287.82 ± 25.18	[38]
Greece	16 ± 6	55 ± 14	305	[90]
Algeria	53.2	50.03	311	[91]
Malaysia(Kedah)	80.63	116.87	200.66	[41]
N.Malaysia(Kedah)	102.08	133.96	325.87	[35]
Iran	20.81 ± 0.37	26.99 ± 0.38	430.43 ± 2.74	[40]
Pakistan	32.66 ± 1.88	58.18 ± 2.12	604.96 ± 21.78	[92]
		Virgin soil samples		
Ethiopia (Dejen)	38.05 ± 2.48	61.78 ± 4.76	240.32 ± 10.79	Present work
Ethiopia (Shoa)	30.51 ± 3.64	14.52 ± 1.11	100.29 ± 14.00	[38]
Malaysia(Penang)	390	165	835	[93]
Malaysia(Pontian)	37	53	293	[42]
Malaysia(Kedah)	51.06	78.44	125.66	[41]
N.Malaysia(Kedah)	65.24	83.29	136.98	[35]
Iran	23.99 ± 0.37	31.74 ± 0.38	461.09 ± 2.68	[40]
Pakistan	25.97 ± 1.48	52.68 ± 1.96	550.08 ± 21.6	[92]

possibly uneven distribution of these radionuclides in the different sampled media.

4.3.2 Radiological Parameters in soil samples

Radioactivity level assessment and interpretation of radiologically related parameters are critical aspects of public awareness and environmental safety. The dose from radionuclides in the observed soil samples that is received by people outside is represented by the absorbed dose rate (ADR). The computed absorbed dose rate from naturally existing radioactive elements is shown in Table 4.13 for samples of agricultural and virgin soil from this investigation. Its value in agricultural soil ranged from 56.70 to 74.12 nGyh^{-1}, with an average value of 67.24 nGyh^{-1}, which is higher than the UNSCEAR global mean value of 60 nGyh^{-1} [5]. Similar to this, in samples of virgin soil, the absorbed dose rate ranged from 58.48 to 73.70 nGyh^{-1}, with a mean value of 67.53 nGyh^{-1}, higher than the UNSCEAR-recommended worldwide mean value [5].

To evaluate the health impacts of the absorbed dose that humans get over

the course of a year, the annual effective dose rate (AEDR) can be determined. As shown in Table 4.13, the calculated annual effective dose rate in agricultural soil samples ranged from 0.070 to 0.091 $mSvy^{-1}$, with an average value of 0.083 $mSvy^{-1}$, whereas it ranged from 0.072 to 0.090 $mSvy^{-1}$, with a mean value of 0.082 $mSvy^{-1}$ in virgin soil samples. In both soil samples, the calculated mean value is slightly higher than the global average annual effective dose of 0.07 $mSvy^{-1}$ [5].

Table 4.13 displays the calculated radium equivalent activity of agricultural and virgin soil samples. The range in agricultural soil samples is 121.82 to 159.64 $Bqkg^{-1}$, with an average value of 144.57 $Bqkg^{-1}$, which is much lower than the allowed limit (370 $Bqkg^{-1}$) and agrees with the Organization for Economic Cooperation and Development's effective dose limit of 1 $mSvy^{-1}$ [94]. The range and mean of Ra_{eq} in virgin soil samples were found to be 125.48 to 158.02 $Bqkg^{-1}$ and 144.90 $Bqkg^{-1}$, respectively, which is significantly lower than the allowed limit. The population is therefore not at risk from radiation in the research area.

Table 4.13: In this study, the estimated hazard indices of the primordial radioisotopes in agricultural and virgin soil samples are calculated

sample code	ADR ($nGyh^{-1}$)	AEDR ($mSvy^{-1}$)	Ra_{eq} ($Bqkg^{-}$)
	Agricultural soil samples		
AS_1	74.12	0.091	159.64
AS_2	67.91	0.083	145.89
AS_3	63.91	0.078	136.71
AS_4	71.52	0.088	154.96
AS_5	56.70	0.070	121.82
AS_6	69.26	0.085	148.41
Range	56.70 - 74.12	0.070 - 0.091	121.82 - 159.64
Mean	67.24	0.083	144.57
	Virgin soil samples		
VS_7	72.95	0.087	156.78
VS_8	73.70	0.090	158.02
VS_9	73.70	0.090	158.02
VS_{10}	63.42	0.078	135.77
VS_{11}	62.96	0.077	135.35
VS_{12}	58.48	0.077	125.48
Range	58.48 - 73.70	0.072 - 0.090	125.48 - 158.02
Mean	67.53	0.082	144.90

According to Table 4.14, the computed values of H_{ex} for agricultural soil samples ranged from 0.33 to 0.43, with an average value of 0.39, and for

virgin soil samples, they ranged from 0.34 to 0.43, with an average value of 0.39. For agricultural soil samples, the computed values of H_{in} ranged from 0.41 to 0.54 with an average value of 0.48, while for virgin soil samples, they ranged from 0.43 to 0.53 with an average value of 0.49 (Table 4.14). The values for H_{ex} and H_{in} are fewer than the upper limit permitted by the European Commission on Radiation Protection [62], as shown in Table 4.14. As a result, the soils in the studied area provide low radiation exposure for residents and agricultural workers while posing no significant radiation risk.

The gamma level associated with natural radionuclides in the soil samples under consideration is assessed using the radioactivity level index (I_γ). The calculated radioactivity level index values for agricultural and virgin soil samples are shown in Table 4.14. For agricultural soil samples, it ranged from 0.87 to 1.13, with an average value of 1.03, and for virgin soil samples, it ranged from 0.89 to 1.13, with an average value of 1.03. For agricultural and virgin soil samples, the average radioactivity level index values are comparable to the recommended upper limit of one.

The excess lifetime cancer risk (ELCR) asserts the chance of getting cancer as a result of gamma irradiation exposure during a person's lifetime. In agricultural soils, the ELCR obtained values varied from 0.25×10^{-3} to 0.32×10^{-3}, with a mean value of 0.29×10^{-3}, while in virgin soils, the ELCR obtained values ranged from 0.25×10^{-3} to 0.32×10^{-3}, with an average value of 0.29×10^{-3}, as shown in Table 4.14. The results are very close to the global allowed standard of 0.29×10^{-3} [5]. As a result, there is no indication of cancer cases in the community.

Comparison of Ra_{eq}, ADR, AEDR, H_{ex}, H_{in} and I_γ with other studies

The mean value of the radium equivalent activity in this study was compared to other international studies in Table 4.15. In comparison to Iran and Egypt, the computed mean value for agricultural soil samples is higher. Similarly, the value is lower for both soil samples than North Malaysia (Kedah) and Malaysia (Kedah), but greater than virgin soil in Iran.

Table 4.15 compares the mean value of the absorbed dose rate in this study

Table 4.14: In this study, the estimated hazard indices of the primordial radioisotopes in agricultural and virgin soil samples are calculated

sample code	H_{ex}	H_{in}	I_γ	ELCR $\times 10^{-3}$
		Agricultural soil samples		
AS_1	0.43	0.54	1.13	0.32
AS_2	0.39	0.47	1.04	0.29
AS_3	0.37	0.45	0.98	0.27
AS_4	0.42	0.50	1.09	0.31
AS_5	0.33	0.41	0.87	0.25
AS_6	0.40	0.50	1.06	0.30
Range	0.33 -	0.41 -	0.87 -	0.25 -
	0.43	0.54	1.13	0.32
Mean	0.39	0.48	1.03	0.29
		Virgin soil samples		
VS_7	0.42	0.53	1.12	0.31
VS_8	0.43	0.53	1.13	0.32
VS_9	0.43	0.53	1.13	0.32
VS_{10}	0.37	0.46	0.97	0.27
VS_{11}	0.37	0.48	0.96	0.27
VS_{12}	0.34	0.43	0.89	0.25
Range	0.34 -	0.43 -	0.89 -	0.25 -
	0.43	0.53	1.13	0.32
Mean	0.39	0.49	1.03	0.29

to that of other studies. The results obtained in agricultural soil samples in this study are higher than those reported in Egypt and Iran. Similarly, it is higher in virgin soil samples than in Iran, but it is lower in both samples than in North Malaysia (Kedah) and Malaysia (Kedah).

Table 4.15 compared this study's annual effective dosage rate's mean value to similar studies from other nations. In comparison to Iran and Egypt, the computed mean value for agricultural soil samples is higher. For virgin soil, it is higher than Iran's, but for both soil samples, it is lower than North Malaysia (Kedah) and Malaysia (Kedah).

Table 4.15 compared the mean value of the external and internal hazard indices in this study to those in other countries. For both soil samples, the value obtained is higher than in Iran. In agricultural samples, the mean value H_{ex} is lower than in Egypt, North Malaysia (Kedah), and Malaysia (Kedah); similarly, the obtained value in virgin samples is lower than in Egypt, North Malaysia (Kedah), and Malaysia (Kedah). In this study, the mean value of H_{in} is lower than that found in Malaysia (Kedah) for virgin soil samples.

Table 4.15: Comparison of the mean values of Ra_{eq}, ADR, AEDR, H_{ex}, H_{in} and I_{γ} in agricultural and virgin soil samples with other studies

Country	Ra_{eq} ($Bqkg^{-}$)	ADR ($nGyh^{-1}$)	AEDR ($mSvy^{-1}$)	H_{ex}	H_{in}	I_{γ}	References
			Agricultural soil samples				
Ethiopia	144.57	67.24	0.083	0.39	0.48	1.03	Present work
N.Malaysia(Kedah)	458.785	141.62	0.169	0.859	-	1.07	[35]
Malaysia(Kedah)	258.36	116.04	0.162	0.708	0.925	-	[41]
Egypt	135	62	0.076	0.4	0.5	-	[39]
Iran	93.92	44.57	0.05	0.25	0.31	0.68	[40]
			Virgin soil samples				
Ethiopia	144.90	67.53	0.082	0.39	0.49	1.03	Present work
N.Malaysia(Kedah)	214.293	87.47	0.106	0.525	-	0.59	[35]
Malaysia(Kedah)	172.7	76.20	0.106	0.464	0.604	-	[41]
Iran	108.08	51.06	0.06	0.29	0.35	0.73	[40]

Table 4.15 compares the mean value of I_{γ} in this study to others studies. For both soil samples, the obtained value in this study is higher than in Iran but lower than in North Malaysia (Kedah).

4.3.3 Discussion

Humans are constantly exposed to ionizing radiation (alpha, beta, and gamma), which is always present naturally in the environment, whether intentional or not. Only radionuclides with half-lives comparable to the earth's age, as well as their decay products, are abundant in the environment. Natural radionuclides, which emanate from the soil and may accumulate in dwellings, expose humans to both external and internal radiation. External sources of irradiation of the human body are primarily gamma radiation, whereas those resulting from inhalation and ingestion via foods and drinking water have internal exposure to humans by alpha, beta, and gamma radiation obtained from ^{238}U and ^{232}Th series, as well as ^{40}K, which are naturally present in the environment [5].

Radon and its short-lived decay products, which emanate from the soil and may be concentrated in dwellings and the atmosphere, are the most significant contributors to human exposure from natural sources. The main route for radiation exposure to the lungs is the inhalation of ^{222}Rn and its short-lived decay products and subsequent deposition along the walls of the bronchial tree's various airways. Although some beta particles and

gamma radiation are emitted during the decay of radionuclides, alpha particles travel a short distance into the airway walls and cause most of the exposure. The main factors that determine an individual's exposure rate are radionuclide concentrations in the soil, time spent outdoors, and the shielding provided by buildings. However, because the majority of building materials contain radionuclides, the shielding of the outdoor radiation field by buildings is frequently outweighed by the presence of additional radionuclides in the building materials [5].

The activity concentration of natural radionuclides emitted by soil varies depending on geological and geographical conditions in each region of the world [5, 6]. The earth was made from stars' materials and many of these materials were radioactive from the beginning of the formation of the earth. Soil is formed continuously, but slowly, as a result of the progressive dissolution of rocks caused by weathering. Weathering can be either physical, chemical, or biological in nature. Water, wind, temperature change, gravity, chemical interaction, living creatures, and pressure changes all contribute to the breakdown and transformation of rocks into soil, thus equilibrium between parent and daughter radionuclides in rocks and in soil takes place. It is an important environmental material that is used for a variety of purposes such as raw material and product construction, playground and street filling, and so on. An individual's total radiation exposure includes both indoor and outdoor radiation exposure from background radiation, which increases the amount in the environment [95]. Soil is the primary source of radiation exposure for humans, as well as a medium for radionuclide transfer to the environment [96].

Soil research is important in the study area because of its contribution to food production, it uses as building material, the ubiquity of human life, and the widespread use of fertilizers in their farmland. Hence, understanding the distribution of radionuclides in soils is necessary for radiological risk management. To assess the risk associated with primordial radionuclides in the study area the following indices were calculated. The radium equivalent activity, annual effective dose rate, absorbed dose

rate,external hazard index, internal hazard index, gamma index, and excess lifetime cancer risk are all determined and discussed in order to provide information on radionuclides found in soil samples and to assess environmental pollution in the study area. The findings were contrasted with average global values given and suggested by the Scientific Committee on the Effects of Atomic Radiation of the United Nations, as well as research from other nations.

Chapter 5
Conclusion and Recommendation

5.1 Conclusion

Using gamma ray spectroscopy coupled with a HPGe detector, the activity concentrations of primordial natural radionuclides obtained in the decay series of ^{238}U and ^{232}Th, as well as ^{40}K, were determined. The radiological health hazards indices in various types of natural gypsum samples collected from gypsum factory stores, some raw material samples used in cement industry collected from their stores, and agricultural and virgin soil samples collected from Berch Giyorgis village, both in Dejen district, were evaluated using these results.

Ten different raw gypsum samples were collected from five different gypsum powder factories in Dejen, and the activity concentration of radionuclides obtained was calculated. The results show that there is natural radioactivity in Abay gorge, with gypsum raw being the main source of ^{238}U, ^{232}Th, and ^{40}K activity concentrations. The specific activity of ^{40}K is much higher than that of ^{238}U and ^{232}Th in all raw gypsum samples studied. This work's average specific activity was discovered to be significantly lower than the global average. The calculated average values of different radiological hazard indices were discovered to be significantly lower than the recommended upper limit. Based on the calculated results, it is possible to conclude that the use of gypsum powder in the construction of residences is safe for occupants, and no radiological complexity is expected to develop inside the buildings.

The total mean values of specific activities ^{226}Ra, ^{232}Th, and ^{40}K in the analyzed raw material samples used for cement production were found to be 13.99 ± 1.07, 21.34 ± 1.79, and 84.21 ± 4.57 Bqkg^{-1}, respectively, which are

significantly lower than the corresponding worldwide mean values. Radiation received doses and radiation hazard parameters were calculated solely for the purpose of screening ready-to-use raw materials. They were found to be below the recommended limits in almost all samples, with the exception of the clay sample. The total mean dose values and radiation hazard indices obtained in the studied samples are below the world-recommended limit, indicating that the studied samples pose no significant radiation risk and can be used safely in cement production. Clay, on the other hand, should be used with caution due to the high radiological risk and received doses. Despite the fact that no restrictions or regulations prohibit its use in the research area.

Natural radioactive element activity levels in agricultural and virgin soil samples were determined. The calculated mean specific activities of ^{226}Ra, ^{232}Th, and ^{40}K in agricultural soil samples were 33.44 $\pm$ 2.01, 66.02 $\pm$ 4.54, and 214.16 $\pm$ 8.90 Bqkg^{-1}, respectively, while in virgin soil samples they were 38.05 $\pm$ 2.48, 61.78 $\pm$ 4.76, and 240.32 $\pm$ 10.79 Bqkg^{-1}, respectively. The mean specific activities of ^{226}Ra in virgin soil samples and ^{232}Th in both samples exceeded the global average value, whereas ^{40}K in both soil samples and ^{226}Ra in agricultural soil samples were lower. The absorbed dose rate, annual effective dose rate, radium equivalent activity, external and internal hazard indices, radioactivity level index, and excess lifetime cancer risk were used to assess radiological hazards. The absorbed dose rate (67.53 nGyh^{-1}) and annual effective dose rate (0.082 mSvy^{-1}) obtained appeared to be slightly higher than the global average (60 nGyh^{-1} and 0.070 mSvy^{-1}, respectively). The values for radium equivalent activity, external and internal hazard indices were lower than the world average, but the values for radioactivity level index and excess lifetime cancer risk were comparable to the UNSCEAR world average. As a result, the soil in this study is suitable for agriculture and as a building material, and it poses no significant health risk to the community.

5.2 Recommendation

Based on the findings, this research, dissertation has recommendations for raw gypsum powder factories, cement factories, and responsible sectors on environmental biosphere in the study areas. The average radioactivity levels measured in natural gypsum samples, some raw material samples used in cement production, and agricultural and virgin soil samples were all below the safe limit for building materials.

The raw gypsum samples used in building construction contained low concentrations of natural radioactivity, and their radiation hazard indices were also lower than the world permissible limit, so the materials were recommended for use as building materials. Except for the clay sample, which has a high activity concentration in the study area, the examined raw materials for cement production have low activity concentrations. It is recommended that the clay ratio be reduced in comparison to the other raw materials used in cement production. The average activity concentration of radium and thorium in the studied agricultural and virgin soil samples is higher than the global average, implying that agricultural activities must be carefully managed.

In general, the results can be regarded as a data base for the distribution of natural radionuclides in building materials to reflect the geological variation of their origin site. To prevent the radiological negative effects of construction materials, a radiation protection management strategy should be implemented, and this research can be used as a baseline for future related studies. Because the Dejen district has abundant construction materials, it is recommended that regular monitoring and further investigation of the level of activity concentration of natural radionuclides be carried out.

Appendix A
Peak Locate Report

Peak Locate Analysis Report 12/7/2021 3:48:58 PM Page 1

****

***** PEAK LOCATE REPORT *****

****

Detector Name: B13010
Sample Title: BUILDING MATERIAL
Peak Locate Performed on: 12/7/2021 3:48:58 PM
Peak Locate From Channel: 1
Peak Locate To Channel: 8192
Peak Search Sensitivity: 3.00

Peak No.	Centroid Channel	Centroid Uncertainty	Energy (keV)	Peak Significance
1	270.62	0.3340	66.15	3.35
2	306.33	0.2284	74.88	5.63
3	315.36	0.2327	77.09	6.35
4	357.48	0.2872	87.38	4.15
5	378.87	0.2530	92.61	4.48
6	760.33	0.2296	185.86	6.69
7	976.04	0.1652	238.59	10.98
8	1001.62	0.3331	244.84	3.19
9	1207.21	0.1757	295.10	9.40
10	1282.99	0.3709	313.62	3.04
11	1383.89	0.2752	338.29	3.76
12	1439.14	0.1378	351.80	14.65
13	1893.26	0.3000	462.81	3.19
14	2089.39	0.1638	510.75	7.91
15	2385.32	0.1494	583.09	10.63
16	2491.74	0.1278	609.11	14.87
17	2973.45	0.2584	726.86	3.25
18	3075.51	0.2923	751.81	3.24
19	3417.28	0.2818	835.36	3.17
20	3726.83	0.1384	911.03	11.11
21	3821.72	0.2696	934.22	3.01
22	3962.99	0.1715	968.76	7.88
23	4582.24	0.1519	1120.13	8.87
24	5063.82	0.2092	1237.86	4.26
25	5632.67	0.2247	1376.91	3.67
26	5974.79	0.0747	1460.55	31.27
27	6117.99	0.2555	1495.55	3.25
28	6495.79	0.2268	1587.90	3.67
29	6628.24	0.2484	1620.28	3.32
30	7074.86	0.2084	1729.46	4.19
31	7216.72	0.1312	1764.14	9.31
32	7556.17	0.2319	1847.12	3.35

? = Adjacent peak noted

Errors quoted at 1.000 sigma
Peak Analysis Report 12/7/2021 3:49:02 PM Page 1

Figure A.1: Peak locate report of GR_1 sample code

Appendix B

Peak Analysis Report

```
*****          P E A K    A N A L Y S I S    R E P O R T          *****
********************************************************************************

     Detector Name:  B13010
     Sample Title:   BUILDING MATERIAL
     Peak Analysis Performed on:  12/7/2021   4:09:09 PM
               Peak Analysis From Channel:      1
               Peak Analysis To Channel:     8192

   Peak  ROI  ROI    Peak     Energy   FWHM  Net Peak  Net Area  Continuum
    No. start end  centroid   (keV)   (keV)  Area      Uncert.    Counts

 M  1   292-  323   297.68    72.76   0.92  2.35E+002   44.16   3.02E+003
 m  2   292-  323   306.48    74.92   0.93  9.07E+002   51.39   3.28E+003
 m  3   292-  323   315.50    77.12   0.93  7.96E+002   50.94   3.29E+003
F   4   374-  386   379.20    92.69   0.95  7.53E+002   51.84   3.64E+003
F   5   755-  767   759.96   185.77   1.07  6.18E+002   56.22   4.31E+003
 M  6   968-  992   976.18   238.63   1.12  2.03E+003   65.68   3.89E+003
 m  7   968-  992   988.69   241.68   1.12  4.71E+002   50.15   2.98E+003
F   8  1200- 1214  1207.60   295.20   1.17  9.28E+002   51.14   2.85E+003
F   9  1375- 1391  1383.65   338.23   1.20  4.66E+002   43.59   2.76E+003
F  10  1433- 1446  1439.49   351.88   1.21  1.64E+003   54.83   1.96E+003
F  11  1888- 1904  1893.88   462.96   1.29  2.51E+002   33.18   1.53E+003
F  12  2079- 2100  2089.88   510.87   1.98  2.47E+003   62.97   2.14E+003
F  13  2374- 2396  2385.52   583.14   1.37  1.24E+003   44.69   1.53E+003
F  14  2481- 2503  2492.36   609.26   1.38  1.78E+003   50.26   1.46E+003
F  15  2964- 2982  2974.56   727.13   1.45  3.04E+002   29.29   9.42E+002
F  16  3239- 3262  3251.32   794.79   1.48  1.95E+002   24.91   9.66E+002
F  17  3508- 3531  3520.73   860.65   1.51  2.01E+002   24.91   9.13E+002
F  18  3716- 3736  3727.06   911.08   1.54  1.16E+003   40.52   7.61E+002
F  19  3814- 3829  3821.28   934.12   1.55  1.47E+002   21.75   4.66E+002
 M 20  3938- 3974  3946.54   964.74   1.56  2.21E+002   25.35   6.70E+002
 m 21  3938- 3974  3963.46   968.87   1.56  6.61E+002   33.39   7.06E+002
F  22  4090- 4102  4096.70  1001.44   1.58  7.37E+001   21.17   4.37E+002
F  23  4573- 4592  4582.39  1120.17   1.63  5.49E+002   30.86   5.79E+002
F  24  5051- 5075  5063.99  1237.90   1.68  2.80E+002   24.48   6.33E+002
F  25  5623- 5646  5634.70  1377.41   1.73  1.83E+002   18.94   3.21E+002
F  26  5749- 5766  5757.71  1407.48   1.75  1.15E+002   16.63   2.21E+002
F  27  5960- 5989  5975.34  1460.68   1.76  8.79E+003   94.63   2.97E+002
F  28  6167- 6182  6173.03  1509.00   1.78  7.72E+001   14.15   1.53E+002
F  29  6488- 6504  6496.16  1588.00   1.81  1.47E+002   16.11   1.34E+002
F  30  6619- 6638  6629.04  1620.48   1.82  8.99E+001   14.34   1.68E+002
F  31  6662- 6680  6671.39  1630.83   1.83  9.46E+001   13.83   1.28E+002
F  32  6788- 6803  6796.07  1661.31   1.84  5.97E+001   11.85   9.18E+001
F  33  7066- 7085  7075.49  1729.61   1.86  1.43E+002   15.52   1.32E+002
F  34  7208- 7229  7217.47  1764.32   1.87  6.50E+002   27.63   1.51E+002
F  35  7551- 7565  7557.92  1847.54   1.90  8.41E+001   13.26   9.44E+001

M = First peak in a multiplet region
m = Other peak in a multiplet region
F = Fitted singlet

Errors quoted at  1.000 sigma
Background Subtract Report            12/7/2021   4:09:17 PM      Page  1
```

Figure B.1: Peak analysis report of GR_3 sample code

Appendix C

Nuclide identification report

```
*************************************************************************
*****   N U C L I D E   I D E N T I F I C A T I O N   R E P O R T   *****
*************************************************************************

     Sample Title:          BUILDING MATERIAL
     Nuclide Library Used: C:\GENIE2K\CAMFILES\Env with outh CD-109

   .....................     IDENTIFIED NUCLIDES     .....................

   Nuclide     Id        Energy     Yield      Activity      Activity     Coinc
   Name     Confidence   (keV)       (%)      (Bq /KG   )   Uncertainty  Corr

   K-40        0.999    1460.81*     10.67    3.64124E+001  2.60251E+000 err
   PB-212      1.000      77.11*     17.50    1.98330E+000  3.16828E-001 err
                         238.63*     44.60    1.51457E+000  1.64890E-001 err
   BI-214      0.999     609.31*     46.30    1.87558E+000  2.07600E-001 err
                        1120.29*     15.10    1.46107E+000  4.65353E-001 err
                        1764.49*     15.80    1.15958E+000  4.57649E-001 err
   PB-214      1.000     295.21*     19.20    1.96393E+000  2.73505E-001 err
                         351.92*     37.20    2.44467E+000  2.47407E-001 err
   AC-228      0.999     911.21*     26.60    2.03254E+000  5.32368E-001 err
                         968.97*     16.20    3.88073E+000  7.83875E-001 err

        * = Energy line found in the spectrum.
        @ = Energy line not used for Weighted Mean Activity
        Energy Tolerance :     1.000 keV
        Nuclide confidence index threshold =    0.30
        Errors quoted at  1.000 sigma
        Coincidence correction performed.
        free = No coincidence correction required.
        miss = Nuclide energy was not found in the coincidence library.
        err  = Error in coincidence correction calculation.
        ISOCS/LabSOCS/Coinc. Corr. Warning/error code =         537199722
```

Figure C.1: Nuclide identification report of GR_3 sample code

Appendix D

Nuclide identification report

```
*******************************************************************************
*****   N U C L I D E   I D E N T I F I C A T I O N   R E P O R T   *****
*******************************************************************************

     Sample Title:          Environmental
     Nuclide Library Used: C:\GENIE2K\CAMFILES\Env with outh CD-109

   .....................     IDENTIFIED NUCLIDES      .....................

   Nuclide     Id         Energy      Yield      Activity      Activity     Coinc
   Name      Confidence    (keV)        (%)      (Bq /Kg   )   Uncertainty  Corr

   K-40        0.990    1460.81*     10.67    2.51738E+002   1.12498E+001 err
   MN-54       0.929     834.83*     99.97    6.36237E-001   5.80793E-002 err
   CS-137      0.993     661.65*     85.12    1.29643E+000   9.64407E-002 err
   PB-212      1.000      77.11*     17.50    7.02234E+001   7.12308E+000 err
                         238.63*     44.60    4.37453E+001   3.56541E+000 err
   BI-214      0.995     609.31*     46.30    3.79093E+001   2.50351E+000 err
                        1120.29*     15.10    3.75592E+001   1.87197E+000 err
                        1764.49*     15.80    3.74138E+001   1.74293E+000 err
   PB-214      0.999     295.21*     19.20    3.84169E+001   3.14751E+000 err
                         351.92*     37.20    3.87897E+001   3.16649E+000 err
   AC-228      0.993     911.21*     26.60    8.33041E+001   5.61861E+000 err
                         968.97*     16.20    8.41468E+001   5.37199E+000 err

       * = Energy line found in the spectrum.
       @ = Energy line not used for Weighted Mean Activity
       Energy Tolerance :    1.000 keV
       Nuclide confidence index threshold =   0.30
       Errors quoted at  1.000 sigma
       Coincidence correction performed.
       free = No coincidence correction required.
       miss = Nuclide energy was not found in the coincidence library.
       err  = Error in coincidence correction calculation.
       ISOCS/LabSOCS/Coinc. Corr. Warning/error code =        537199722
```

Figure D.1: Nuclide identification report of VS_9 sample code

Appendix E

Interference Corrected Activity Report

Interference Corrected Activity Report 4/13/2022 2:01:43 PM Page 2

****
***** I N T E R F E R E N C E C O R R E C T E D R E P O R T *****
****

Nuclide Name	Nuclide Id Confidence	Wt mean Activity (Bq /kg)	Wt mean Activity Uncertainty
K-40	0.937	6.901051E+000	1.405022E+000
MN-54	0.982	1.752315E-001	3.536907E-002
CS-137	0.969	2.986438E-001	4.322137E-002
PB-212	0.999	1.820379E+001	1.186809E+000
BI-214	0.962	8.757420E+000	3.787709E-001
PB-214	0.996	1.072184E+001	6.463958E-001
AC-228	0.966	2.496909E+001	1.255213E+000

? = nuclide is part of an undetermined solution
X = nuclide rejected by the interference analysis
@ = nuclide contains energy lines not used in Weighted Mean Activity

Errors quoted at 1.000 sigma

Figure E.1: Interference corrected activity report of S_1 sample code

Appendix F

Gamma Spectrum Analysis

```
*************************************************************************
*****       G A M M A   S P E C T R U M   A N A L Y S I S         *****
*************************************************************************


Filename: C:\GENIE2K\CAMFILES\GEZACHEW AAU\ERTL-C5-2022.CNF

Report Generated On             : 4/14/2022   9:59:19 AM

Sample Title                    : environmental
Sample Description              :
Sample Identification           : ERTL-C5-2022
Sample Type                     : Clay
Sample Geometry                 : 538G-E

Peak Locate Threshold           :  3.00
Peak Locate Range (in channels) :     1 -  8192
Peak Area Range (in channels)   :     1 -  8192
Identification Energy Tolerance :    1.000 keV

Sample Size                     :  6.100E-001 kg

Sample Taken On                 :
Acquisition Started             : 4/13/2022   7:38:57 AM

Live Time                       :    28800.0 seconds
Real Time                       :    28963.2 seconds

Dead Time                       :   0.56 %


             Energy Calibration Used Done On       : 3/23/2022
             Efficiency Calibration Used Done On   : 3/3/2021
             Efficiency ID                         :
```

Figure F.1: Gamma spectrum analysis of C_5 sample code

Appendix G

Nuclear decay law equations

The change in radioactive nuclei during an infinitesimal time interval dt is

$$\frac{dN(t)}{N} = -\lambda dt, \tag{G.1}$$

The number of nuclei at any later time t is

$$\int \frac{dN(t)}{N} = -\int \lambda dt, \Rightarrow N(t) = N_0 e^{-\lambda t} \tag{G.2}$$

The activity of radionuclide is

$$A(t) = \lambda N(t) = \lambda N_0 e^{-\lambda t} = A_0 e^{-\lambda t} \tag{G.3}$$

The mean lifetime of a radioactive nuclei is

$$\tau = \int \frac{t\lambda N(t)dt}{N_0} = \lambda \int t e^{-\lambda} dt = \frac{1}{\lambda} \tag{G.4}$$

Bibliography

[1] Adams F., Dams R. (1970). Experiments in Nuclear Science, Second Edition, Published by ORTEC, USA.

[2] UNSCEAR (1993). Sources and effects of ionizing radiation. Report to the General Assembly, with Scientific Annexes. United Nations, New York.

[3] Santawamaitre, T., Malain, D., Al-Sulaiti, H.A., Matthews, M., Bradley, D.A., and Regan, P. (2011). Study of natural radioactivity in riverbank soils along the Chao Phraya river basin. Nuclear Instrument and Methods in Physics Research Section A, 652: 920-924.

[4] L'Annunziata M. F. (2007). Radioactivity: Introduction and History. (Elsevier).

[5] UNSCEAR (2000). United Nations Scientific Committee on the Effects of Atomic Radiation, Report to General Assembly, with Scientific Annexes, Sources and Effects of Ionizing Radiation, United Nations, New York.

[6] Tzortzis, M., Tsertos, H., Christofides, S., Christodoulides, G. (2003). Gamma radiation measurements and dose rates in commercially-used natural tiling rocks (granites). Journal of Environmental Radioactivity, 70, P:223-235.

[7] Stochioiu A., et. al., (2013), Environmental radioactivity assessment studies on placement area of the new extreme light infrastructure nuclear physics facility. Romanian Journal Physics, 59: 808-816.

[8] Saad, M. H., Tamboul, J. Y., Yousef, M., (2014). Evaluation of Natural Radioactivity in Different Regions in Sudan. Journal of American Science, 10 (2).

[9] European Cooperation in Science and Technology, (2017). Naturally occurring radioactive materials in construction. WOODHEAD, P: 1-338.

[10] Das A., Ferbel T. (2003). Introduction to nuclear and particle physics (Second Edition). World Scientific New Jersey London, 65(5):1-395.

[11] Ahmed S. N. (2007). Physics and engineering of radiation detection. (Academic Press).

[12] Merril Eisenbud, (1987). Environmental radioactivity. Third edition. (Academic Press, INC.)

[13] Neeb Karl-Heinz, (1997). The Radiochemistry of Nuclear Power Plants with Light Water Reactors.

[14] Khandaker M. U., Jojo P. J., Kassim H. A, Amin Y. M. (2012). Radiometric analysis of construction materials using HPGe gamma-ray spectrometry. Radiation Protection Dosimetry, 152, P:33-37.

[15] Shultis J. K. and Faw R. E. (2002). Fundamentals of Nuclear Science and Engineering, Marcel Dekker, Inc, U.S.A.

[16] Ali Abdulwahab Ridha, (2013). Determination of Radionuclides Concentrations in Construction Materials Used in Iraq.

[17] Auday Tariq Subhi Al Bayati, (2017). Determination of the Concentrations for Radioactive Elements Around Al-Tuwaitha Center Using Gamma Ray Spectroscopy and CR-39 Detector. PhD Thesis, University of Baghdad, Iraq.

[18] Xhixha, G. (2010). Advanced Gamma-Ray Spectrometry for Environmental Radioactivity Monitoring. PhD Thesis, University of Ferrara, Italy.

[19] Flakus F. N. (1981). Detecting and measuring ionizing radiation-a short history. IAEA BULLETIN, 23(4):31-36.

[20] Milbrath B. D., Peurrung A. J., Bliss M., Weber W. J. (2008). Radiation Detector Materials: An Overview. Journal of Materials Research, 23(10):2561-2581.

[21] Richard B. Firestone, (2005). Physics of Gamma-ray Spectroscopy Measurements, Lawrence Berkeley National Laboratory, Berkeley, CA 94720 USA.

[22] WHO (2009). Hand book on Indoor Radon. A Public Health Perspective, World Health Organizatin.

[23] Byrnes M.E., King D.A., Tierno P.M. (2003). Nuclear, Chemical, Biological: Terrorism Emergency Response and Public Protection, Lewis Publishers, A CRC Press Company, Boca Raton, London, New York, Washington, p:124-135.

[24] Sofiya Choudhary (2018). Deterministic and Stochastic Effects of Radiation. Short communication. Cancer Therappy and Oncology international Journal, 12(2):1-2.

[25] ICRP 1991. Annals of the ICRP, Recommendations of the International Commission on Radiological Protection, ICRP publication 60, Pergamon Press.

[26] Reid J (1980). Nuclear physics. Nature, 283(5750): P:1-95.

[27] Nafaa Reguigui, (2006). Gamma Ray Spectrometry.

[28] Khandaker M. U. (2011). High purity germanium detector in gamma-ray spectrometry. International Journal of Fundamental Physical Sciences, 1,P:42-46.

[29] Poschl M., Nollet L. M. (2006). Radionuclide concentrations in food and the environment. (Taylor and Francis Group, LLC).

[30] Knoll, F.G. (2000). Radiation Detection and Measurement, Third Edition, John Wiley and Sons, Inc. New York, USA.

[31] Korna A. H., Fares S. S., El-Rahman M. A. (2014). Natural radioactivity levels and radiation hazards for gypsum materials used in Egypt. Natural Science, 06(01):5-13.

[32] Isola G. A., Ayanlola P. S., Ayantunji O. I., Bayode O. P. (2021). Comparative Study on the Contribution of Asbestos and Gypsum Building Materials to Environmental Radioactivity and Its Radiological Implications. International Journal of Sciences: Basic and Applied Research (IJSBAR) International Journal of Sciences: Basic and Applied Research, 56(2):263-271.

[33] Shala F., Xhixha G., Kaçeli Xhixha M., Hasani F., Xhixha E., Shyti M., Sadiraj Kuqi D., Prifti D., Qafleshi M. (2017). Natural radioactivity in cements and raw materials used in Albanian cement industry. Environmental Earth Sciences, 76(20):1-7.

[34] Turhan S., (2010), Radioactivity levels of limestone and gypsum used as building raw materials in Turkey and estimation of exposure doses. Radiation Protection Dosimetry, 140(4):402-407.

[35] Alzubaidi G., Hamid F. B. S., Abdul Rahman I. (2016). Assessment of Natural Radioactivity Levels and Radiation Hazards in Agricultural and Virgin Soil in the State of Kedah, North of Malaysia, Hindawi Publishing Corporation, Scientific World Journal Volume 2016, P:1-9.

[36] Thabayneh K. M., Jazzar, M. M. (2012). Natural Radioactivity Levels and Estimation of Radiation Exposure in Environmental Soil Samples from Tulkarem Province-Palestine. Open Journal of Soil Science, 02(01):7-16.

[37] Abiama P. E., et al., (2010). High background radiation investigated by gamma spectrometry of the soil in the southwestern region of Cameroon. Journal of environmental radioactivity, 101 (9):739-743.

[38] Geremew H., Chaubey A. K. (2019). Investigations of Natural Radioactivity Levels and the Possible Radiation Hazards in Floriculture Soil , Holeta , Shoa , Ethiopia , Using Gamma Ray Spectrometry. International Journal of Current Research, 11 (02):1535-1540.

[39] Issa, S. A. M. (2013). Radiometric assessment of natural radioactivity levels of agricultural soil samples collected in dakahlia, egypt. Radiation Protection Dosimetry, 156 (1):59-67.

[40] Mohebian M., Pourimani, R. (2020). Radiometric properties of virgin and cultivated soil around the shazand refinery complex in Iran. International Journal of Radiation Research, 18(4):723-732.

[41] Nisar A., Jaafar S. (2015). Natural radioactivity in virgin and agricultural soil and its environmental implications in Sungai Petani, Kedah, Malaysia. Pollution, 1(3):305-313.

[42] Saleh M. A., Ramli A. T., Alajerami Y., Aliyu A. S. (2013). Assessment of natural radiation levels and associated dose rates from surface soils in Pontian district, Johor, Malaysia. Journal of Ovonic Research, 9(1):17-27.

[43] Ismail A.F., Yasir M.S., Amran A., Majid B., Bahari I., Yahaya R., Rahman I., (2009). Radiological studies of naturally occurring radioactive materials in some Malaysia's sand used in building construction, The Malaysian Journal of Analytical Sciences, 13 (1): 29-35.

[44] Abdel-Ghany H.A., El-Zakla T., Hassan A.M. (2009). Environmental Radioactivity Measurements of some Egyptian Sand Samples. Romanian Journal of Physics, 54 (1-2):213-223.

[45] Turhan, S. (2007). Assessment of the natural radioactivity and radiological hazards in Turkish cement and its raw materials. Journal of Environmental Radioactivity, 99(2):404-414.

[46] Saadi, E., Benrachi, F., Azbouche, A. (2020). An overview of natural and anthropogenic radioactivity distribution in various building materials used in Algerian dwellings. International Journal of Environmental Analytical Chemistry, 00(00):1-18.

[47] Kolo, M. T., Khandaker, M. U., Amin, Y. M., Abdullah, W. H. B. (2016). Quantification and radiological risk estimation due to the presence of natural radionuclides in Maiganga coal, Nigeria. PLoS ONE, 11(6):1-13.

[48] Aslam, M., Gul, R., Ara, T., Hussain, M. (2012). Assessment of radiological hazards of naturally occurring radioactive materials in cement industry. Radiation Protection Dosimetry, 151(3):483-488.

[49] Akkurt I., Mavi B., Akyildirim H., Günoglu K., (2009). Natural radioactivity of coals and its risk assessment. International Journal of Physical Sciences, 4(7):403-406.

[50] Khan, K., Khan, H. M. (2001). Natural gamma-emiting radionuclides in Pakistani Portland cement. Applied Radiation and Isotopes, 54(5):861-865.

[51] Zalewski M., Tomczak M., Kapata J. (2001). Radioactivity of Building Materials Available in Northeastern Poland. Polish Journal of Environmental Studies, 10(3):183-188.

[52] Abu Samreh, M. M., Thabayneh, K. M., Khrais, F. W. (2014). Measurement of activity concentration levels of radionuclides in soil samples collected from Bethlehem Province, West Bank, Palestine. Turkish Journal of Engineering and Environmental Sciences, 38(2):113-125.

[53] Knoll Glennn P. (2000). Radiation Detection and Measurements. 3rd ed. New York: Jhon Wiley and Sons, Inc. ISBN: 0-471-07338-5.

[54] Krane, Kenneth S. (1988). Introductory nuclear physics, Kentheth S. Krane. Chichester:Wiley. New York. ISBN: 047180553X.

[55] Canberra (2008). Standard Electrode Coaxial Ge Detectors. [cited 18 March 2009].

[56] Pourimani R., Shahroodi S. M. M. (2018). Radiological assessment of the artificial and natural radionuclide concentrations of wheat and barley samples in Karbala, Iraq. Iranian Journal of Medical Physics, 15(2):126-131.

[57] IAEA (1989). Measurement of Radionuclides in Food and the Environment,(a Guidebook, Technical Reports Series No. 295, International Atomic Energy Agency, Vienna).

[58] Gilmore G. R. (2008). Practical Gamma-ray Spectrometry. 2nd Edition, Wiley-VCH Verlag, Wenheim, Germany.

[59] NRC (National Research Council). (1999). Arsenic in drinking water. Washington, DC. p. 251-257.

[60] Ben Fredj A., Hizem N., Chelbi M., Ghedira L. (2005). Quantitative analysis of gamma-ray emitters radioisotopes in commercialised bottled water in Tunisia. Radiation Protection Dosimetry, 117(4):419-424.

[61] Quindos L. S., Fernandez P. L., Rodenas C., Gomez-Arozamena J. A. (2004). convertion factors for external gamma dose drived from natural radionuclides in soil. Journal of environmental radioactivity, 71, p.139-145.

[62] EC (1999). Radiological protection principles concerning the Natural radioactivity of Building materials, Directorate General Environment, Nuclear Safety, and Civil protection.

[63] Beretka J., Mathew P. J. (1985). Natural radioactivity of australian building materials, industrial wastes and by-products. Health Physics, 48(1):87-95.

[64] ICRP (1994). Protection against Rn-222 at home and at work. Publication No. 65, Annals of the ICRP,23, Pergamon, Oxford, Pergamon press.

[65] Buonanno G., Giovinco G., Morawska L., Stabile L. (2015). Lung cancer risk of airborne particles for Italian population. Environmental Research, 142:443-451.

[66] UNSCEAR (2010). Report of the united nations scientific committee on the effects of atomic radiation. In United Nations, New York.

[67] Yasir M. S., Ab Majid A., Yahaya R. (2007). Study of natural radionuclides and its radiation hazard index in Malaysian building materials. Journal of Radioanalytical and Nuclear Chemistry, 273(3):539-541.

[68] El-Taher A. (2009). Gamma spectroscopic analysis and associated radiation hazards of building materials used in Egypt. Radiation Protection Dosimetry, 138(2):166-173.

[69] El-Taher A., (2012). Assessment of natural radioactivity levels and radiation hazards for building materials used in Qassim area, Saudi Arabia. Romanian Reports of Physics, 57(3-4):726-735.

[70] Al-Dadi M. M., Hassan H. E., Sharshar T., Arida H. A., and Badran H. M., (2014) Environmental impact of some cement manufacturing plants in Saudi Arabia. Journal of Radioanalytical and Nuclear Chemistry, 302(3):1103-1117.

[71] Baykara O., Karatepe S., Dogru M. (2011). Assessments of natural radioactivity and radiological hazards in construction materials used in Elazig, Turkey. Radiation Measurements, 46(1):153-158.

[72] ICRP (1999). Protection of the public institutions of prolonged radiation exposure. Stockholm, Sweden,Elsevier sciences.

[73] Otto R. (2008). Gypsum processing and Use. Appropriate Technology Magazine, 23(4):1-7.

[74] Sakthieswaran S. M., Babu G. (2016). Gypsum as a Construction Material-A Review of Recent Developments. IJIRST-International Journal for Innovative Research in Science and Technology, 2(12):315-322

[75] Sharaf J. M. Hamideen M. S. (2013). Measurement of natural radioactivity in Jordanian building materials and their contribution to the public indoor gamma dose rate. Applied Radiation and Isotopes, 80, 61-66.

[76] Joel E. S., Maxwell O., Adewoyin O. O., Ehi-Eromosele C. O., Embong Z., Oyawoye F. (2018). Assessment of natural radioactivity in various commercial tiles used for building purposes in Nigeria. MethodsX, 5, 8-19.

[77] Matiullah N. A., Hussein A. J. A. (1998). Natural radioactivity in Jordanian soil and building materials and the associated radiation hazards. Journal of Environmental Radioactivity, 39(1):9-22.

[78] Chowdhury M. I., Alam M. N., Ahmed A. K. S. (1998). Concentration of radionuclides in building and ceramic materials of Bangladesh and evaluation of radiation hazard. Journal of Radioanalytical and Nuclear Chemistry, 231(1-2): 117-123a.

[79] Bou-Rabee F. Bem H. (1996). Jointly published by Else qer Science S. A., Lausanne and A ”kaddmiai Kiad6, Btdapest. Building, 213(2):143-149.

[80] Papaefthymiou H., Gouseti O. (2008). Natural radioactivity and associated radiation hazards in building materials used in Peloponnese, Greece. Radiation Measurements, 43(8):1453-1457.

[81] El-Taher A., Makhluf S., Nossair A., Abdel Halim A. S. (2010). Assessment of natural radioactivity levels and radiation hazards due to cement industry. Applied Radiation and Isotopes, 68(1):169-174.

[82] Tso M. Y. W., Leung J. K. C. (1996). Radiological impact of coal ash from the power plants in Hong Kong. Journal of Environmental Radioactivity, 30(1):1-14.

[83] Papaefthymiou H., Symeopoulos B. D., Soupioni M. (2007). Neutron activation analysis and natural radioactivity measurements of lignite and ashes from Megalopolis basin, Greece. Journal of Radioanalytical and Nuclear Chemistry, 274(1):123-130.

[84] Mora J. C., Baeza A., Robles B., Corbacho J. A., Cancio D. (2009). Behaviour of natural radionuclides in coal combustion. Radioprotection, 44(5):577-580.

[85] Xinwei L., Lingqing W., Xiaodan J. (2006). Radiometric analysis of Chinese commercial granites. Journal of Radioanalytical and Nuclear Chemistry, 267(3):669-673.

[86] IAEA (1982). Basic safety standards for radiation protection IAEA, safety series No.9, International Atomic Energy Agency, Vienna (Issue 9).

[87] Sharma N., Singh J., Esakki S. C., Tripathi R. M. (2016) A study of the natural radioactivity and radon exhalation rate in some cements used in India and its radiological significance. Journal of Radiation Research and Applied Sciences, 9(1):47-56.

[88] Kabir K., Islam S., Rahman M. (1970). Distribution of Radionuclides in Surface Soil and Bottom Sediment in the District of Jessore, Bangladesh and Evaluation of Radiation Hazard. Journal of Bangladesh Academy of Sciences, 33(1):117-130.

[89] Singh S., Rani A., Mahajan R. K. (2005). ^{226}Ra, ^{232}Th and ^{40}K analysis in soil samples from some areas of Punjab and Himachal Pradesh, India using gamma ray spectrometry. Radiation Measurements, 39(4):431-439.

[90] Ioannides K. G., Mertzimekis T. J., Papachristodoulou C. A., Tzialla C. E. (1997). Measurements of natural radioactivity in phosphate fertilizers. Science of the Total Environment, 196(1):63-67.

[91] Boukhenfouf W., Boucenna A. (2011). The radioactivity measurements in soils and fertilizers using gamma spectrometry technique. Journal of Environmental Radioactivity, 102(4):336-339.

[92] Akhtar N., Tufail M., Ashraf M. (2005). Natural environmental radioactivity and estimation of radiation exposure from saline soils. International Journal of Environmental Science and Technology, 1(4):279-285.

[93] Almayahi B. A., Tajuddin A. A., Jaafar M. S. (2012). Radiation hazard indices of soil and water samples in Northern Malaysian Peninsula. Applied Radiation and Isotopes, 70(11):2652-2660.

[94] NEAOECD. (1979). Exposure to Radiation From The Natural Radioactivity in Building Materials. Report By An NEA Group of Experts (p. 40).

[95] Porstendorfer J., Buttenveck G., Reineking A. (1994). Daily Variation of the Radon Concentration. Health Physics, 67(3):283-287.

[96] Ramli A. T., Hussein A. W. M. A., Wood A. K. (2005). Environmental ^{238}U and ^{232}Th concentration measurements in an area of high level natural background radiation at Palong, Johor, Malaysia. Journal of Environmental Radioactivity, 80(3):287-304.

DECLARATION

ADDIS ABABA UNIVERSITY
COLLEGE OF NATURAL AND COMPUTATIONAL SCIENCES
DEPARTMENT OF PHYSICS

PhD Dissertation

Study of Natural Radioactivity Levels
in Environmental samples (Building Material)
in Dejen district, East Gojjam, Ethiopia

Name of Candidate: Gizachew Zihon Cherie

I the under signed declare that the thesis is my original work and no part of it can be claimed as an intellectual property of anybody else except me and my advisors.

Signature: _____